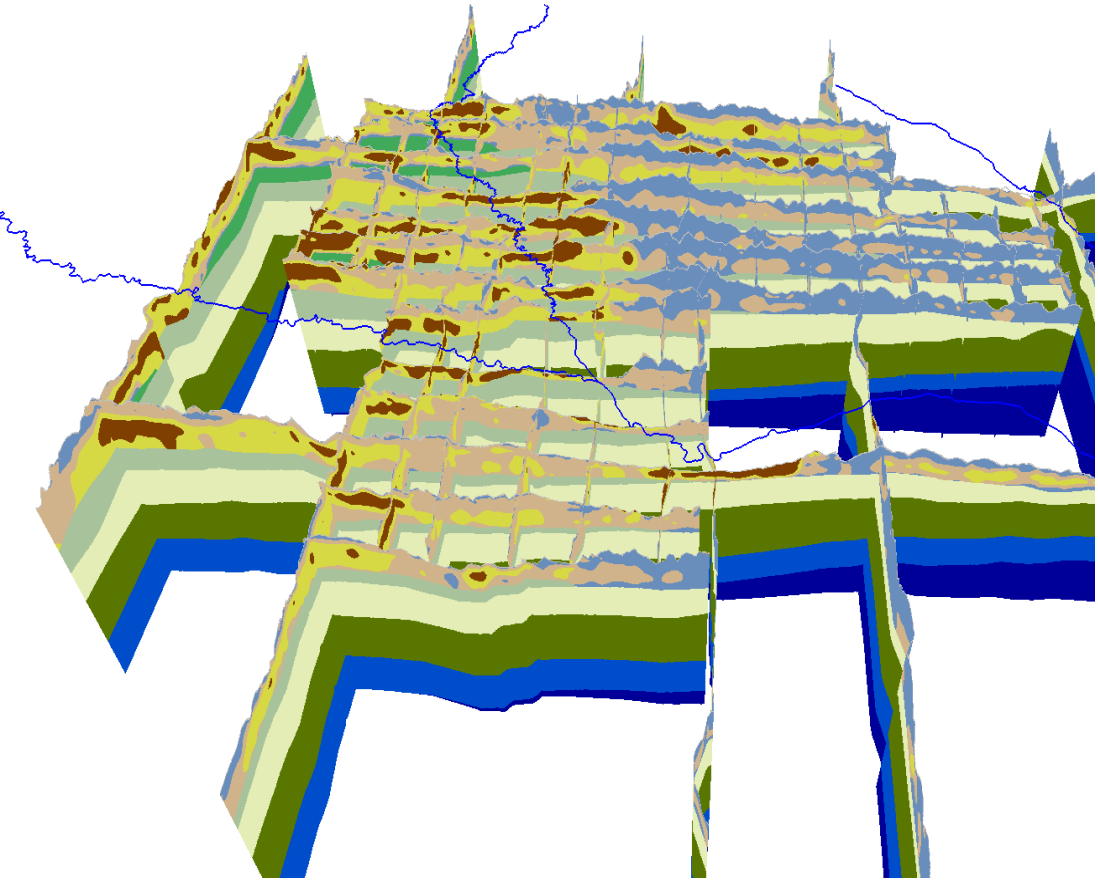
Airborne Electromagnetic Geophysical Surveys and Hydrogeologic Framework Development for Selected Sites in the Lower Elkhorn Natural Resources District, Northeastern Nebraska



Prepared for:

Lower Elkhorn Natural Resources District
601 E. Benjamin Ave. Suite 101
Norfolk, NE 68702

Revision Version 2.0 May 12, 2015
replacing March 30, 2015 Version 1.0

EXPLORATION RESOURCES INTERNATIONAL

May 12, 2015

Airborne Electromagnetic Geophysical Surveys and Hydrogeologic Framework Development for Selected Sites in the Lower Elkhorn Natural Resources District

Revision Version 2.0 May 12, 2015 replacing March 30, 2015 Version 1.0

Prepared for:
Lower Elkhorn Natural Resources District
601 East Benjamin Avenue
Norfolk, NE 68701

Submitted by:
Exploration Resources International Geophysics, LLC
6207 Hwy 80 East
Vicksburg, MS 39180
Phone: (866) 974-6867



Table of Contents

1 Introduction 1
1.1 Purpose of Project 1
1.2 Previous Work 1
1.3 Description of Project Area 2
2 Project Area Hydrogeology 4
2.1 Geologic Setting 4
2.1.1 Surficial Geology 4
2.1.2 Tertiary Geology 7
2.1.3 Cretaceous Geology 7
2.1.4 Jurassic and Triassic Geology 8
2.1.5 Paleozoic System 8
2.2 Hydrogeologic Characteristics in the Quaternary System 9
2.2.1 Aquifer Characteristics 13
2.2.2 Connectivity to Surface Water 14
2.2.3 Connectivity to other Aquifers 14
2.3 Bedrock Aquifer Conditions 15
2.3.1 Extent/Structure of Aquifer 15
2.3.2 Aquifer Characteristics 16
2.3.3 Connectivity to Surface Water 16
2.3.4 Connectivity to other Aquifers 16
2.4 Water Quality 16
2.4.1 Quaternary Aquifer Water Quality 18
2.4.2 Bedrock Aquifer Water Quality 22
2.5 Water Use 23
3 Additional Background Information 25
3.1 Borehole Data 25
3.2 Historic Geologic Cross Sections 28
4 Geophysical Methodology, Acquisition and Processing 33
4.1 Geophysical Methodology 33

4.2 Utility Mapping 34
4.3 AEM Survey Instrumentation 35
4.4 Data Acquisition 38
4.5 Data Processing 41
4.5.1 Primary Field Compensations 41
4.5.2 Automatic Processing 41
4.5.3 Manual Processing and Laterally-Constrained Inversions 41
4.5.4 Power Line Noise Intensity (PLNI) 43
4.5.5 Magnetic Field Data 44
4.6 Spatially-Constrained Inversions 46
4.6.1 Determination of the DOI 53
5 Results and Interpretation 56
5.1 AEM Results and Interpretation 57
5.1.1 Interpretation of the Quaternary and Tertiary Hydrogeologic Framework 60
5.1.2 Interpretation of Bedrock Geology 65
5.1.3 Cretaceous Stratigraphic Sequence 66
5.1.4 Paleozoic Stratigraphic Sequence 67
5.1.5 Resistivity-Lithology Relationship 68
5.1.6 Comparison with CSD Geologic Cross Sections and Test holes 78
5.2 Summary and Recommendations 84
5.2.1 Key AEM Survey Findings 84
5.2.2 AEM Survey Gridline Spacing 85
5.2.3 Applicability and Recommendations Regarding Future Groundwater Investigations 87
6 Description of Data Delivered 92
7 References 98
Appendix 1: AEM Profiles and Interpretation A1-1
Appendix 2: Comparison of CSD Holes with AEM Profiles A2-1
Appendix 3: Depth of Investigation A3-1
Appendix 4: Data Deliverables

List of Figures

Figure 1-1: Map of LENRD project area, including principal cities. 3

Figure 1-2: Elevation of the LENRD project area. 3

Figure 2-1: Bedrock geology of the LENRD project area, derived from Burchett (1986). 4

Figure 2-2: Geologic time scale with lithostratigraphic sequence underlying Nebraska as defined by UNL-CSD (Korus and Joeckel, 2011). 6

Figure 2-3: Generalized till thickness map of Quaternary deposits in eastern Nebraska (University of Nebraska-Lincoln School of Natural Resources, 2014). 7

Figure 2-4: Map displaying the major streams and rivers within the project area. 10

Figure 2-5: Elevation of ground water surface in the LENRD area. 13

Figure 2-6: Thickness of the Dakota aquifer system/Maha aquifer in eastern Nebraska (Ellis, 1984). 15

Figure 2-7: Concentrations (x-axis) of TDS, calcium, chloride, and sodium in water samples verses depth (y-axis) Data are from the US Geological Survey NWIS database. 17

Figure 2-8: Public supply wells within the LENRD project area. 24

Figure 2-9: Registered wells within the LENRD area with depth to static water level indicated by color. 24

Figure 3-1: Locations of CSD tests holes drilled subsequent to 2003 that were provided by ENWRA. 26

Figure 3-2: Locations of boreholes used containing lithologic information across the project area. 26

Figure 3-3: Locations of boreholes used containing stratigraphic information within the project area. 27

Figure 3-4: Locations of boreholes containing geophysical logs that were used in the analysis of the AEM data. 28

Figure 3-5: Locations of geologic cross sections across the project area. 29

Figure 3-6: Original cross section from CSD OFR 109 (left) and the digitized cross section (right). 31

Figure 3-7: 3D view of geo-referenced geologic cross sections used to aid AEM interpretation. 32

Figure 4-1: Schematic of an AEM survey. 33

Figure 4-2: A) Example of a dB/dt sounding curve. B) Corresponding inverted model values. C) Corresponding resistivity earth model. 34

Figure 4-3: Map of the expected utilities across the project area. 35

Figure 4-4: SkyTEM 508 frame including instrumentation locations and X and Y axes. 37

Figure 4-5: Photos of the SkyTEM508 system. 38

Figure 4-6: Flights lines as collected, organized by date. 39

Figure 4-7: Example locations of EM coupling with pipelines or power lines. 42

Figure 4-8: A) AEM data affected by coupling, shown in Figure 4-7, in Aarhus Workbench editor. The top group of lines is the Low Moment and the bottom is the High Moment. B) AEM data with area affected by coupling removed. 42

Figure 4-9: A) Inversion results where AEM data affected by coupling with pipelines and power lines were not removed. B) Inversion results where AEM data affected by coupling were removed. 43

Figure 4-10: Power Line Noise Intensity (PLNI) map of the LENRD survey area. 44

Figure 4-11: Magnetic field data corrected for diurnal drift, with IGRF removed. 45

Figure 4-12: Regional magnetic field data within the LENRD boundary. Derived from Bankey et al. (2002). 45

Figure 4-13: 3D magnetic field analytical signal calculated from the diurnal and IGRF corrected magnetic field data. 46

Figure 4-14: An example AEM profile illustrating the increase in model layer thickness with depth. 47

Figure 4-15: Borehole resistivity logs compared with inverted AEM models. A: Well 3-A-52, 1,700 ft from the AEM line. B: Well 3-A-53, 2,512 ft from AEM line. C: Well 4-A-52, 527 ft from AEM line. 49

Figure 4-16: Borehole resistivity logs compared with inverted AEM models. A: Well 5-GT-80, 721 ft from the AEM line. B: Well 8-A-53, 1,768 ft from AEM line. C: Well 15-A-55, 3,132 ft from AEM line. 51

Figure 4-17: Borehole resistivity logs compared with inverted AEM models. A: Well 8-LE-03, 1,540 ft from AEM line. A: Well 13-LS-99, 2,349 ft from AEM line. 51

Figure 4-18: Cross-plot resistivities compared with the resampled borehole resistivity for the 13 boreholes within the closer spaced flight lines. 52

Figure 4-19: Difference between data point residuals produced by SCIs with and without using the borehole conductivity data as a-priori information. Red indicates an improvement in the residuals by greater than 0.1. 52

Figure 4-20: Data residuals distribution produced by the SCIs in the three-mile grid area with and without use of resistivity logs as a-priori information. 53

Figure 4-21: Data residuals distribution produced by the SCIs in the 10-mile recon lines with and without the resistivity logs as a-priori information. 53

Figure 4-22: Sample of AEM resistivity inversion model with the DOI marked as grey boxes at the bottom of the image. 55

Figure 5-1: Locations of inverted data along the AEM flight lines. 56

Figure 5-2: AEM flight lines with line numbers. 57

Figure 5-3: A northeastward view of the 3D hydrostratigraphic framework of the LENRD project area, including geologic materials ranging from Quaternary deposits to Paleozoic bedrock. The image includes the seven labeled areas of sand-rich, coarse principal aquifer materials (brown colored zones). The Elkhorn and North Fork of the Elkhorn Rivers are also displayed on the framework, and some of the ENWRA reconnaissance lines are displayed beyond the district flight block. 63

Figure 5-4: A 3D view of the northwest-trending buried channel in the sand-rich area 2 of the principal aquifer (brown intervals). 64

Figure 5-5: Box and whisker plots for the resistivity ranges for the nine most common unconsolidated materials encountered in the Quaternary system. 69

Figure 5-6: Histogram plot displaying the distribution of resistivities by major aquifer material color categories (blue- non-aquifer material, tan- marginal aquifer, yellow- principal aquifer, brown- sand-rich, coarse intervals of the principal aquifer). 71

Figure 5-7: Pie charts of the distribution of material within each resistivity range for the four aquifer materials used in the interpretation of the AEM data- 0-12 ohm-m and 12-20 ohm-m. 71

Figure 5-8: Pie charts of the distribution of material within each resistivity range for the four aquifer materials used in the interpretation of the AEM data- 20-50 ohm-m, and 50 ohm-m and above. 72

Figure 5-9: Pie chart of the overall lithology indicated in the 33 e-logs used to characterize the relationship of lithology and resistivity in the project area. 72

Figure 5-10: Pie charts showing overall percentage of lithologies in selected CSD test holes. 74

Figure 5-11: Box and whiskers plot of the resistivity distribution of the Cretaceous and Paleozoic bedrock units discussed in the interpretation of the AEM data. 74

Figure 5-12: Deep Oil and Gas borehole resistivity logs compared with inverted AEM models. A: Well 2616719000, 5,186 ft from the AEM line, B: Well 2616721003, 12,838 ft from AEM line. 75

Figure 5-13: Histogram of the distribution of the fractional difference in the thickness of the principal aquifer materials using 20 and 21 ohm-m resistivity thresholds. 77

Figure 5-14: Example cross section illustrating the small difference between selecting a 20 ohm-m threshold or a 21 ohm-m threshold to define the principal aquifer. The solid black line enclosing the yellow (principal aquifer material) represents the 20 ohm-m threshold and the dotted black line enclosing the principal aquifer material represents the 21 ohm-m threshold. 77

Figure 5-15: Northwestward view of LENRD project area displaying the locations of historic and contemporary CSD geologic cross sections. 79

Figure 5-16: Northeastward view of LENRD project area displaying the locations of historic and contemporary CSD geologic cross sections. 80

Figure 5-17: Comparison of the TEM inversion model, borehole log, lithology, and stratigraphy at CSD test hole 5-GT-80. 80

Figure 5-18: Combined display of AEM data (second panel), hydrostratigraphic interpretation (third panel), and CSD cross section (bottom panel) for flight line 100501 near Wayne, NE. The locations of the AEM flight line and CSD cross section are displayed in the top panel. 81

Figure 5-19: Zoomed-in view along the eastern extent of AEM flight line 100501, demonstrating the thin intervals of material indicated in the test hole logs that correspond to only the averaged resistivity data across intervals of greater thickness. This is particularly evident in 31-A-51 and 9-A-64. 82

Figure 5-20: Combined display of AEM data (second panel), hydrostratigraphic interpretation (third panel), and CSD cross section (bottom pane) for flight line 101601 near Oakland, NE. The locations of the AEM flight line and CSD cross section are displayed in the top panel. 83

Figure 5-21: Display of aquifer material near Clarkson, NE with a 700 ft grid line spacing. The yellow lines demonstrate how some portion of the aquifer would have been missed if the AEM flight line spacing were set at 0.5 or 1.0 miles. 86

List of Tables

Table 2-1: Aquifers in Quaternary to Cretaceous-age stratigraphic units, eastern Nebraska 12

Table 2-2: Statistical results of water-quality analyses from groundwater samples collected in or near the project area, from all wells. Units in milligrams per liter unless stated otherwise. Data are from the US Geological Survey NWIS database. 18

Table 2-3: Statistical results of water quality analyses from groundwater samples collected in or near the project area, from stream-valley/alluvial wells. Units are in milligrams per liter unless stated otherwise. Data are from the US Geological Survey NWIS database. 20

Table 2-4: Statistical results of water quality analyses from groundwater samples collected in or near the project area from glacial wells. Units are in milligrams per liter unless stated otherwise. Data are from the US Geological Survey NWIS database. 21

Table 2-5: Statistical results of water quality analyses from groundwater samples collected in or near the project area from *Kd* wells. Units are in milligrams per liter unless stated otherwise. Data are from the US Geological Survey NWIS database. 22

Table 3-1: Geologic cross sections from CSD OFR-109 that were digitized and geo-referenced. 30

Table 4-1: Positions of instruments on the SkyTEM508 frame, using the center of the frame as the origin in feet. 37

Table 4-2: Positions of corners of the SkyTEM508 transmitter coil, using the center of the frame as the origin in feet. 37

Table 4-3: Locations of magnetic field base station instruments. 37

Table 4-4: Airports and state parks used for landing and refueling by date of acquisition. 40

Table 4-5: Production log displaying the number of production flights conducted on each day and total line miles and kilometers surveyed. 40

Table 4-6: Thickness and depth to bottom for each layer in the SCI inverted AEM models. The thickness of the model layers increase with depth as the resolution of the AEM system decreases with depth. 47

Table 4-7: List of wells with borehole resistivity logs used as a-priori information for the SCI. 50

Table 6-1: Channel name, description, and units for 20141126_345_Nebraska_XRI.xyz with EM, mag, DGPS, Inclinometer, altitude, and associated data. 93

Table 6-2: Channel name, description, and units for Gridlines_SCIresults.xyz and Reconlines_SCIresults.xyz with EM inversion results. 94

Table 6-3: Files containing borehole information. 95

Table 6-4: Channel name, description, and units for collar files 95

Table 6-5: Channel name description and units for borehole data 96

Table 6-6: Channel name description and units for the interpretation results file. 97

List of Abbreviations

1D	One-dimensional
2D	Two-dimensional
3D	Three-dimensional
A* m^2	Ampere meter squared
AEM	Airborne Electromagnetic
Bgl	Below Ground Level
dB/dt	Change in amplitude of magnetic field with time
CSD	Conservation and Survey Division, Nebraska Geological Survey
DOI	Depth of Investigation
DGPS	Differential global positioning system
ENWRA	Eastern Nebraska Water Resources Assessment
Ft	Feet
Ft/d	Feet per day
Ft^2/d	Feet squared per day
GIS	Geographic Information Systems
gpd/ft	Gallons per day per foot
GX	Geosoft executable
IGRF	International Geomagnetic Reference Field
in/year	Inches per year
km	Kilometers
LCI	Laterally-Constrained Inversion
LENRD	Lower Elkhorn Natural Resources District
MAG	Magnetic (data); Magnetometer (instrument)
MCG	Minimum curvature gridding
mg/L	Milligrams per liter
mi	Miles
mi^2	Square miles
µS/cm	Microsiemens per centimeter
NAD83	North American Datum of 1983
NDNR	Nebraska Department of Natural Resources
NRD	Natural Resources District
NOGCC	Nebraska Oil and Gas Conservation Commission
NWIS	National Water Information System
OM	Oasis Montaj
PFC	Primary Field Compensation
PLNI	Power Line Noise Intensity
ρ_{model}	Modeled Resistivity
Rx	Receiver
SCI	Spatially-Constrained Inversion
STD	Standard Deviation
SWL	Static Water Level
TDS	Total Dissolved Solids
TEM	Transient Electromagnetic
TDEM	Time-Domain Electromagnetic
Tx	Transmitter

USGS	United States Geological Survey
UTM	Universal Transverse Mercator
V/m^2	Volts per meter squared
XRI	Exploration Resources International

Executive Summary

Exploration Resources International (XRI) is pleased to submit our report to the Lower Elkhorn Natural Resources District (LENRD) titled "**Airborne Electromagnetic Geophysical Surveys and Hydrogeologic Framework Development for Selected Sites in the Lower Elkhorn Natural Resources District.**" This project was conducted to address the water resource concerns of the LENRD in the area near Norfolk, Nebraska. This hydrogeologically complex area has undergone increased groundwater development in recent years, which prompted the LENRD to seek additional information on the aquifers underlying this part of the district. XRI entered into an agreement with LENRD to undertake this study on September 24, 2014.

The scope of work for this project was as follows:

1. SCOPE OF WORK:

   An Airborne Electromagnetic (AEM) and magnetic survey was flown over a specified area of the LENRD to support creation of the hydrogeological framework of this area. This framework will be provided as preliminary AEM data and as a final product in a data report. The AEM survey will be flown in a reconnaissance grid format at approximately 3 miles separation of flight lines over the areas indicated as priorities by the LENRD. Limited ground time-domain electromagnetic data will be collected in areas selected after the completion of the AEM data acquisition.

   A. The Contractor shall acquire an AEM survey flown over the LENRD to provide the hydrogeological framework, commencing October 11, 2014.

   B. The Contractor shall process and provide quality assurance/quality control for all of the data collected from the AEM and ground system.

   C. The Contractor shall invert the AEM data and then derive an electrical model of the surveyed area. These inverted georeferenced data will be delivered to the LENRD.

   D. The Contractor shall provide a hydrogeologic framework report that will include maps of aquifer(s), map of aquifer(s) relationship to current test holes and production groundwater wells, a map of estimated potential recharge areas for the areas flown. The report will also include all data and metadata files. Aquifer maps will be presented in an attributed Google Earth file format. The report will be delivered in PDF digital format.

2. SCHEDULE OF WORK 2014:

   Upon completion of the AEM survey, the Contractor will begin on or before October 20, 2014, the geophysical processing, including numerical inversions to create a preliminary dataset to be shared with the LENRD.

> Post geophysical processing, the Contractor will begin development of the hydrogeologic framework. At times during its development, interaction with LENRD staff will be needed to keep both parties apprised of progress. After completion of the framework, an interpretive publication will be produced and reported out to the LENRD. The final report will be delivered by June 30, 2015.

The AEM data was successfully collected October 11-19, 2014, including all quality control, quality assurance, and initial inversions of the data. In total, 1471 line-miles of data were collected during the survey. Data interpretation and report writing started in October 2014 and will be completed with final delivery of this report to LENRD. All contracted activities within the scope and schedule of work were met or exceeded.

Interpretation of the AEM data collected in 2014 provided a subsurface characterization of the various geologic materials that correlated with pre-existing geologic information. The AEM provided detailed verification and quantification of the geology that underlies the project area. The interpretation also provided a new understanding of the glacial and bedrock features present in the subsurface. Lithologic descriptions from test holes (University of Nebraska-Conservation and Survey Division) and oil and gas records (Nebraska Oil and Gas Conservation Commission) provided the most useful historical information in the development of the new hydrogeologic framework. Additional supporting data included historic cross sections and a limited number of geophysical logs from the Conservation and Survey Division.

Characterization of unconsolidated subsurface materials (Within the Quaternary system and the Tertiary Ogallala Group) was divided into four categories based on resistivity thresholds- 1) non-aquifer (aquitard) (0-12 ohm-m); 2) marginal aquifer (12-20 ohm-m); 3) principal aquifer (20-50 ohm-m) and 4) the sand-rich portion of the principal aquifer with resistivities greater than 50 ohm-m. Principal aquifer material is most abundant in the western half of the survey area and included Tertiary Ogallala Group materials. Within the extent of the principal aquifer, seven unique areas of sand-rich areas were identified. Marginal aquifer material is present mostly east of the North Fork of the Elkhorn River, and is typically overlain by thick sequences of glacial till and loess as identified by materials in the 0-12 ohm-m range. The ranges of resistivity for each of these categories were determined by an empirical relationship of resistivity to lithology based on comparisons of local resistivity and lithology logs. As expected, coarse material (sand, sand and gravel, gravel and boulders) have the highest median resistivity, all exceeding 50 ohm-m, whereas silty clay had the lowest median resistivity of 9 ohm-m. To assess the influence of the resistivity thresholds, a sensitivity analysis was conducted to determine the difference of the thickness of principal aquifer material with the lower threshold initially set at 20 ohm-m and then again at 21 ohm-m. This test revealed little change in the overall interpreted thickness (less than 10%).

Within the project area, the principal aquifer is made up of the Quaternary sediments and the Tertiary Ogallala Group sediments that are aquifer material. Often aquifer materials of these formations are in hydrogeologic connection with each other. Within the Quaternary and Tertiary Ogallala Group, the

aquifer materials were divided into marginal, principal, and coarse sand rich materials. These aquifer types are located mostly in the western and southern thirds of the project area. The marginal aquifer is the predominant groundwater source in the eastern one-third of the project area. Aquitards occur mostly in the central and eastern extents of the project area. Potential Cretaceous Dakota Formation bedrock aquifers are detected only as areas of high resistivity because limited test hole information is available in the area which limits the ability to fully characterize aquifer conditions based on resistivity values alone. The Pennsylvanian and Mississippian strata are detected in the AEM survey but minimal information on water quality and test hole logs limit conclusive hydrogeologic interpretation on these units. In the LENRD, brackish and saline groundwater are known to exist in the bedrock strata. While these groundwater types can be mapped by AEM methods, there is, however, limited historical data or new supporting data available to confirm that these waters are present beneath the project area. The body and appendices of the report contain the information used in the AEM interpretation and development of the hydrogeologic framework.

The nature of the AEM reconnaissance line flight pattern (widely spaced flight lines) limits the display of the imaged subsurface to two-dimensional (2D) sections along the flight lines and no information on aquifer volumes nor the amount of groundwater in storage can be deduced. However, the 2D sections do provide the location, orientation, groundwater level (from the 1995 CSD water table map), and connectivity between the deposits comprising the principal aquifer and the local streams that in the project area. Also revealed in the hydrogeologic framework are locations at the land surface where the potential for recharge to the principal aquifer is likely the greatest. The 2D sections of the glacial till and loess areas provide limited insight into the confined and unconfined nature of the groundwater system and where water quality management could be impacted by the presence or absence of these materials.

1 Introduction

1.1 Purpose of Project

Sound management of groundwater and surface water in eastern Nebraska has become increasingly important in recent years. There are expanding pressures placed on the resource by the ever growing demands for agricultural production, population growth and urbanization, potential contamination from natural and anthropogenic sources, industrial needs, and the persistent threat of drought. The combination of these stresses on water resources has increased the need for detailed hydrogeologic frameworks of the subsurface

This report describes the general hydrogeologic conditions, assessed using data collected from an airborne electromagnetic (AEM) survey in 2014, within the Lower Elkhorn Natural Resources District (LENRD). In addition to the AEM data, reports from previous studies, analysis of historic groundwater levels, and geologic descriptions from University of Nebraska-Lincoln Conservation and Survey Division test holes and drillers logs obtained from registered wells at the Nebraska Department of Natural Resources (NDNR) were used. The AEM survey data were collected along both reconnaissance (recon) lines spaced approximately 20 miles apart and a tighter grid of 3 mile-spaced lines surrounding the city of Norfolk, NE.

1.2 Previous Work

Use of AEM technology to map and evaluate groundwater resources has gained momentum over the last 20 years in the United States and abroad. The state of Nebraska has been on the forefront of implementing AEM for water resources management over the last decade with projects across the state in a variety of geologic settings. In recent years, the Eastern Nebraska Water Resources Assessment (ENWRA) has coordinated efforts between area Natural Resources Districts (NRDs), Conservation and Survey Division, University of Nebraska-Lincoln (CSD), the U.S. Geological Survey (USGS), and Exploration Resources International Geophysics, LLC (XRI) in support of several projects designed to characterize glacial outwash and buried paleovalley aquifers across the eastern part of the state.

In March 2007, AEM methods were implemented to characterize the hydrogeologic conditions in the Platte River valley near Ashland, as well as in areas underlain by glacial till near Firth and Oakland, Nebraska (Abraham et al., 2011, Korus et al., 2012). In the following years, individual reports utilizing the AEM data collected in 2007 were released by the USGS and CSD. In 2009, a multi-faceted investigation incorporating the 2007 AEM data and 2009 ground-based geophysical techniques was conducted by the USGS to characterize the hydrogeologic setting near Oakland, Nebraska. In 2009, the Lower Platte South NRD funded development of a 3D hydrostratigraphic framework of the subsurface near Swedeburg, Nebraska based on an AEM survey. Also in 2009, the Lower Platte South NRD funded a similar investigation of the hydrostratigraphy near Sprague, Nebraska (Smith et al., 2009; Divine and Korus, 2012). In 2013, the Lower Elkhorn NRD funded XRI to conduct an AEM survey near the towns of Clarkson and Howells, Nebraska in order to characterize the extent of the Quaternary aquifer beneath

the area following the drought of 2012 (Abraham et al., 2013). Also in 2013, XRI completed an AEM survey covering over 800 line-miles in Butler and Saunders counties northwest of the city of Lincoln, Nebraska (Carney et al., 2014). This survey revealed extensive, buried paleovalley aquifers beneath thick sequences of till. Additionally, intervals of Cretaceous bedrock units were revealed in the survey. Thus, AEM surveys of the glacial terrain of eastern Nebraska have followed a progressive, long-term plan spanning nearly 8 years. This body of work shows continuing advancements in the science and application of AEM to support groundwater management.

1.3 Description of Project Area

The LENRD spans approximately 4,050 square miles (mi^2) in northeast Nebraska (Figure 1-1). The elevation of the area, presented in Figure 1-2, ranges from 835 ft to 2235 ft above sea level**.** It is underlain by parts of five of Nebraska's eight topographic regions—Dissected Plains, Plains, Rolling Hills, Sandhills, and Valleys (Elder et al., 1951). This area stretches from the rolling, loess-mantled, glacially-derived landscape (Gosselin et al., 1996) on the east to the Holocene, sand-covered, non-glaciated areas on the west.

Principal cities within the project area, based on 2010 population estimates, include (largest to smallest) Norfolk (24,210), Wayne (5,660), Madison (2,438), Pierce (1,767), Stanton (1,577), and Wisner (1,170) (U.S. Census Bureau, 2013).

Land use/land cover within the project area is primarily agricultural, including irrigated and non-irrigated corn and soybeans. Secondary land use is rangeland, pastureland, and grasslands with some alfalfa crops, urban areas, riparian forest and woodlands (School of Natural Resources University of Nebraska-Lincoln, 2005). Center-pivot irrigation is the primary groundwater irrigation method within the project area, using approximately 6,273 registered irrigation wells.

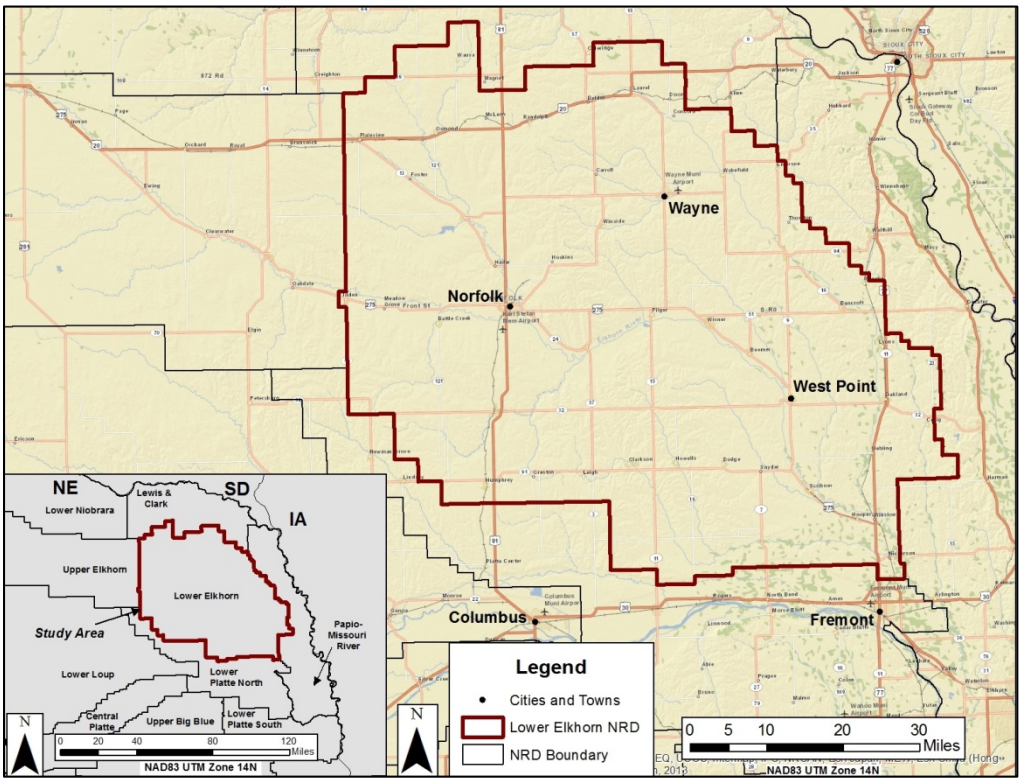


Figure 1-1: Map of LENRD project area, including principal cities.

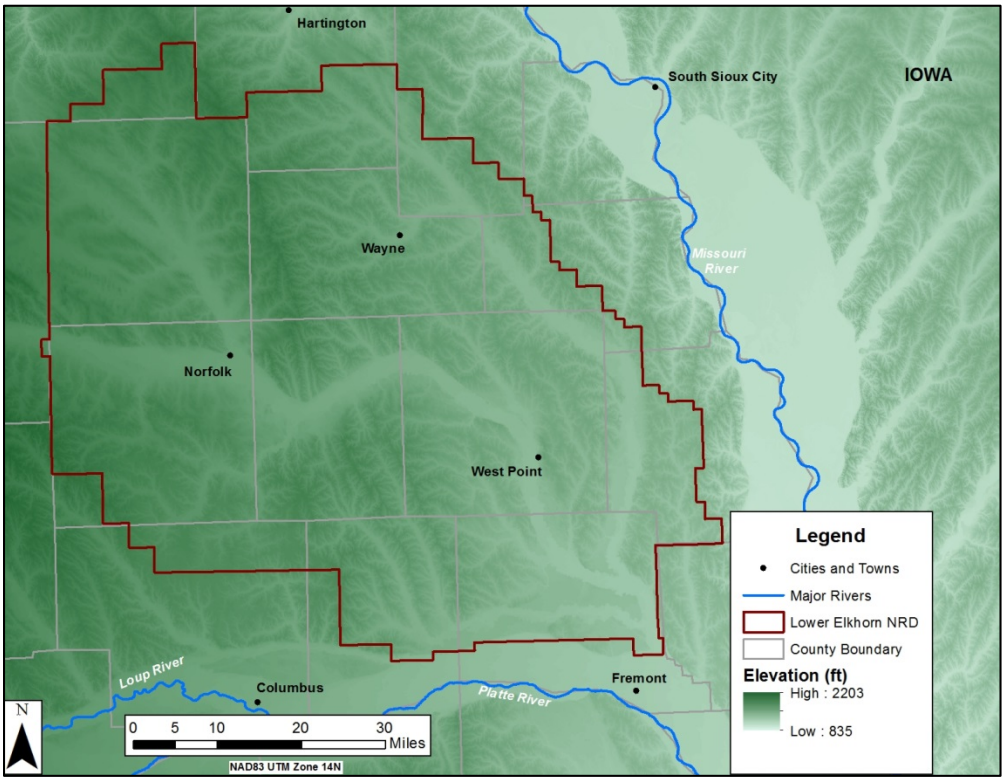


Figure 1-2: Elevation of the LENRD project area.

2 Project Area Hydrogeology

2.1 Geologic Setting

Bedrock geology (Figure 2-1) in the project area is comprised of Tertiary, Cretaceous, and Paleozoic deposits. Paleozoic bedrock consists of undifferentiated Pennsylvanian (*[P*) and Mississippian (*M*) strata. Cretaceous bedrock units include the Pierre Shale (*Kp*), Niobrara Formation (*Kn*), Carlile Shale (*Kc*), Greenhorn Limestone and Graneros Shale (*Kgg*), and the Dakota Formation (*Kd*). The Tertiary bedrock present consists of the Ogallala Group (*To)*, which also serves as a principal aquifer in the western part of the project area. The Tertiary deposits are present only in the western third of the project area. The Cretaceous and Paleozoic deposits underlie the entire area. The southeast portion of the area (east of and south of West Point) is underlain by *Kd*, which locally can yield potable water.

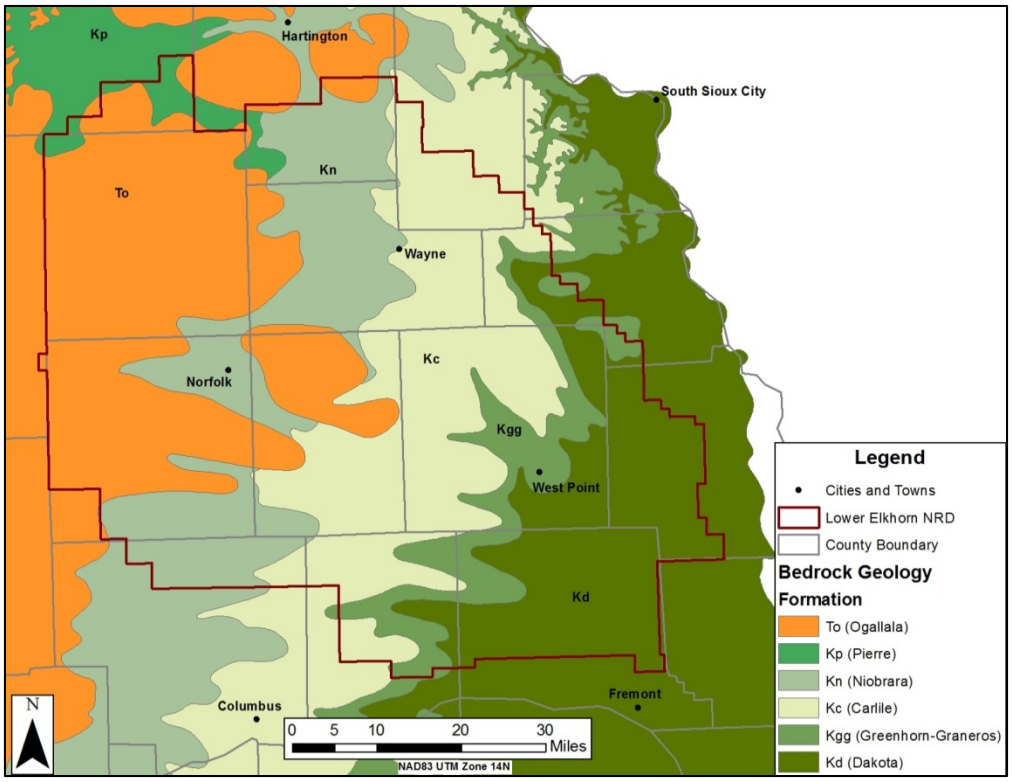


Figure 2-1: Bedrock geology of the LENRD project area, derived from Burchett (1986).

2.1.1 Surficial Geology

The complex Pleistocene and Holocene (Quaternary) geology in northeastern Nebraska consists of myriad sequences of clay, silt, till, sand, and gravel overlying bedrock units. These materials are capped by loess deposits in many locations. Figure 2-2 displays the geologic time scale with CSD's lithostratigraphic sequence that underlies the state of Nebraska (Korus and Joeckel, 2011). The surficial geology of the project area is typical of western mid-continental glaciated areas of North America where buried Quaternary sand and gravel glacial outwash deposits or paleovalleys, comprised of

unconsolidated Plio-Pleistocene sand and gravel units, underlie extensive areas of glacial till. In much of northeastern Nebraska glacial till often underlies loess units (e.g., Peoria, Gillman Canyon Formation, and Loveland loess deposits). Present day surface water systems have incised the loess and till to create wide stream valleys in some locations.

CSD test holes and drillers logs obtained from NDNR indicate glacial till units are prevalent across the project area and make up the majority of the surficial geologic deposits. These units, which can often exceed 200 ft in thickness, serve as upper confining layers to hydrogeologically buried paleovalley aquifers. Figure 2-3 displays a generalized map of till thickness across eastern Nebraska (University of Nebraska-Lincoln School of Natural Resources, 2014). These can impede or reduce recharge to groundwater systems because of the low permeability of the clay within the till. Comprised of localized sand and gravel, the till is consistent with glaciated areas experiencing lateral, push, and terminal moraines.

Plio-Pleistocene and Holocene sand and gravel units, deposited as glacial outwash or by fluvial systems sit unconformably on Cretaceous bedrock in many locations beneath the project area. Thicknesses of the sand and gravel deposits vary by location but generally do not exceed 300 ft (Gosselin et al., 1996). The paleovalley units appear to be preglacial, synglacial, or interglacial in origin and are not well understood (Gates et al., 2014). The paleovalley units underlying thick till sequences in eastern Nebraska can be greater than 6 miles wide, 62 miles long (Gates et al., 2014) and can be up to 200 ft thick (Fredrick et al., 2006). Locally, CSD test holes indicate that the sand and gravel units are, typically, not clean, and are interlayered with silts and clays. Some of the paleovalleys are “deeply covered” by Loveland loess, or Peorian loess. Certain paleovalleys in eastern Nebraska extend eastward (Divine et al., 2009) and some trend southeastward (Condra and Reed, 1959). Easterly to southeasterly trends for paleovalley aquifers in eastern Nebraska appear to be the most common orientations for these subsurface features.

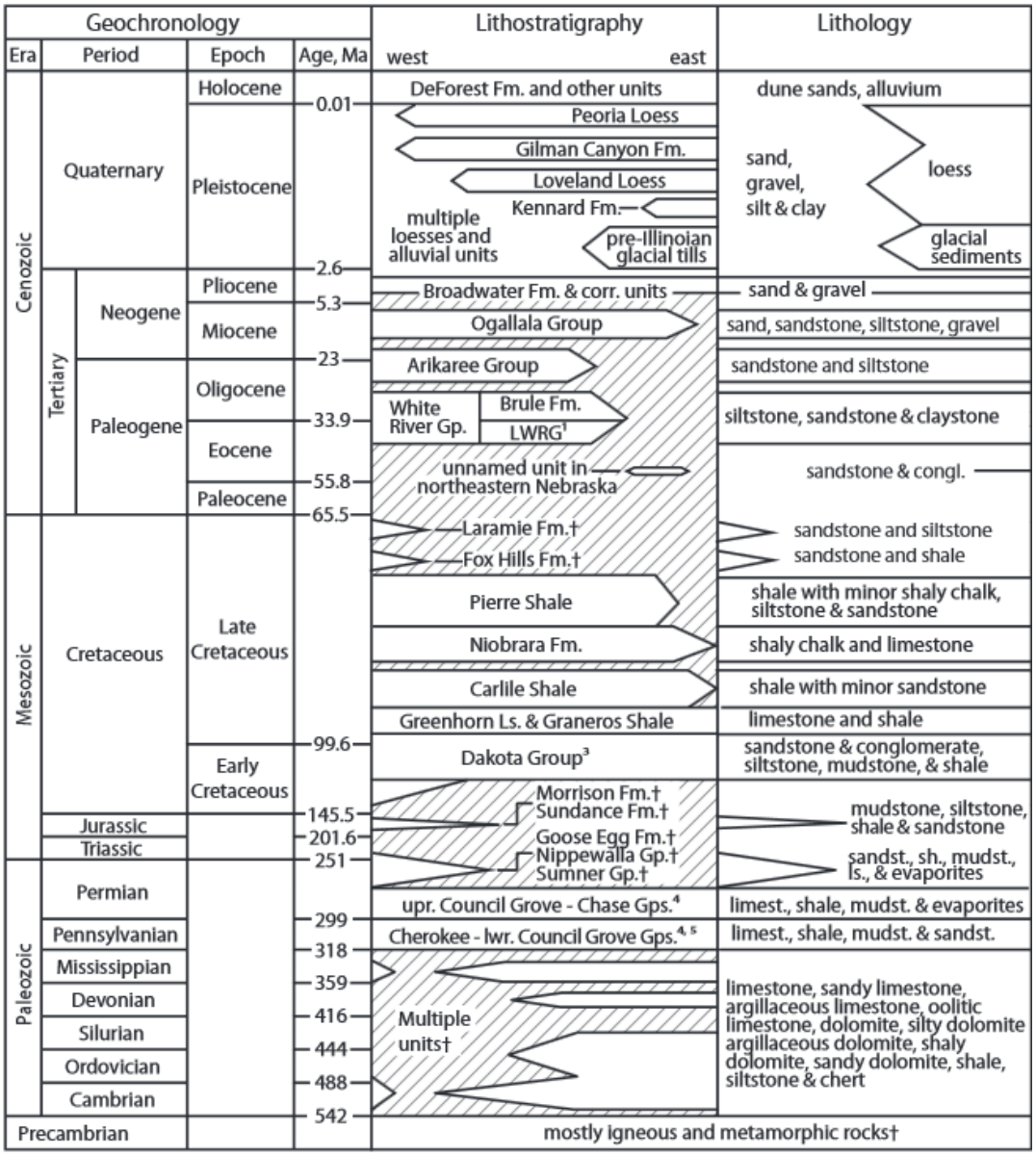


Figure 2-2: Geologic time scale with lithostratigraphic sequence underlying Nebraska as defined by UNL-CSD (Korus and Joeckel, 2011).

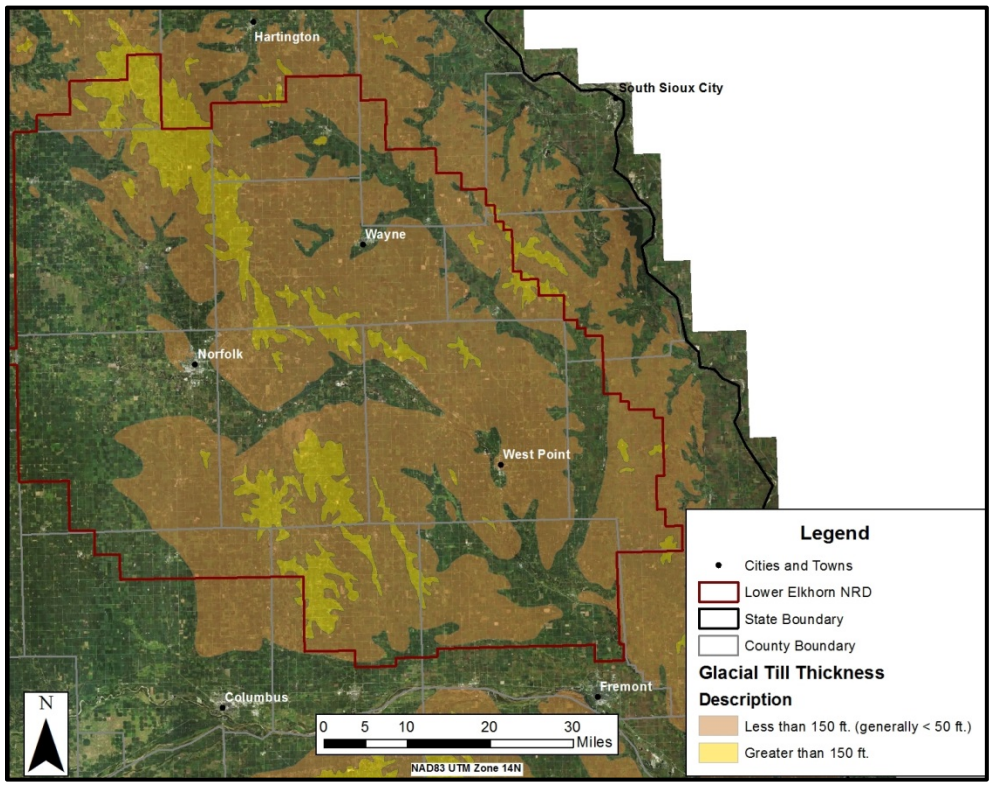


Figure 2-3: Generalized till thickness map of Quaternary deposits in eastern Nebraska (University of Nebraska-Lincoln School of Natural Resources, 2014).

2.1.2 Tertiary Geology

The *To* is the sole major Tertiary geologic unit in the project area and is composed predominantly of fluvial material which comprised of unconsolidated to consolidated irregularly distributed beds of silt, clay, sand, and gravel (Souders, 2000). Some members of the *To* contain partially cemented friable sands or sandstone (Condra and Reed, 1959). The *To* thins and pinches out to the east and rests unconformably above underlying Cretaceous strata (Divine, 2012). The *To* is found primarily in the western half of the project area. Where present, the *To* acts as a primary aquifer and, generally, is saturated and yields sufficient quantities of groundwater for irrigation purposes. Areas of the *To* with the greatest abundance of groundwater occur where the Platte River or its ancestral drainages developed (Diffendal, 1995).

2.1.3 Cretaceous Geology

Both Upper and Lower Cretaceous units are present in the project area. The Upper Cretaceous bedrock formations are the *Kp, Kn*, *Kc* (CSD TH 24-A-51), *Kgg* (CSD TH 26-A-51 and TH 25-B-63), which lie unconformably over the *Kd*. Together these formations are comprised of interbedded to sandy shale, indurated to shaly chalk, thin layers of bentonite, limestone, and massive sandstone (Condra and Reed, 1959; Gutentag et al., 1984). These formations thin and pinch out to the east (Divine, 2012), but where present act as a lower confining unit to saturated Quaternary deposits. None of the Upper Cretaceous formations yield beneficial amounts of potable groundwater within the project boundaries. However,

some areas of eastern Nebraska, the *Kn*, where fractured, is known to yield water for irrigation purposes (Gutentag et al., 1984; Miller and Appel, 1997).

Underlying the Upper Cretaceous formations is the regionally extensive *Kd*. This formation is comprised primarily of massive to interbedded sandstone with ironstone and some argillaceous to slightly sandy shale (Condra and Reed, 1959). The sandstone in the *Kd* typically has low permeability and storage compared to the unconsolidated units overlying it. A hydraulic connection can exist in locations where the *Kd* is in contact with overlying saturated Quaternary deposits (Gutentag et al., 1984).

2.1.4 Jurassic and Triassic Geology

Strata considered to correlate with Jurassic and Triassic deposits have been identified in cuttings in western Nebraska. However, these units are not known to exist in eastern Nebraska (Condra and Reed, 1959).

2.1.5 Paleozoic System

Historic cross sections and lithologic logs from deep oil and gas wells allow for the identification of Paleozoic units in limited locations of the project area.

2.1.5.1 Permian Geology

Permian deposits, composed primarily of massive to bedded limestone, fossiliferous limestone that can be dolomitic with interbedded shale, evaporites, sandstone, and siltstone are present beneath southern and eastern Nebraska. Although some of these units crop out in southeast Nebraska, they are missing in the stratigraphic sequence immediately beneath the project area. This information on the strata's absence in the project area is based on stratigraphic selections described in Nebraska Oil and Gas Conservation Commission (NOGCC) test holes.

2.1.5.2 Carboniferous Geology

Carboniferous deposits, Upper (Pennsylvanian) and Lower (Mississippian) subsystems, are thought to underlie all of Nebraska except for a few square miles in the northeast part of the state (Condra and Reed, 1959). Undifferentiated deposits of the Carboniferous System include the Wabaunsee, Shawnee, Douglas, Pedee, Lansing, Kansas City, Bronson, Marmaton, Cherokee, Osage-Meramec, and Kinderhook Groups. Korus (2012) reports *[P* deposits that extend beneath parts of the project area are the undifferentiated Kansas City and Lansing Groups, and the undifferentiated Marmaton and Pleasanton Groups. Similar to the Permian deposits, these Carboniferous groups are comprised of massive to bedded and fossiliferous limestone that can be dolomitic with interbedded shale, evaporites, sandstone, and siltstone. Shale deposits can be substantial sequences that are a mixture including argillaceous, arenaceous, fissile, and/or limy type shale (Condra and Reed, 1959). The Kansas City and Lansing Groups are primarily inter-bedded limestone and shale (Hanson et al., 2012). In addition, the Kansas City, Lansing, Marmaton, and Pleasanton Groups are part of the Western Interior Plains confining system overlying the upper aquifer unit of the Western Interior Plains aquifer system- which includes the Kinderhook Group (Jorgensen et al., 1993; Signor et al., 1996).

2.1.5.3 Devonian Geology

Devonian deposits unconformably underlie Carboniferous through the southeastern third of Nebraska. The Devonian deposits are largely a sequence of limestones, dolomites, and shales that thin westward and northwestward and are absent over the Cambridge Arch (Condra and Reed, 1959). It is unknown to what extent Devonian rocks exist in the project area.

2.1.5.4 Silurian Geology

Silurian deposits underlie the east to southeast quarter of Nebraska and are thickest in the extreme southeast part of the State and then thin northward. While most Silurian rocks in Nebraska have been dolomitized, they act as an important groundwater reservoir in the Omaha, NE area (Condra and Reed, 1959).

2.1.5.5 Ordovician Geology

Ordovician deposits underlie parts of eastern Nebraska including the principle units of the Richmond and Trenton Groups. These deposits generally are oolitic and hematitic shales overlying dolomites. Similar to the Silurian deposits, they produce some groundwater in deep wells in the Omaha area. While the presence of groundwater from Ordovician deposits increases to the west, these water resources are highly mineralized (Condra and Reed, 1959).

2.2 Hydrogeologic Characteristics in the Quaternary System

A map showing the major streams in rivers within the project area is shown in Figure 2-4. Across much of the project area, stream-dissected glacial till have created a dendritic pattern of perennial and seasonal streams. The largest surface-water system in the project area is the Elkhorn River (U.S. Geological Survey, 2015) which flows easterly to southeast from the Sand Hills west of the project area to its confluence with the Platte River west of Omaha, NE. Mean annual discharge in 2013 at Norfolk, NE (USGS station number 06799000) was 287.3 cubic feet per second (ft^3/s) and 517.9 ft^3/s at West Point, NE. Tributaries to the Elkhorn River include the North Fork of the Elkhorn River near Pierce, NE (USGS station number 06799100; 2013, 34.3 ft^3/s), Logan Creek (USGS station number 06799445; 2013, at Wakefield, NE 84.8 ft^3/s; USGS station number 06799500; 2012, near Uehling, NE, 243 ft^3/s) (U.S. Geological Survey, 2015), and Maple Creek near Nickerson, NE (USGS station number 06800000, 34.3 ft^3/s), as well as many smaller streams. The North Fork of the Elkhorn River and Logan Creek drain southward and discharge into the Elkhorn River.

A limited number of surface-water impoundments are present in the project area, with the largest feature located at the Willow Creek State Recreation Area (700 acre flood control reservoir) southwest of Pierce, NE, and many other smaller lakes, sandpits, and reservoirs. Numerous sandpits and small lakes are located adjacent, or in close proximity, to the Elkhorn River or other major streams.

Regional groundwater-flow direction for the project area is primarily northeast to southwest (Bentall, 1971, Flowerday et al., 1998) and locally can be hydraulically connected to shallower aquifers or surface water systems (Stanton,et al. 2007). Groundwater levels are located at shallower depths in the alluvial valleys and at deeper depths under glaciated areas, and typically reach maximum depths from extensive

groundwater pumpage during the crop growing months. Groundwater levels typically return to shallower, pre-stress levels in the March to June timeframe. Annual depths of drawdown and recharge of aquifers highly depend on the type of aquifer (e.g., confined or unconfined), proximity of the aquifer to the land surface, and the magnitude of stress exhibited on the system during the pumping season, combined with the amount of recharge available to the aquifer. Groundwater under confined systems, such as in aquifers beneath glacial till, typically exhibits more drawdown than groundwater in unconfined systems that are present in alluvial settings.

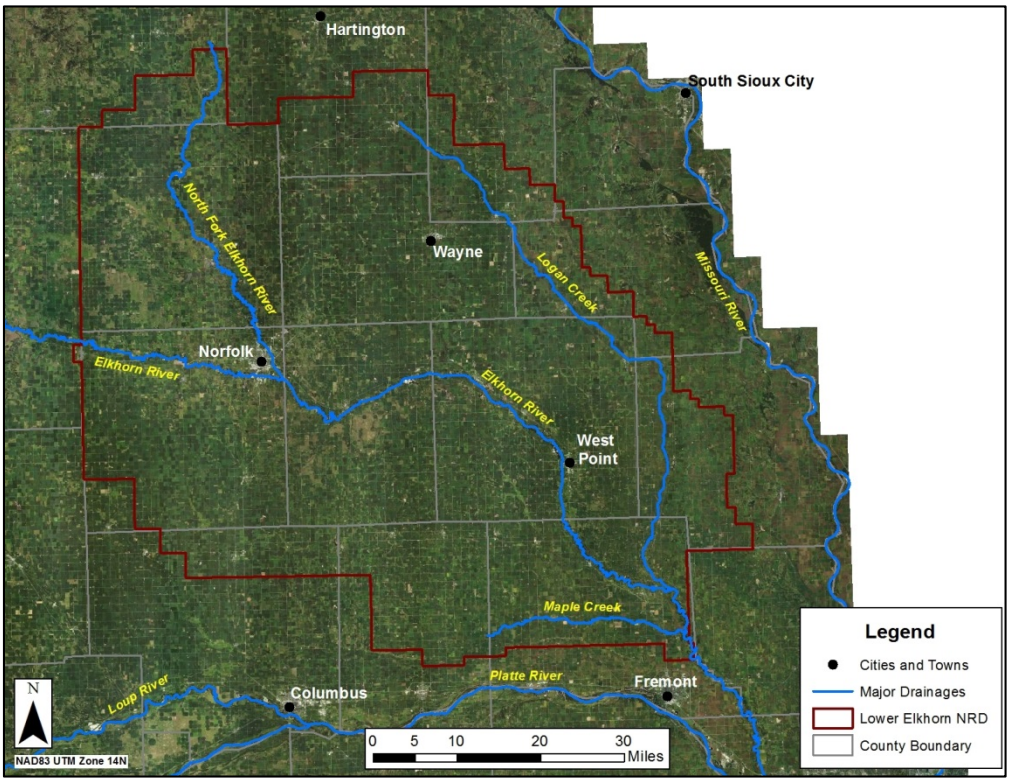


Figure 2-4: Map displaying the major streams and rivers within the project area.

Potentiometric gradients show groundwater movement from upland areas toward stream valleys. Hilly topography and complex heterogeneity within the glacial-drift terrain can create local flow systems (Gates et al., 2014). Contrasts of hydraulic conductivity within the principal aquifers of eastern Nebraska, including the Maha aquifer, can commonly cause significant vertical groundwater flow gradients (Summerside et al., 2001).

There are two principal Quaternary hydrogeologic units within the LENRD boundaries. The first are saturated alluvial deposits that make up the stream-valley (valley fill) aquifers. The second are glacial-drift aquifers which are alluvial and paleo-alluvial or paleo-glacial deposits of Plio-Pleistocene age that underlie till and loess deposits in the uplands and/or that make up the paleovalley deposits. Saturated Quaternary deposits in northeast Nebraska are a complex mixture of unconsolidated, saturated sand and gravel deposits. These saturated deposits can be confined to unconfined, deep to shallow, and/or regional and local, and, in places, interbedded with glacial till (Bentall, 1971; Miller and Appel, 1997;

Flowerday et al, 1998; Stanton et al., 2007). Stream-valley and glacial-drift systems locally can be hydraulically connected with other, similar systems and/or bedrock aquifers. In addition, aquifers in the project area are typically associated with modern or abandoned stream valleys or with elongated paleovalleys (Gates et al., 2014; Szilagyi et al., 2005). Alluvium near the glacial-till border, deposited from Platte River tributaries are Pliocene to Holocene in age (Diffendal, 1995). Table 2-1 contains summary information for each known aquifer (Quaternary through Cretaceous) within the area. Included in this table are the geologic system hosting the aquifer, aquifer thickness, a general discussion regarding the aquifer framework, groundwater flow system characteristics, and aquifer parameters.

The stream-valley aquifers yield groundwater at rates that support the widespread use of wells for irrigation and other industrial needs, specifically near the Elkhorn River, the North Fork of the Elkhorn, and the Logan and Maple Creeks. Most of the water in stream-valley or alluvial aquifers is under unconfined or water-table conditions with local confined conditions where overlying fine-grained sediments cap the aquifers. Stream-valley aquifers consist mostly of Holocene sand and gravel. The stream-valley sand and gravel deposits in many locations have been reworked from older glacial-drift deposits and are difficult to distinguish from glacial outwash (Miller and Appel, 1997). Locally, stream-valley aquifers can be hydraulically connected to underlying semi-consolidated or bedrock aquifers, such as the *To* or *Kd*. In much of the project area, stream-valley aquifers are associated with the High Plains Aquifer whose primary unit is the *To*.

Availability of groundwater in glacial-drift aquifers is highly variable. The potentiometric head in glacial-drift aquifers is often a composite surface. The aquifers are comprised of unconfined and confined systems due to the complex interbedding of deposits with varying permeability and large numbers of locally confining units (Miller and Appel, 1997). Consequently, groundwater in glacial-drift aquifers could be under confined conditions in one area and unconfined conditions in others. Results of a composite aquifer test conducted in a glacial-drift aquifer west of Oakland, NE indicated a transmissivity for a paleovalley aquifer of about 67,000 gpd/ft (9,000 ft^2/d) and a hydraulic conductivity of about 72 ft/day (U.S. Geological Survey, personal comm., 2009).

Recharge to stream-valley aquifers is largely from local precipitation, although additional sources of recharge can occur from downward percolation of irrigation waters or inflow from underlying permeable aquifers. Estimated regional mean annual recharge rates for stream valleys within the project area range from about 3.7 to 5.5 inches per year (in/year) with local annual recharge rates up to 6.4 in/year. In the uplands beyond the stream valleys, regional estimated annual recharge rates generally range from 2.4 to 5.5 in/year (Szilagyi et al., 2005). An analysis of statewide data determined that the total recharge for the Nebraska glaciated region averaged about 2.2 in/year (56 mm/year) Szilagyi and Jozsa, 2013; Gates et al., 2014) and was similar to rates determined using other methods (Nolan et al., 2007; Gates et al., 2014).

Table 2-1: Aquifers in Quaternary to Cretaceous-age stratigraphic units, eastern Nebraska

System	Series	Hydrologic unit	Maximum thickness, ft.
Quaternary	Holocene, Pleistocene	Aquifer in undifferentiated alluvial deposits	Generally less than 100 ft
Undifferentiated sand and gravel units in stream-valley systems. Stream-aquifer systems can be intermixed with older glacial sand and gravel making the deposits difficult to distinguish from older glacial outwash. Hydraulic head is typically unconfined. Recharge is principally from local precipitation and rapid if the source area is primarily sand and gravel. Wells are capable of yielding up to several thousand gallons per minute.			
Quaternary	Holocene, Pleistocene	Aquifer in undifferentiated glacial-drift deposits	Up to 300 ft
Undifferentiated sand and gravel units in glacial-drift aquifers. Hydraulic head generally under confined conditions, but can be under unconfined conditions elsewhere. Thickness of glacial-drift aquifers vary greatly. Comprised largely of sand and gravel from ancestral river channels or glacial outwash that became capped by till or loess. Some paleovalleys several miles wide and tens of miles long. Recharge mostly from precipitation infiltration or inflow from adjacent hydraulically connected aquifers. Wells yields are highly variable; some capable of up to several thousand gallons per minute but vary greatly by location. Isolated aquifers capable of sustaining good quality water only for domestic or stock purposes only.			
Tertiary	Miocene	Aquifer in Ogallala Group	Up to 300 ft, typically 100 ft or less, thins west to east
Generally unconsolidated to semi-consolidated sand, gravel, silt, and clay, underlying saturated Quaternary deposits. Serves as principal hydrogeologic unit of the eastern part of project area and of the High Plains aquifer. Hydraulic head unconfined to confined. Recharge largely from local precipitation or inflow from adjacent hydraulically connected aquifers. Irrigation wells capable of producing yielding several thousand gallons per minute.			
Cretaceous	Upper	Confining units of the Pierre, Niobrara, Carlile, or Greenhorn–Graneros Formations	Variable
Where present, largely serve as regional confining units. Niobrara Formation may produce water where secondary fracturing occurs.			
Cretaceous	Lower	Aquifer in Dakota Sandstone	Total thickness variable. Up to 600 ft in the project area (Miller and Appel, 1997).
Locally the Dakota can serve as an aquifer or as a confining unit. Aquifer generally located in loosely-cemented, medium- to fine-grained sandstone. Hydraulic head typically confined with local unconfined conditions encountered. Groundwater more potable in eastern part of state where Dakota underlies hydraulically connected with overlying saturated Quaternary deposits. Westerly, the Dakota becomes more mineralized and is found deeper beneath the subsurface. Where Dakota units lie in close proximity to the land surface, recharge is primarily from local precipitation, otherwise largely from inflow from adjacent hydraulically-connected aquifers. Sandstones capable of producing potable water to irrigation and municipal wells. Yields can be as much as 1,000 gallons per minutes locally (Miller and Appel, 1997).			

2.2.1 Aquifer Characteristics

The overall elevation of the water table within the project area is shown in Figure 2-5.

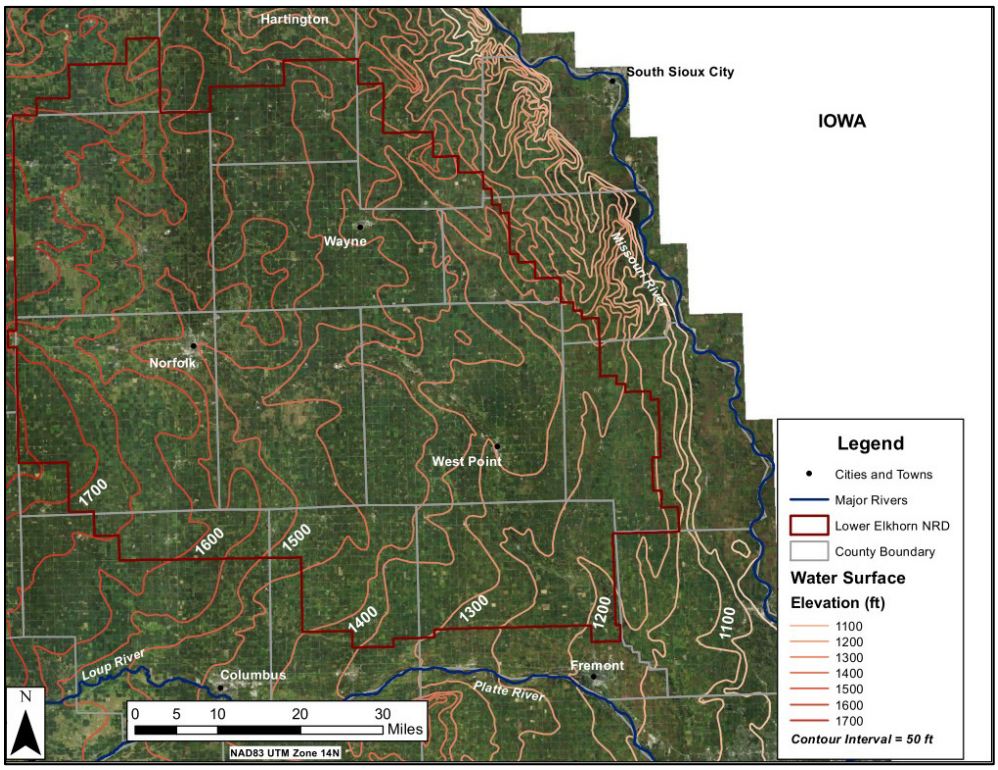


Figure 2-5: Elevation of ground water surface in the LENRD area.

Overall specific yield in the project area ranges from 0.05 to 0.20, with 0.15 to 0.20 in alluvium and unconfined systems in and adjacent to the Elkhorn and the North Fork of the Elkhorn River and 0.05 to 0.10 in confined areas underlying the till. Locally the specific yield is 0.20 in larger areas west and northwest of Wayne, NE. Conditions in the *To* generally range from 0.10 to 0.20 (Olafsen-Lackey, 2005a; Olafsen-Lackey and Summerside, 2005).

Lower and upper transmissivity values range from 20,000 gpd/ft (2,700 ft^2/d) to 150,000 gpd/ft (20,000 ft^2/d). Transmissivity values are predominantly 50,000 gpd/ft in alluvium and unconfined systems with local areas of 20,000 or 100,000 gpd/ft. One area along the Elkhorn River west of Norfolk, NE shows a transmissivity of 150,000 gpd/ft. Confined systems are predominantly 20,000 gpd/ft with local areas of 50,000 gpd/ft found northwest of Wayne (Olafsen-Lackey, 2005b; Olafsen-Lackey and Summerside, 2005). An aquifer test in the Oakland area indicated transmissivity values in the glacial-drift pale valley aquifer at approximately 67,000 gpd/ft. This value is of the same magnitude as the 50,000 gpd/ft reported previously for this area (Olafsen-Lackey and Summerside, 2005).

Lower and upper ranges of horizontal hydraulic conductivity in Madison and Pierce Counties were reported between 30 to 50 ft/d (Stanton et al., 2010). Horizontal hydraulic conductivity from a paleovalley aquifer test in the Oakland area show values in the glacial-drift aquifer of 100 to 120 ft/day

with a composite value of 72 ft/day. Overall, most horizontal conductivity values within the project area likely range from 10 ft/day in wells open to the *To* to 100 ft/day in wells screened in alluvium and glacial-drift sand and gravel.

2.2.2 Connectivity to Surface Water

Groundwater flow connectivity to surface water features is largely undocumented in the glaciated areas of eastern Nebraska. However, Peterson and Strauch (2007) report streamflow measurements at 531 sites conducted in November 2006 in the Elkhorn and Loup River basins and selected streams in the Niobrara and Platte River basins in north-central Nebraska. Most of these sites were located throughout the Elkhorn and Loup River basins, while 49 were located in the project area. Results at these 49 sites showed streamflow increasing in a downstream direction, indicating surface-water baseflow increasing downstream in these areas. Streamflow measurements were not collected in the highly glaciated areas of the project area.

Springs are common along several tributaries of the Elkhorn River. Logan Creek and Maple Creek basins experience spring flow and locally have drains installed to keep groundwater levels from flooding farmland. Many of the springs flow primarily during early- to mid-growing season in smaller tributaries; whereas they flow perennially in the major tributaries (Fredrick et al., 2006).

Goeke (2010) reports estimates of 50 to 90% of baseflow in the Elkhorn is made up of groundwater. This is thought to be due to less overland runoff in comparison to areas such as the Republican River basin, and much more groundwater contribution from coarse-textured, sandy soils. Overland flow in the project area is more prominent during periods of frequent precipitation and depending on antecedent conditions, can become groundwater recharge or continue as overland flow (Fredrick et al., 2006).

2.2.3 Connectivity to other Aquifers

Locally, Plio-Pleistocene deposits are hydraulically connected to shallower aquifers and streams (Gosselin et al., 1996). Where connected, the deeper aquifers can discharge into the shallow or into the streams and play an important role in water chemistry. The amount of communication between the two systems (stream-valley and glacial-drift) is unknown and not well understood. Communication, either horizontally or vertically, likely occurs temporally and/or aerially between stream-valley aquifers and glacial-drift aquifers. It is thought that temporal communication changes with increased pumping during irrigation season (June to September). During this time groundwater gradients change and communication between the two systems can be enhanced. Aerial communication also occurs as it is very possible that a glacial-drift aquifer (such as a paleovalley aquifer) could be in communication with an aquifer or stream at one location and not another.

2.3 Bedrock Aquifer Conditions

2.3.1 Extent/Structure of Aquifer

Two regionally extensive bedrock aquifers exist in the project area. The western half is underlain in areas by the High Plains aquifer, which is comprised primarily of the *To*. This unit extends eastward into the project area from the main body of the aquifer that extends from South Dakota to Texas. A smaller, isolated portion of the *To* covering around 150 square miles is present east of Norfolk, NE and underlies the city of Stanton. The High Plains aquifer in this area typically ranges from 25 to around 100 ft in thickness, but can approach 300ft in some locations (Gutentag et al., 1984).

The second regional bedrock aquifer system is composed of permeable sandstone within the *Kd* and is named the Maha aquifer (Miller and Appel, 1997; Gosselin et al., 2001). Ellis (1984) presented a structural map of the "Dakota aquifer system" (Maha) in eastern Nebraska which indicates the unit thinning eastward with a relatively steep gradient immediately beneath the project area (Figure 2-6). From west to east the unit thins from approximately 600 ft to about 100 ft. Regionally, the system thickens northwestward to over 900 ft in north-central Nebraska.

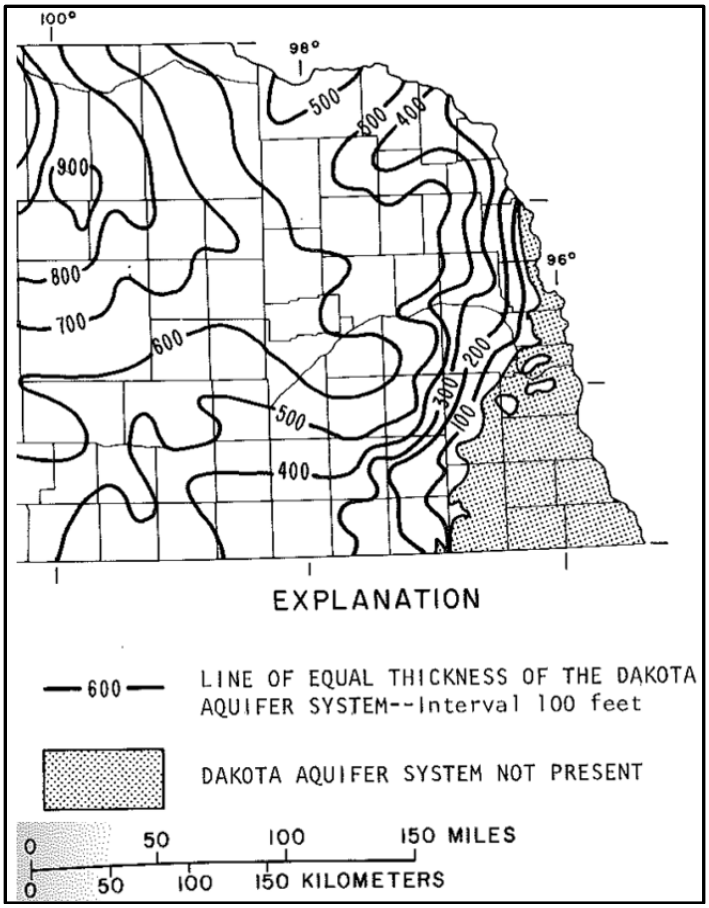


Figure 2-6: Thickness of the Dakota aquifer system/Maha aquifer in eastern Nebraska (Ellis, 1984).

2.3.2 Aquifer Characteristics

Available aquifer parameter data are based primarily on regional aquifer evaluations. Transmissivity within the Maha aquifer beneath the project area ranges from around 7,500 to 75,000 gpd/ft (1,000 to 10,000 ft^2/day). In the south-central portion of the project area, transmissivities exceed 75,000 gpd/ft (10,000 ft^2/day) beneath Colfax and northern Butler Counties (Helgesen et al., 1993).

Limited information exists on the porosity of the Maha aquifer. Helgesen et al. (1993) present a regional porosity map within this aquifer based on borehole geophysical logs and laboratory-derived values from literature originating in the oil and gas industry. The nearest contour to the project area, which sits north-south across central Nebraska indicates a porosity value of 0.3. Specific yield estimates for sandstones in the Dakota aquifer in Kansas and Colorado range from 0.1 to 0.2. No storage coefficient values for the confined portion of the system have been identified. However, a specific storage value of 9.5×10^{-7} per ft of aquifer was reported (Helgesen et al., 1993). Multiplying this by 400 ft, the average thickness of the Maha aquifer beneath of the project area, results in a storage coefficient of 3.8×10^{-4}.

2.3.3 Connectivity to Surface Water

Recharge to the Maha aquifer beneath the project area is limited to locations where the bedrock is close to the surface. This occurs most often along deeply-incised surface drainages. In other regions of the Maha aquifer, recharge occurs via infiltration of precipitation along exposed outcrops or shallow subcrops (Helgesen et al., 1993).

Connection to surface water features is limited to where outcrops of the *Kd* are in direct contact with streams at the surface or where permeable bedrock and or fractures are separated from the surface streams by highly permeable streambed sediments.

2.3.4 Connectivity to other Aquifers

Communication with overlying buried glacial outwash aquifers likely occurs, but specific quantification of these fluxes is not known. Gosselin et. al (2001) identified specific geochemical groundwater signatures that indicated a source from overlying glacial outwash. The degree of communication between the Quaternary and Cretaceous groundwater flow systems is not well understood and likely varies considerably due to local, ambient vertical gradients or through influence of pumping that occurs from both aquifers. Upward vertical communication of groundwater from underlying bedrock units is also possible. The highly saline sources in the Maha Aquifer southeast of the project area in Lancaster County have been attributed to sources from the underlying Paleozoic units (Helgesen et al., 1993).

2.4 Water Quality

A total of 740 historic water quality samples were analyzed from the USGS National Water Information System (NWIS) to determine water chemistry characteristics of the project area, — 423 water samples from 184 stream-valley or alluvial wells, 192 water samples from 62 glacial-fill wells, 32 water samples

from 31 High Plains wells, and 93 water samples from 29 wells tapping Cretaceous strata (most likely *Kd*). The water-quality samples from the High Plains wells likely were collected from wells screened in or open to the *To*. The High Plains aquifer also includes Quaternary deposits.

Median specific electrical conductance for all groundwater samples was 718 µS/cm (Table 2-2). Median calcium, sodium, chloride, and total dissolved solids (TDS) were 99.5, 25.9, 3.6, 39.0, and 448 mg/L, respectively (Figure 2-7 [sulfate not shown], Table 2-2). The maximum specific conductance value was 4,710 µS/cm and the maximum calcium, sodium, chloride, sulfate, and TDS concentrations were 527, 281, 110, 1,390, and 2,470 mg/L, respectively. The maximum value for both specific conductance and TDS was from a sample in a shallow glacial well open to loess or till deposits. Specific conductance values averaged 2,550 µS/cm from 5 water samples. So the 4,710 µS/cm reading would appear as or approach an outlier value.

Most groundwater in the area appears fresh. In some locations, larger specific conductivity, sulfate, and total dissolved solids concentrations were observed. The quality of the groundwater in the project area should pose no interference for interpretation of AEM data.

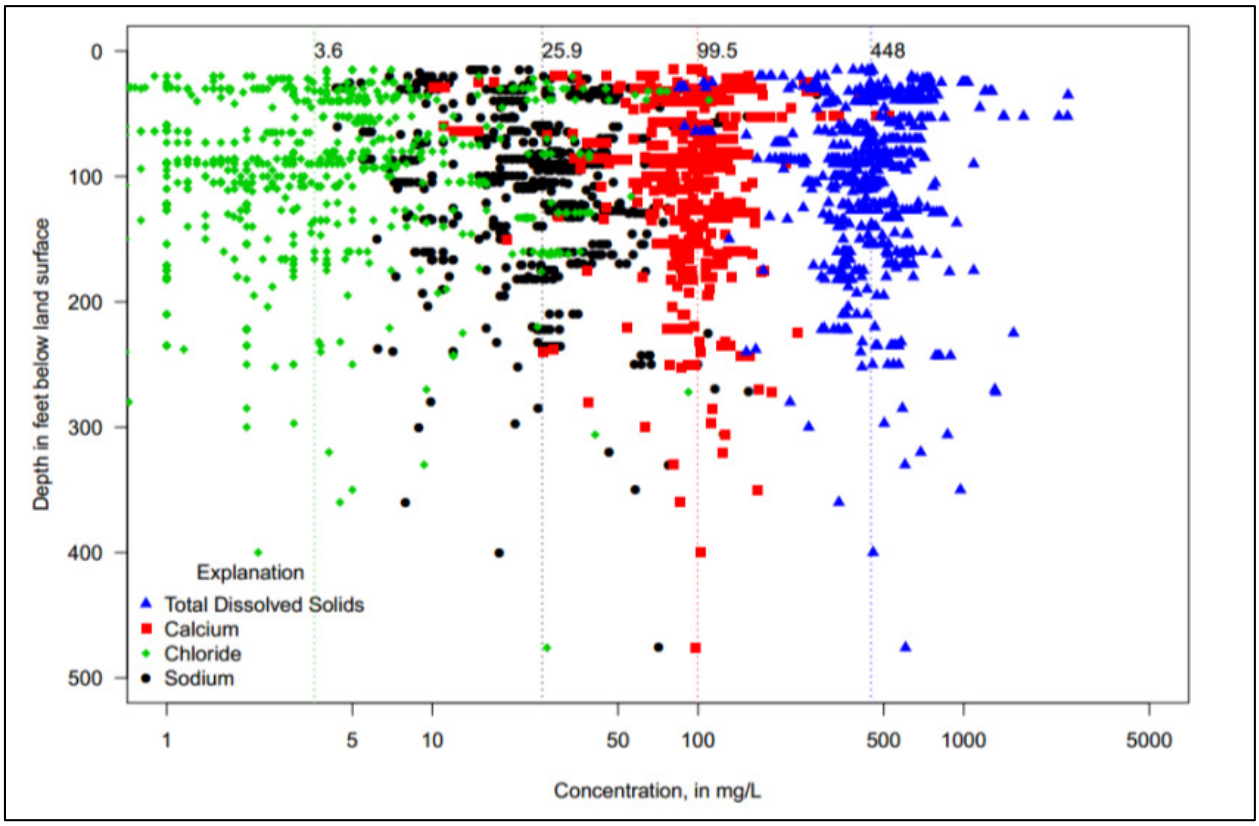


Figure 2-7: Concentrations (x-axis) of TDS, calcium, chloride, and sodium in water samples verses depth (y-axis) Data are from the US Geological Survey NWIS database.

Table 2-2: Statistical results of water-quality analyses from groundwater samples collected in or near the project area, from all wells. Units in milligrams per liter unless stated otherwise. Data are from the US Geological Survey NWIS database.

	Water temperature, in °C	Specific conductance, in uS/cm at 25°C	pH, in standard units	Dissolved oxygen	Total dissolved solids	
Minimum	8.30	96.0	5.90	0.10	85.0	
25th	11.5	597	7.00	0.20	355	
Median	12.5	718	7.20	0.70	448	
Mean	12.7	764	7.31	2.44	483	
75th	13.9	890	7.60	4.10	571	
Maximum	22.2	4,710	8.50	17.2	2,470	
NA's	18	2	83	384	23	
	Calcium	**Magnesium**	**Sodium**	**Sodium adsorption ratio**	**Potassium**	
Minimum	10.1	1.90	4.34	0.13	1.41	
25th	82.0	16.0	17.0.	0.40	4.1	
Median	99.5	21.9	25.9	0.60	6.34	
Mean	104	23.6	30.7	0.70	7.14	
75th	120	29.0	36.0	0.80	9.00	
Maximum	527	90.5	281	3.52	29	
NA's	0	0	0	0	18	
	Chloride	**Sulfate**	**Fluoride**	**Silica**	**Alkalinity, as $CaCO_3$**	**Bicarbonate, as $CaCO_3$**
Minimum	0.54	<0.18	0.09	8.20	30.3	37.0
25th	1.80	16.0	19.0	27.8	332	390
Median	3.60	39.0	23.0	33.0	360	440
Mean	8.08	77.9	28.7	32.5	371	465
75th	7.20	89.0	35.0	39.0	400	494
Maximum	110	1,390	93.0	66.8	1,020	1,240
NA's	2	1	213	200	454	628

2.4.1 Quaternary Aquifer Water Quality

Groundwater quality in both stream-valley and glacial-fill (Quaternary surficial aquifers) depends largely on overlying deposits. In areas where low yield deposits (i.e., till and loess) overlie aquifers, groundwater quality largely is less impacted than those where sand and gravel deposits are near land surface. In stream-valley systems, groundwater is in close proximity to the land surface and therefore subject to water quality changes due to land use/land cover.

Median specific conductance values from water-quality samples collected from stream-valley and glacial wells were 663 µS/cm (Table 2-3) and 779 µS/cm (Table 2-4), respectively. These values are lower than water samples from the *Kd* wells where median specific conductance was 845 µS/cm (Table 2-5). For

stream-valley wells the median calcium, sodium, chloride, sulfate, and total dissolved solids concentrations were 91.0, 20.2, 3.20, 40.0, and 413 mg/L, respectively (Table 2-3). The maximum specific conductance value was 1,930 µS/cm and the maximum calcium, sodium, chloride, sulfate, and TDS concentrations were 237, 116, 56.0, 875, and 1,540 mg/L, respectively (Table 2-3). For glacial-fill wells the median calcium, sodium, chloride, sulfate, and TDS concentrations were 104, 33.4, 3.37, 29.0, and 468 mg/L, respectively (Table 2-4). The maximum specific conductance value was 4,710 µS/cm and the maximum calcium, sodium, chloride, sulfate, and TDS concentrations were 527, 281, 110, 1,390, and 2,470 mg/L, respectively (Table 2-4).

Generally, median concentrations of ions and TDS in groundwater were slightly higher in water samples from glacial-fill wells than from stream-valley wells. Sulfate was the only exception where the stream-valley systems contained higher sulfate concentrations than glacially derived systems. This is thought to be due to the larger dissolved oxygen concentrations observed in the glacial systems than the stream-valley aquifers (2.50 to 0.65 mg/L). Small dissolved oxygen concentrations would help promote oxidation-reduction reactions (redox), which can increase SO_4 concentrations. Dissolved oxygen, however, was not collected in most stream-valley groundwater samples.

Table 2-3: Statistical results of water quality analyses from groundwater samples collected in or near the project area, from stream-valley/alluvial wells. Units are in milligrams per liter unless stated otherwise. Data are from the US Geological Survey NWIS database.

	Water temperature, in °C	Specific conductance, in µS/cm at 25°C	pH, in standard units	Dissolved oxygen	Total dissolved solids	
Minimum	8.30	96.0	5.90	0.10	85.0	
25th	11.7	513	7.10	0.20	320	
Median	12.9	663	7.30	0.65	413	
Mean	12.9	682	7.44	1.77	434	
75th	14.0	857	7.80	1.82	537	
Maximum	22.2	1,930	8.50	9.00	1,540	
NA's	10	2	17	343	13	
	Calcium	**Magnesium**	**Sodium**	**Sodium adsorption ratio**	**Potassium**	
Minimum	10.1	1.90	4.34	0.20	1.53	
25th	68.0	14.0	11.0	0.32	4.10	
Median	91.0	20.0	20.2	0.50	6.10	
Mean	93.7	21.8	23.4	0.55	6.42	
75th	120.	28.0	29.0	0.68	8.10	
Maximum	237.	89.0	116.	1.80	17.0	
NA's	0	0	0	0	9	
	Chloride	**Sulfate**	**Fluoride**	**Silica**	**Alkalinity, as $CaCO_3$**	**Bicarbonate, as $CaCO_3$**
Minimum	0.54	0.80	0.10	12.0	30.3	37.0
25th	1.70	15.0	0.30	29.8	330	44
Median	3.20	40.0	0.30	33.0	352	413
Mean	6.43	67.4	0.35	33.8	326	330
75th	5.94	84.8	0.40	39.0	392	437
Maximum	56.0	875	0.9	53.0	574	699
NA's	2	1	50	46	369	402

Table 2-4: Statistical results of water quality analyses from groundwater samples collected in or near the project area from glacial wells. Units are in milligrams per liter unless stated otherwise. Data are from the US Geological Survey NWIS database.

	Water temperature, in °C	Specific conductance, in µS/cm at 25°C	pH, in standard units	Dissolved oxygen	Total dissolved solids	
Minimum	9.10	418	6.50	0.10	261	
25th	11.6	687	6.90	0.40	408	
Median	12.3	779	7.00	2.50	468	
Mean	12.5	910	7.08	3.51	576	
75th	13.2	915	7.20	6.40	618	
Maximum	20.8	4,710	8.20	17.2	2,470	
NA's	7	0	48	24	1	
	Calcium	**Magnesium**	**Sodium**	**Sodium adsorption ratio**	**Potassium**	
Minimum	63.0	11.0	8.73	0.13	1.41	
25th	94.0	19.2	25.0	0.59	3.81	
Median	104	24.4	33.4	0.73	5.44	
Mean	122	27.7	42.8	0.94	7.67	
75th	117	29.9	47.0	1.04	8.98	
Maximum	527	90.5	281	3.52	29.0	
NA's	0	0	0	0	0	
	Chloride	**Sulfate**	**Fluoride**	**Silica**	**Alkalinity, as $CaCO_3$**	**Bicarbonate, as $CaCO_3$**
Minimum	<1.00	<0.18	0.17	14.9	158	192
25th	1.58	15.8	0.30	30.8	349	429
Median	3.37	29.0	0.40	33.6	368	477
Mean	7.76	78.5	0.49	32.5	402	545
75th	5.99	58.2	0.60	37.6	400	514
Maximum	110	1,390	1.22	50.4	1,020	1,240
NA's	0	0	104	104	30	123

Table 2-5: Statistical results of water quality analyses from groundwater samples collected in or near the project area from *Kd* wells. Units are in milligrams per liter unless stated otherwise. Data are from the US Geological Survey NWIS database.

	Water temperature, in °C	Specific conductance, in µS/cm at 25°C	pH, in standard units	Dissolved oxygen	Total dissolved solids	
Minimum	10.8	582	6.70	0.10	292	
25th	11.0	755	7.00	0.10	460	
Median	11.5	845	7.10	0.30	534	
Mean	13.4	880	7.10	0.48	559	
75th	13.0	938	7.20	0.60	602	
Maximum	143.	2,050	7.70	2.40	1,490	
NA's	1	0	18	11	9	
	Calcium	**Magnesium**	**Sodium**	**Sodium adsorption ratio**	**Potassium**	
Minimum	70.1	14.2	16.0	0.40	<3.21	
25th	104.	21.5	27.4	0.63	6.73	
Median	119.	23.7	32.7	0.73	9.90	
Mean	118.	25.3	43.3	0.94	9.74	
75th	129.	29.7	43.7	0.99	11.4	
Maximum	215.	47.0	186.	3.00	28.0	
NA's	0	0	0	0	9	
	Chloride	**Sulfate**	**Fluoride**	**Silica**	**Alkalinity, as $CaCO_3$**	**Bicarbonate, as $CaCO_3$**
Minimum	<1.00	<2.00	0.71	8.20	295	367
25th	2.00	68.9	0.87	12.7	317	372
Median	14.0	90.0	0.92	14.0	368	384
Mean	17.3	127.3	1.10	13.9	367	385
75th	25.6	157	1.10	14.8	417	392
Maximum	106	755	2.80	21.9	507	410
NA's	0	0	59	50	45	87

2.4.2 Bedrock Aquifer Water Quality

Water quality within the bedrock aquifers varies considerably by location and depth. Quality in the *Kd* in eastern Nebraska varies from (1) a Ca(±Mg)HCO_3-type water associated with local precipitation and where the Maha aquifer is unconfined, (2) a $CaSO_4$ and Ca-Na SO_4-type water associated with meltwater from Pleistocene glaciers and where the confining unit is thick, or (3) mixed waters of either $CaSO_4$ and Ca-Na SO_4-type water or NaCl-type water, which represent a possible interaction of the first

two types of water or recharge waters have been displaced by NaCl at depth (Gosselin et al., 2001). In the project area, water quality in the *Kd* likely is a $CaSO_4$ and Ca-Na SO_4-type water.

Groundwater can be potable in areas where the *Kd* is unconfined or subject to recharge from local precipitation. Dissolved-solids concentrations at these locations can be 500 mg/L or less (Ellis, 1984). Elsewhere, groundwater in the *Kd* can be highly mineralized (Stanton et al., 2007).

The median specific conductance value from water quality samples collected from *Kd* wells was 845 µS/cm (Table 2-5). As mentioned, this median value is higher than median specific conductance water samples from the stream-valley and glacial wells (Table 2-3 and Table 2-4). For *Kd* wells, the median calcium, sodium, chloride, sulfate, and TDS concentrations were 119, 32.7, 14.0, 19.0, and 534 mg/L, respectively (Table 2-5). These values are also larger than water samples collected from stream-valley and glacial wells. The single glacial well has large specific conductance and total dissolved solids values. Maximum calcium, sodium, chloride, sulfate, and TDS concentrations from *Kd* wells were 215, 186, 106, 755, and 1,490 mg/L, respectively (Table 2-5). Maximum calcium, chloride, and TDS concentrations were smaller than samples from glacial wells, a condition which is likely due to samples collected from the glacial well discussed above.

2.5 Water Use

The public supply wells within the LENRD area are displayed in Figure 2-8. The greatest concentrations of public wells are near the more populated area of northeast Madison County. Registered wells other than public supply wells are found throughout the LENRD, with irrigation wells being the most numerous. The densest concentrations of irrigation wells are in the western third of the LENRD as well as in smaller areas near the center of the district and along the district's southern boundary northwest of Fremont, NE. Domestic wells are scattered throughout the LENRD, with the greatest concentration surrounding the Norfolk, NE area.

Figure 2-9 displays the depth to groundwater in the registered wells. Relatively shallow groundwater (less than 50 ft below the subsurface) is present along the surface drainages that slope east/southeastward across the district, most notably along the Elkhorn and North Fork of the Elkhorn River valleys. Trending north/south through the middle of the project area is a zone of wells where groundwater is typically 150 ft deep or greater. In the western third of the area, depth to groundwater is slightly more variable, with the static levels typically between 50 and 150 ft. This variation could be due to wells tapping different aquifers, as the *To* is present in this area. Similar patterns in depth to groundwater are also apparent in the north-central portion of the project area.

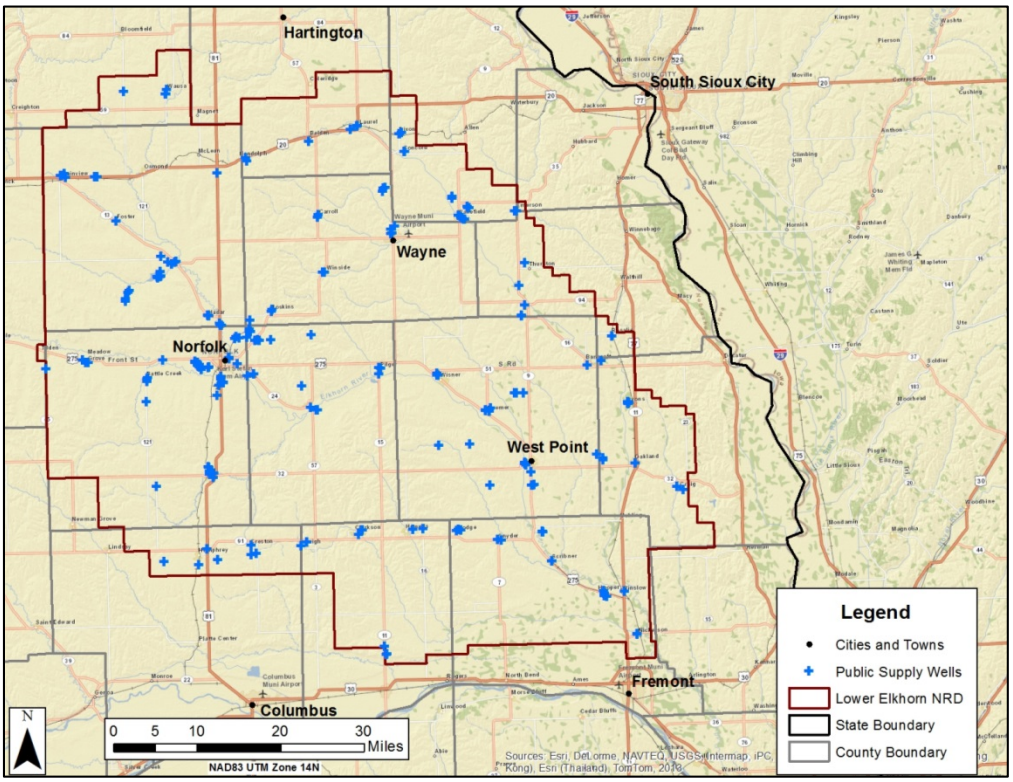


Figure 2-8: Public supply wells within the LENRD project area.

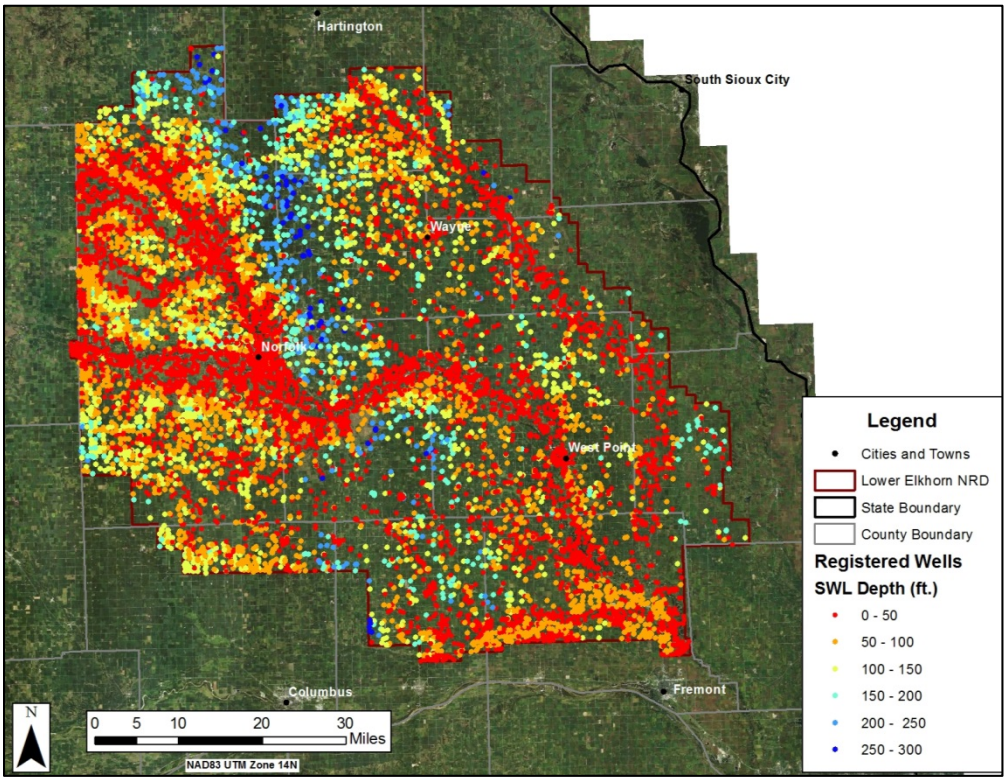


Figure 2-9: Registered wells within the LENRD area with depth to static water level indicated by color.

3 Additional Background Information

Various sources of background information were used to interpret the AEM data, which is discussed in Section 5.

3.1 Borehole Data

Borehole data for this project consisted of a combination of lithologic, stratigraphic, and downhole geophysical logs. Appendix 4 contains all borehole data utilized. The majority of borehole data were acquired from the Nebraska Statewide Test Hole Database (University of Nebraska-Lincoln School of Natural Resources, 2014), which contains information from boreholes drilled between 1930 and 2003 by the CSD and other cooperating agencies. CSD test holes drilled subsequent to 2003 were provided as a dataset directly from ENWRA and are shown in Figure 3-1. Additional borehole data were also acquired from the Nebraska Oil and Gas Conservation Commission (NOGCC) (Nebraska Oil and Gas Conservation Commision, 2008).

The CSD test holes are more numerous and generally much shallower than the oil and gas boreholes, typically less than 500 feet in depth and most do not extend far into bedrock material. Oil and gas boreholes can extend to depths greater than the AEM earth-resistivity models (discussed in Section 5). However, they typically lack the level of near-surface detail provided by the CSD boreholes.

The lithologic and stratigraphic borehole data from both the CSD and oil and gas boreholes were examined in detail. In some instances, specific interval descriptions were generalized to present both datasets with concise lithology and stratigraphy logs. A total of 695 lithology logs and 476 stratigraphy logs were obtained from CSD boreholes; 7 lithology logs and 7 stratigraphy logs were obtained from oil and gas boreholes. The locations of the boreholes containing lithology and stratigraphy data used are depicted in Figure 3-2 and Figure 3-3.

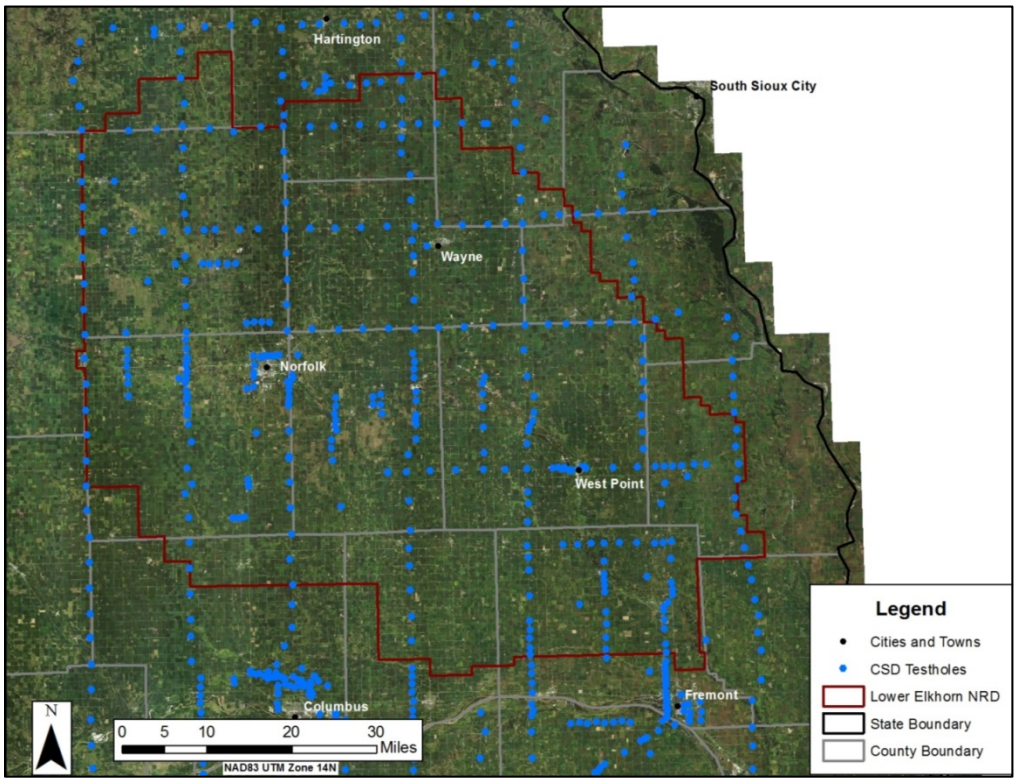


Figure 3-1: Locations of CSD tests holes drilled subsequent to 2003 that were provided by ENWRA.

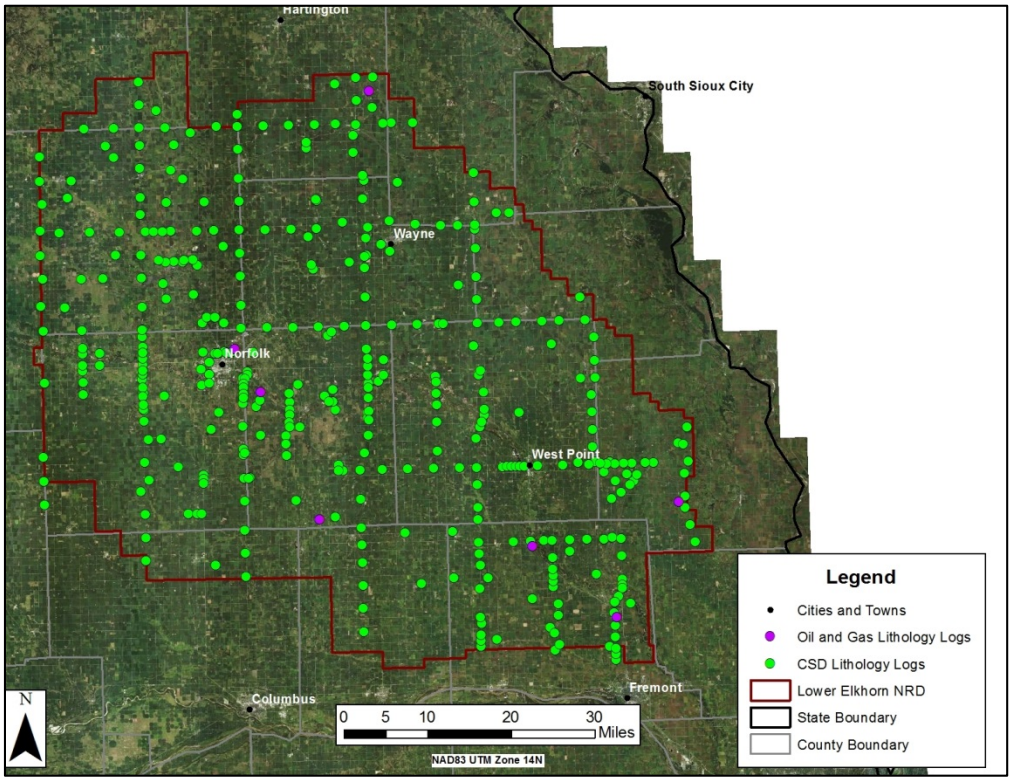


Figure 3-2: Locations of boreholes used containing lithologic information across the project area.

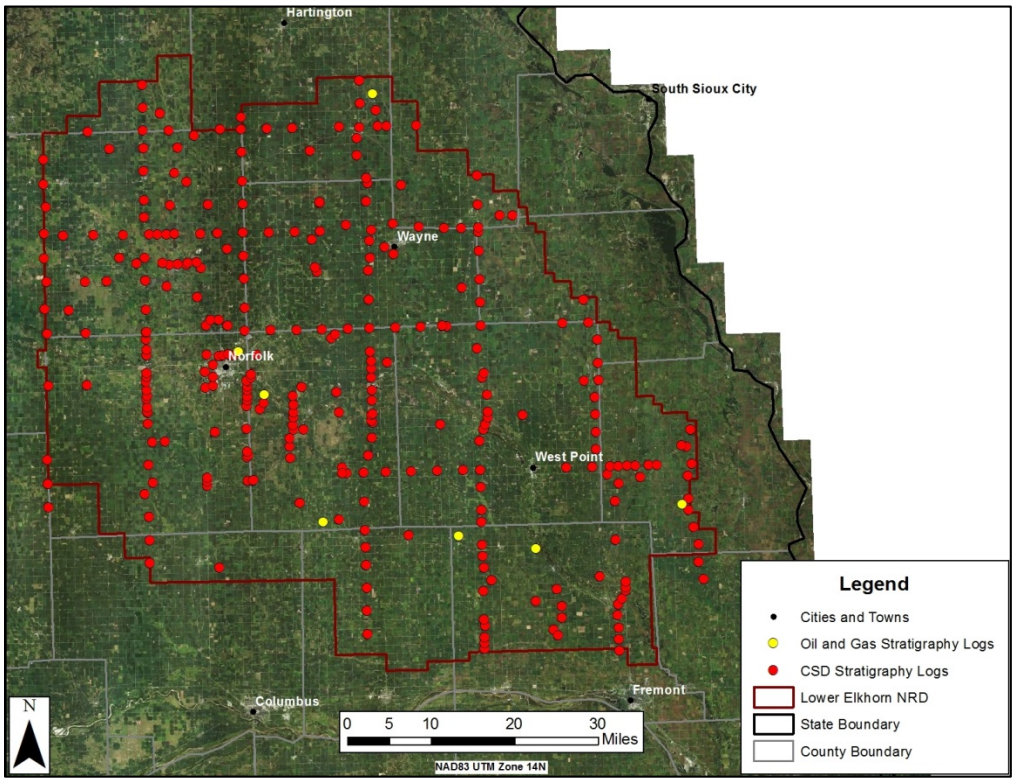


Figure 3-3: Locations of boreholes used containing stratigraphic information within the project area.

Geophysical logs from both CSD boreholes and oil and gas boreholes contained resistivity logs collected from a variety of downhole resistivity and/or induction tools. A total of 104 resistivity logs were obtained from CSD boreholes, with 80 of these logs from boreholes drilled prior to 1998 and 24 from wells drilled after 1998. The geophysical logs from boreholes drilled prior to 1998 usually contain both self-potential data and single-point resistivity data. The geophysical logs from boreholes drilled after 1998 contain a combination of natural gamma, self-potential, single-point resistivity, 16-inch normal resistivity, 64-inch normal resistivity, lateral resistivity, specific conductance of borehole fluid, and borehole fluid temperature data. Geophysical logs were also obtained from two oil and gas wells. These data were acquired as an image of the original paper log which was then converted into digital format. Oil and gas borehole geophysical logs contain a combination of self-potential, short normal resistivity, lateral resistivity, spherically-focused resistivity and deep- and medium-induction log data. A variety of factors can lead to geophysical borehole data that does not accurately measure subsurface physical properties, such as drilling fluid infiltration and improper or infrequent borehole tool calibration.

Each resistivity log was compared to the initial AEM data for correlation, both in magnitude of the reported resistivity values and structural interval delineation. A total of 34 resistivity logs were considered to be high quality data and were located in close proximity to the AEM flight lines. These logs were used as constraints in the final AEM data inversion (Section 4.6). The locations of the boreholes containing geophysical logs used in this project are displayed in Figure 3-4.

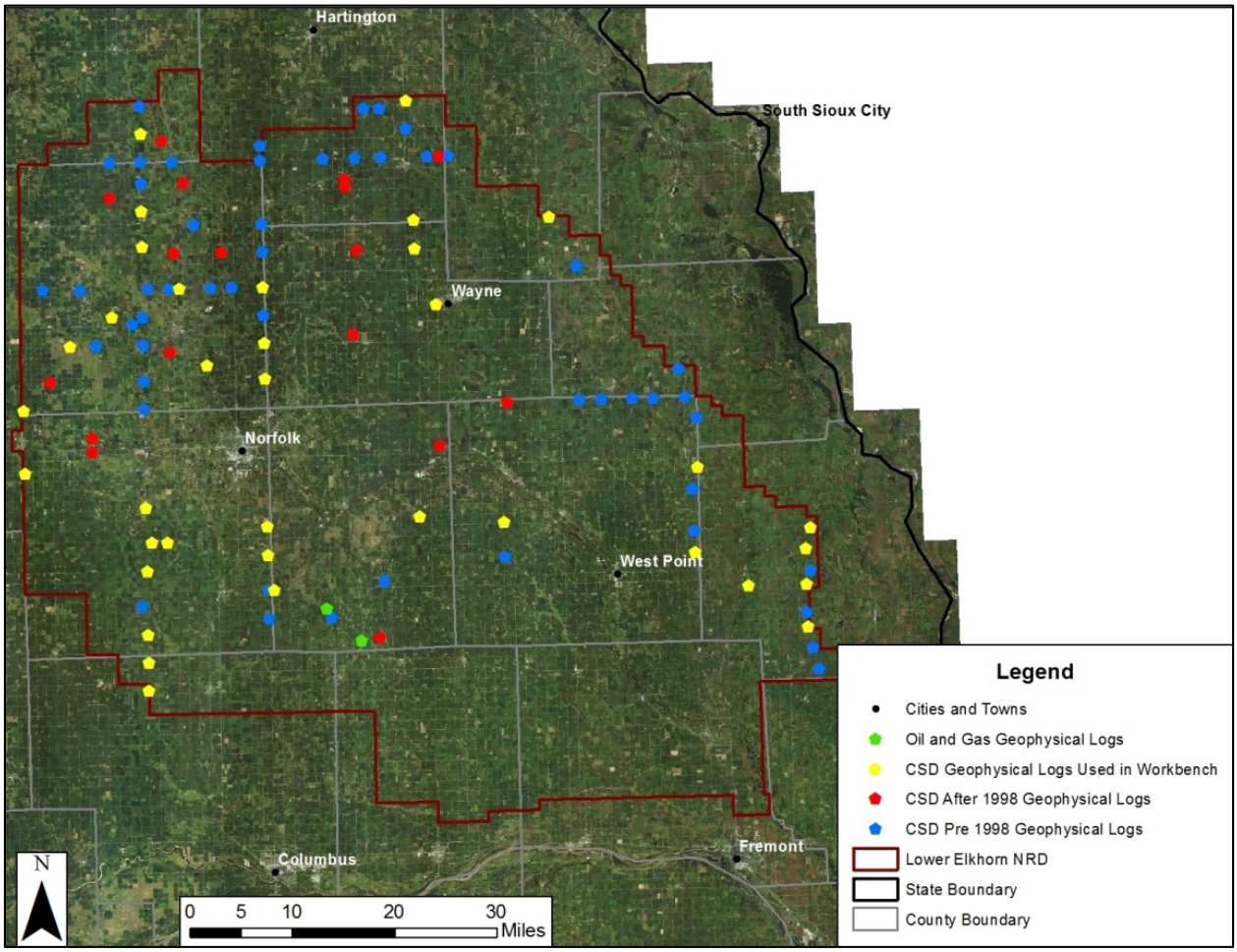


Figure 3-4: Locations of boreholes containing geophysical logs that were used in the analysis of the AEM data.

3.2 Historic Geologic Cross Sections

Ten published and previously unpublished geologic cross sections were digitized and geo-referenced (Divine et al., 2010; Korus et al., 2012). The quality of the sections ranged from rough pencil drafts to publishable quality. Table 3-1 lists the cross sections used and Figure 3-5 shows their locations.

Care was taken to properly place identified CSD borings as these were used to geo-reference each image. Each digitized image was broken up into smaller panels, where each panel began and ended at a known borehole. Encom Profile Analyst (PA) was used to apply positional data to each panel. Figure 3-6 shows an example of the digitized profiles in comparison with the original image that were used in the interpretation of the AEM results discussed in Section 5. Corel Draw was used to digitize and add color fill for each cross section (right side of Figure 3-6). Figure 3-7 displays the cross-sections in a 3D view produced in PA.

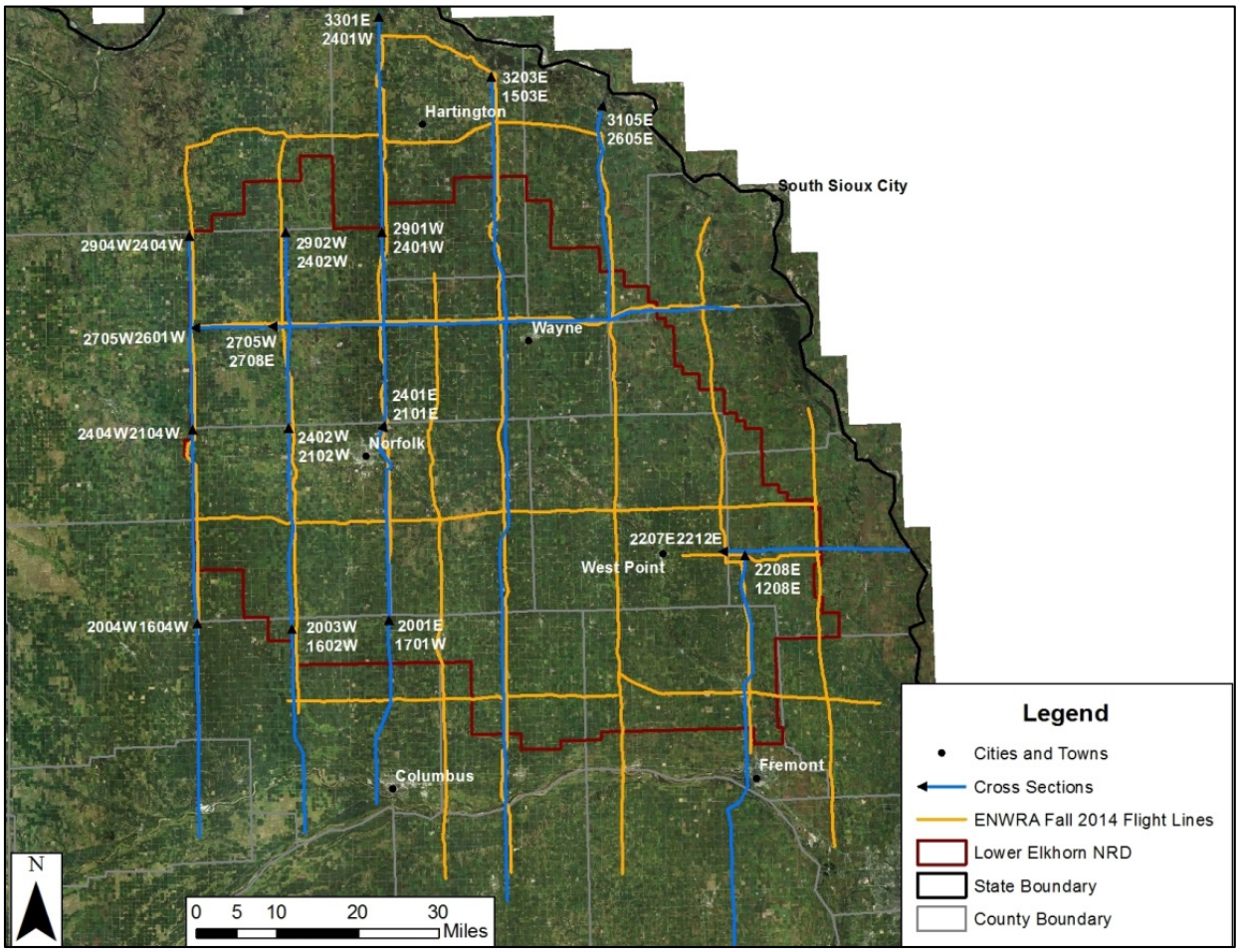


Figure 3-5: Locations of geologic cross sections across the project area.

Table 3-1: Geologic cross sections from CSD OFR-109 that were digitized and geo-referenced.

Image Name	Associated Line Name
Burt_gen.jpg	2207E2212E
Burt_Saunders.jpg	2208E1208E
Cedar_Madison.jpg	3301E2401W
Dixon_NS.jpg	3105E2605E
Madison_sections.jpg	2401W2101W (top profile)
Madison_sections.jpg	2402W2102W (middle profile)
Madison_sections.jpg	2404W2104W (bottom profile)
Pierece_3NS_EW.jpg	2705W2601W (D-D')
Pierece_3NS_EW.jpg	2901W2401W (C-C')
Pierece_3NS_EW.jpg	2902W2402W (B-B')
Pierece_3NS_EW.jpg	2904W2404W (A-A')
Pierece_Thurston.jpg	2705W2708E
Platte.jpg	2001W1701W (top profile)
Platte.jpg	2003W1602W (middle profile)
Platte.jpg	2004W1604W (bottom profile)

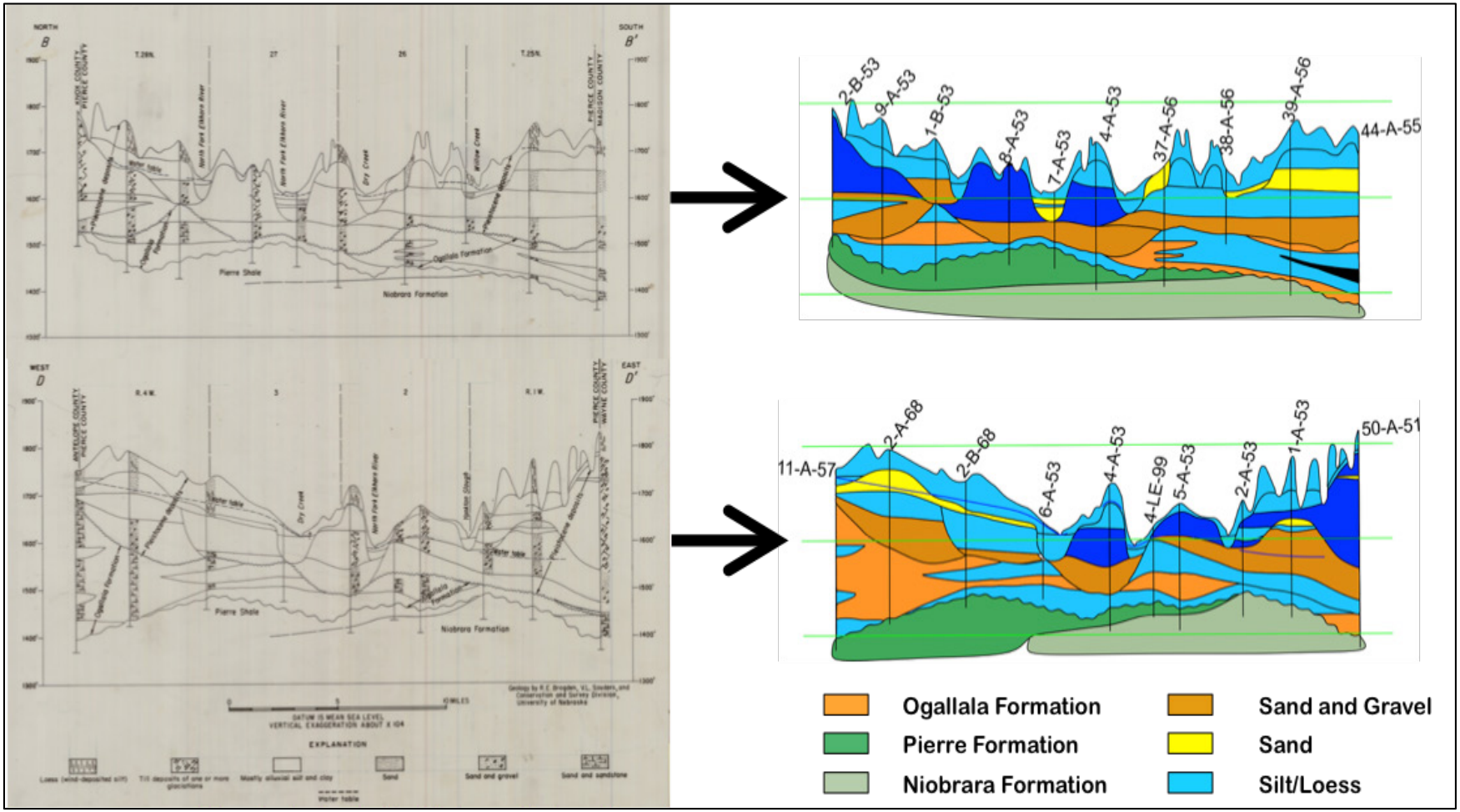


Figure 3-6: Original cross section from CSD OFR 109 (left) and the digitized cross section (right).

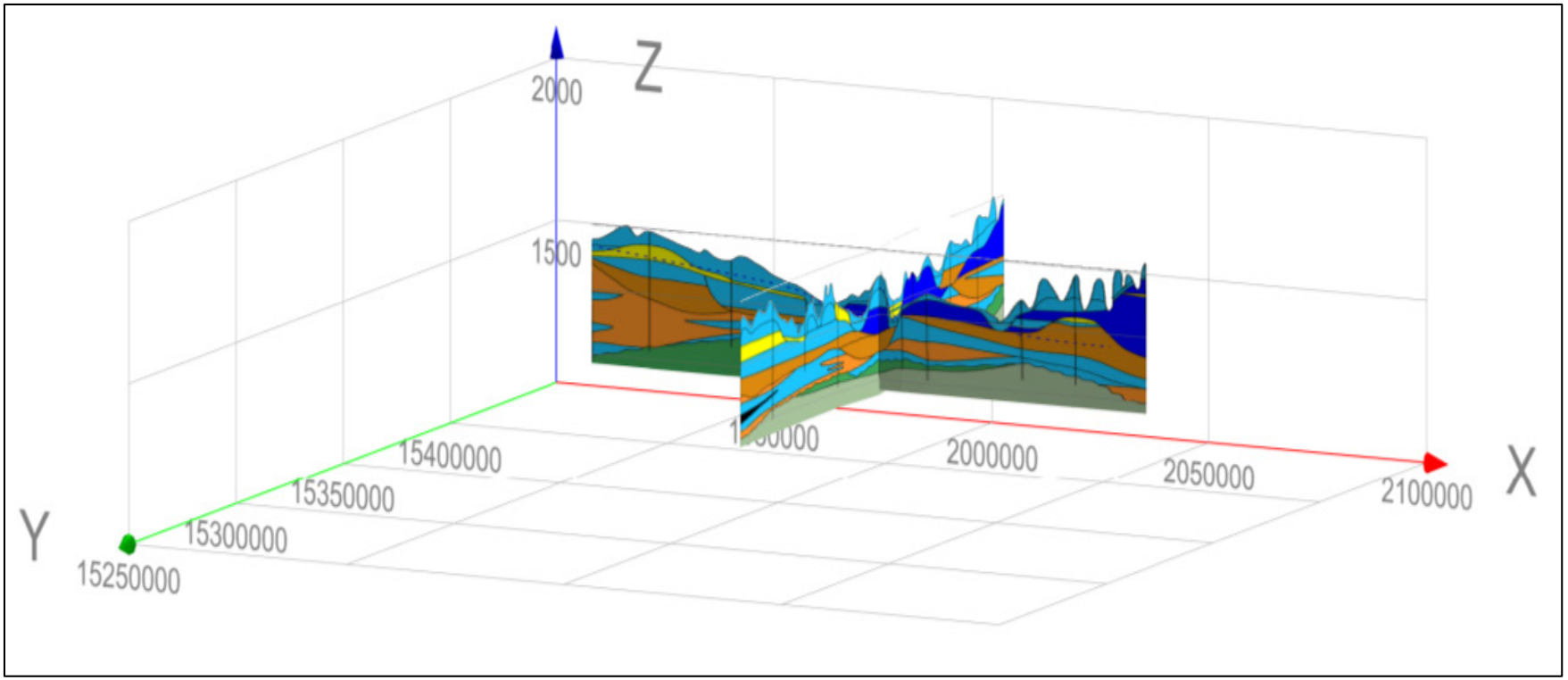


Figure 3-7: 3D view of geo-referenced geologic cross sections used to aid AEM interpretation.

4 Geophysical Methodology, Acquisition and Processing

4.1 Geophysical Methodology

AEM (Airborne Transient Electromagnetic (TEM)) surveys provide characterization of electrical properties of earth materials from the land surface downward using electromagnetic induction. Figure 4-1 gives a conceptual illustration of the airborne TEM method.

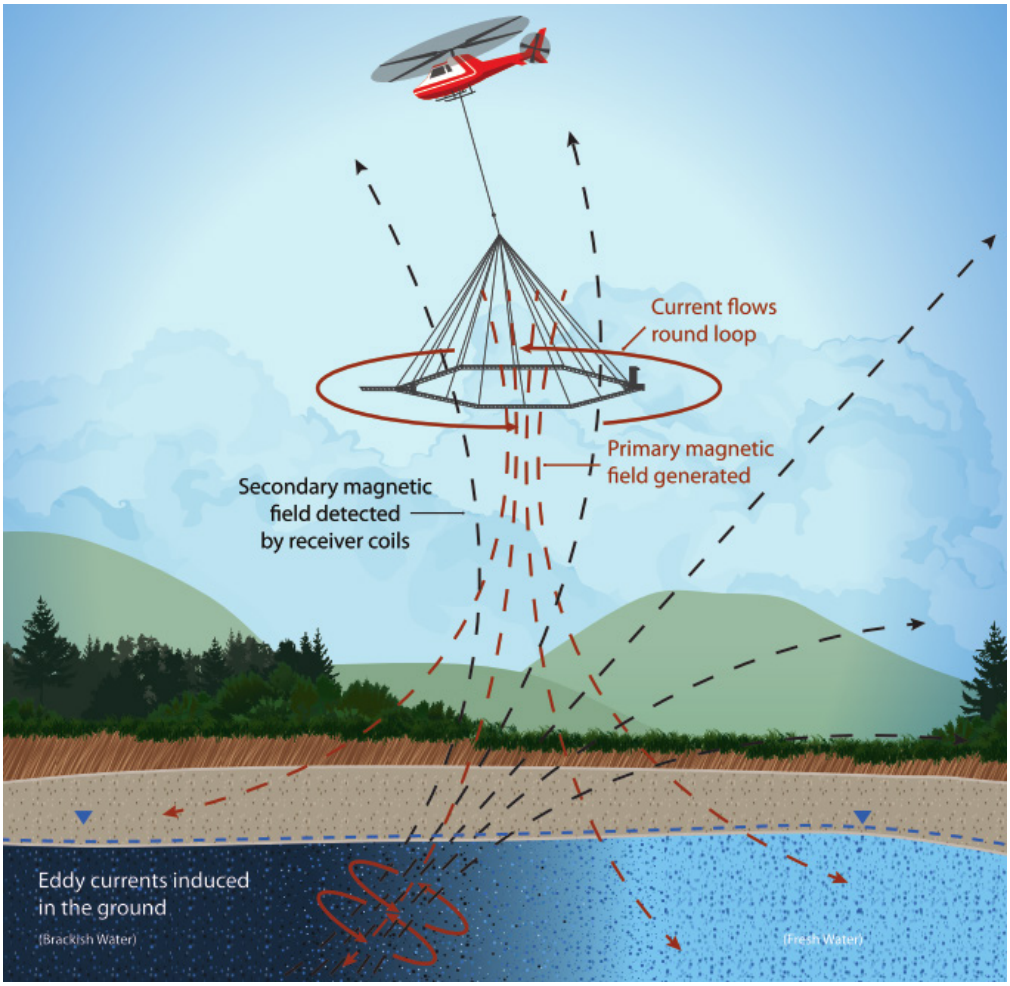
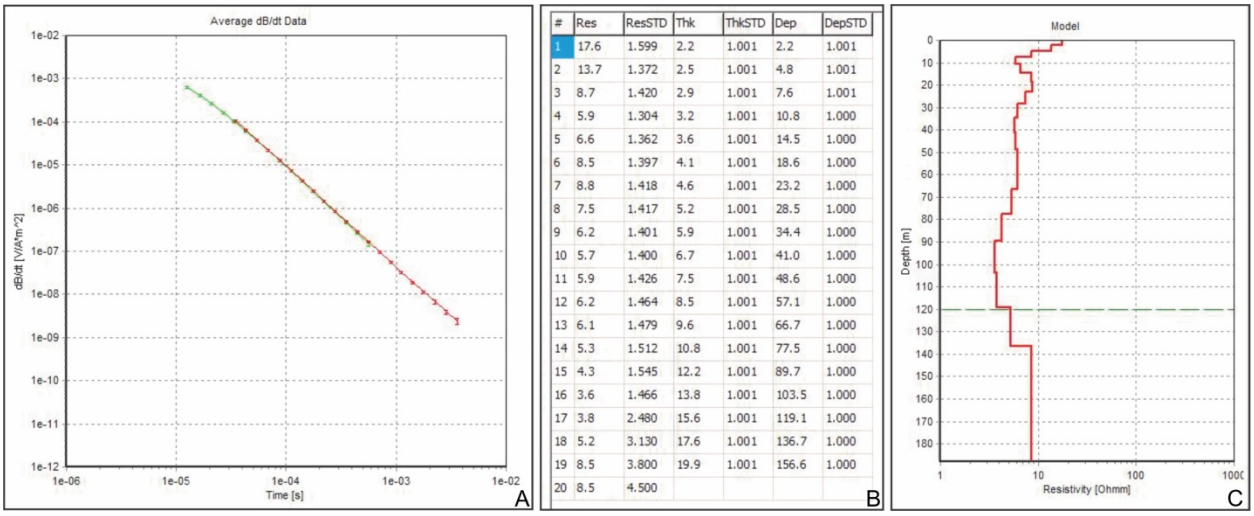


Figure 4-1: Schematic of an AEM survey.

To collect TEM data, an electrical current is generated with a large loop of wire consisting of multiple turns which is called the transmitter (Tx) coil. This current is switched off as abruptly as possible. The current dissipates and decays with time traveling deeper into the subsurface and spreading wider. The rate of dissipation is dependent on the electrical properties of the subsurface (controlled by the material composition of the geology including the amount of mineralogical clay, the water content, the amount of dissolved solids, the metallic mineralization, and the percentage of void space). At the moment of turnoff, a secondary current, which also begins to decay, is generated within the subsurface. The decaying secondary current generates a magnetic field, which in turn generates a current in a receiver

(Rx) coil, per Amperes Law. This current is measured at several different moments in time (time gates). From this current, the time rate of decay of the magnetic field (dB/dt) is determined. When compiled, these measurements become a "sounding" at that location. Each AEM measurement produces an electrical sounding at one point on the surface.

The sounding curves are numerically inverted to produce a model of subsurface resistivity as a function of depth. Inversion relates the measured geophysical data to probable physical earth properties. Figure 4-2 shows an example of a dual-moment TEM dB/dt sounding curve and the corresponding inverted electrical resistivity model.



#	Res	ResSTD	Thk	ThkSTD	Dep	DepSTD
1	17.6	1.599	2.2	1.001	2.2	1.001
2	13.7	1.372	2.5	1.001	4.8	1.001
3	8.7	1.420	2.9	1.001	7.6	1.001
4	5.9	1.304	3.2	1.001	10.8	1.000
5	6.6	1.362	3.6	1.001	14.5	1.000
6	8.5	1.397	4.1	1.001	18.6	1.000
7	8.8	1.418	4.6	1.001	23.2	1.000
8	7.5	1.417	5.2	1.001	28.5	1.000
9	6.2	1.401	5.9	1.001	34.4	1.000
10	5.7	1.400	6.7	1.001	41.0	1.000
11	5.9	1.426	7.5	1.001	48.6	1.000
12	6.2	1.464	8.5	1.001	57.1	1.000
13	6.1	1.479	9.6	1.001	66.7	1.000
14	5.3	1.512	10.8	1.001	77.5	1.000
15	4.3	1.545	12.2	1.001	89.7	1.000
16	3.6	1.466	13.8	1.001	103.5	1.000
17	3.8	2.480	15.6	1.001	119.1	1.000
18	5.2	3.130	17.6	1.001	136.7	1.000
19	8.5	3.800	19.9	1.001	156.6	1.000
20	8.5	4.500				

Figure 4-2: A) Example of a dB/dt sounding curve. B) Corresponding inverted model values. C) Corresponding resistivity earth model.

4.2 Utility Mapping

The primary source of noise in geophysical electromagnetic surveys are other electromagnetic devices that are part of typical municipal utility infrastructure. These include, for example, power lines, railroads, pipelines, and water pumps. Prior to AEM data acquisition in the LENRD, three types of utilities (pipelines, railroads, and power lines) were located. Various public power districts in Eastern Nebraska provided power line locations, in either a Google Earth ".kmz" or ".cad" format, that were then converted to a Geographic Information Systems (GIS) Arc shapefile format. Public power entities that provided power line location data included: Auburn Board of Public Works, Burt County Power District, Butler County Power District, Cedar-Knox Power District, City of Freemont, Cornhusker Public Power District, Cuming County Power District, Elkhorn Rural Public Power District, Lincoln Electric Systems, Loup Power District, Nebraska Public Power District, Nemaha-Marshall Electric Cooperative, Norris Public Power District, North Central Public Power District, Northeast Nebraska Public Power District, Omaha Public Power District, Polk County Rural Public Power District, Seward County Public Power District, and the Stanton County Public Power District.

A GIS Arc shapefile of railroads in Nebraska was downloaded from the United States Department of Agriculture's Natural Resource Conservation Service (United States Department of Agriculture, 2014) and a shapefile of the pipelines in Nebraska was purchased from Platts (Platts, 2014). Mapsof the three utilities, an example of which is shown in Figure 4-3, were exported in GeoTIFF and .kmz formats and used during data processing and interpretation.

The locations of the flight lines were initially organized into a regularly spaced grid and then to one with flight lights optimized in order to avoid electromagnetic coupling with the previously mentioned utilities.

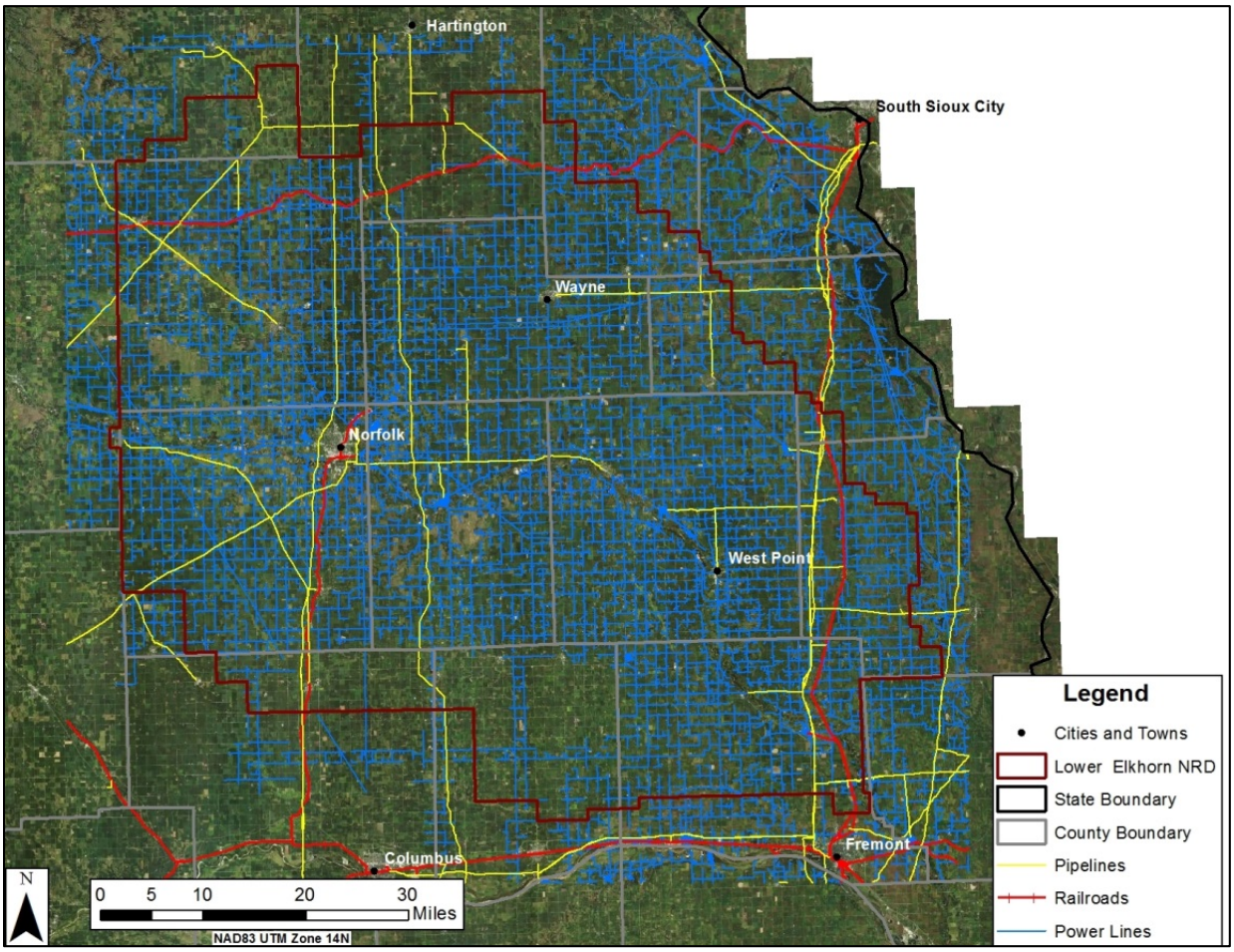


Figure 4-3: Map of the expected utilities across the project area.

4.3 AEM Survey Instrumentation

AEM data were acquired using the SkyTEM 508 (508) airborne electromagnetic system (SkyTem Airborne Surveys Worldwide, 2015). The 508 is a rigid frame, dual-moment (Low and High) transient airborne electromagnetic (TEM) system. The area of the 508 Tx coil is 5,769.5 ft2 (536 m2) and the coil contains eight (8) turns of wire. A peak current of 8.6 amps is passed through one turn of wire in the Tx for Low Moment measurements and a peak current of 127 amps is passed through the eight turns of

wire for High Moment measurements. This results in peak Tx Low and High magnetic moments of ~4,600 Ampere- meter squared ($A*m^2$) and ~540,000 $A*m^2$, respectively.

The SkyTEM 508 system utilizes an offset Rx positioned slightly behind the Tx resulting in a 'null' position which is a location where the intensity of the primary field from the system transmitter is minimized. This is desirable because you want to minimize the amplitude of the primary field at the Rx to maximize the sensitivity of the Rx to the secondary fields. The SkyTEM 508 multi-turn Rx coil has an effective area of 1,130 ft^2 (105 m^2). In addition to the Tx and Rx that constitute the TEM instrument, the SkyTEM 508 is also equipped with a Total Field magnetometer and data acquisition systems for both of these instruments. The SkyTEM 508 also includes two each of laser altimeters, inclinometers/tilt meters, and differential global positioning system (DGPS) receivers. Positional data from the frame mounted DGPS receivers are recorded by the AEM data acquisition system. The magnetometer includes a third DGPS receiver whose positional data is recorded by the magnetometer data acquisition system. Figure 4-4 gives a simple illustration of the SkyTEM 508 frame and instrument locations. The image is viewed along the +z axis looking at the horizontal x-y plane. The axes for the image are labeled with distance in meters. The magnetometer is located on a boom off the front of the frame (right side of image). The Tx coil is located around the octagonal frame and the Rx Coil is located at the back of the frame (left side of image).

The coordinate system used by the 508 defines the +x direction as the direction of flight, the +y direction is defined 90° to the right and the +z direction is downward. The center of the transmitter loop, mounted to the octagonal SkyTEM frame is used as the origin in reference to instrumentation positions. Table 4-1 lists the positions of the instruments (in feet) and Table 4-2 lists the corners of the transmitter loop (marked with red circles in Figure 4-4).

The DGPS and magnetometer mounted on the frame of the SkyTEM508 require the use of base stations, which are located on the ground and are positioned in an area with low cultural noise. Data from the magnetometer and DGPS base stations were downloaded each day after the end of the day's AEM flights. The DGPS and magnetometer base stations were placed at the Universal Transverse Mercator (UTM) coordinate system locations listed in Table 4-5. The horizontal geodetic reference used is North American Datum of 1983 (NAD83 in feet). All elevations are from USGS's National Elevation Dataset, referenced to the North American Vertical Datum of 1988; with feet as the unit of measurement.

For this LENRD survey, the 508 was flown at an average speed of 50.0 mi/hr (80.5 kilometers/hr) at an average flight height of 141.4 ft (43.1 m) above land surface using the sling-load cargo system of an AS350 FX2 helicopter. The higher than usual flight height was due to tree heights along the flight lines. Figure 4-5 displays pictures of the 508 on the ground and in operation.

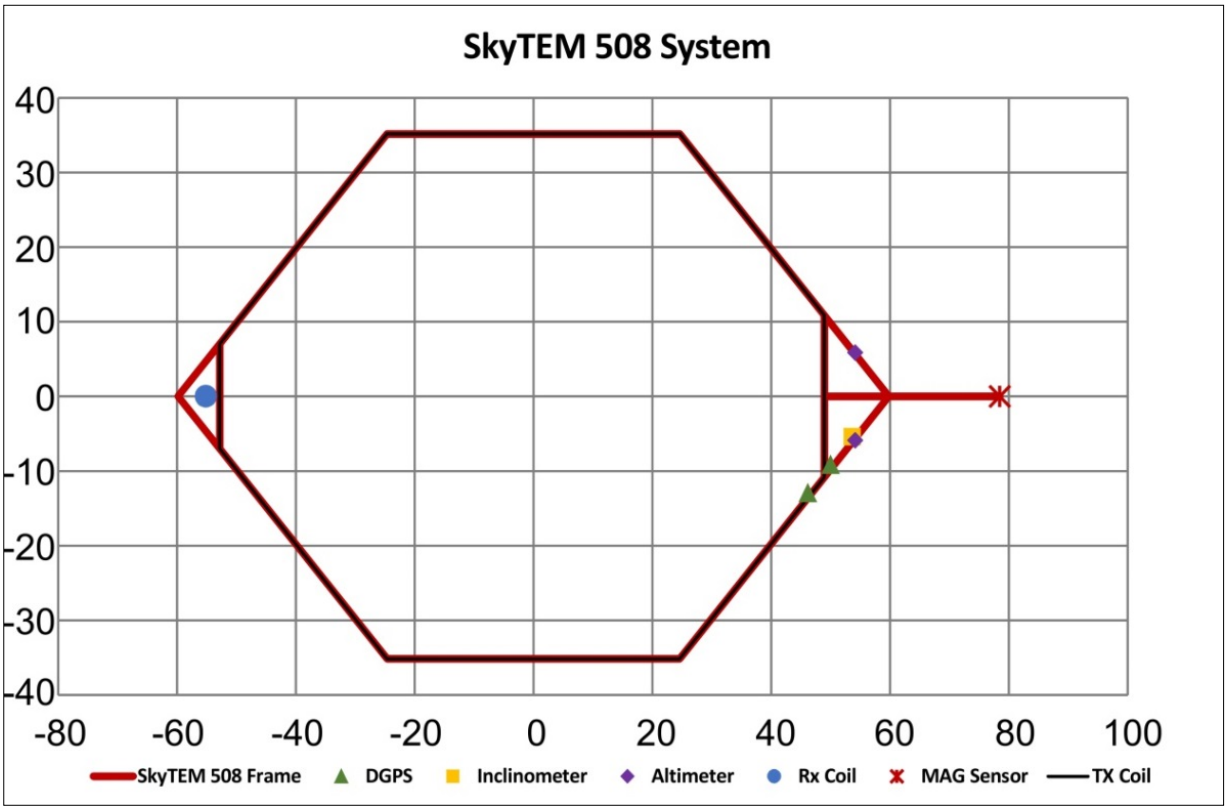


Figure 4-4: SkyTEM 508 frame including instrumentation locations and X and Y axes.

Table 4-1: Positions of instruments on the SkyTEM508 frame, using the center of the frame as the origin in feet.

	DGPS 1	DGPS 2	Inclinometer 1	Inclinometer 2	Altimeter 1	Altimeter 2	MAG Sensor	Rx Coil
X	50.00	46.16	53.64	53.64	54.13	54.13	79.79	-55.12
Y	9.15	12.96	5.38	5.38	5.87	-5.87	0.00	0.00
Z	-0.52	-0.52	-0.39	-0.39	-0.39	-0.39	-1.51	-6.56

Table 4-2: Positions of corners of the SkyTEM508 transmitter coil, using the center of the frame as the origin in feet.

Tx Corners	1	2	3	4	5	6	7	8
X	24.64	48.95	48.95	24.64	-24.64	-52.82	-52.82	-24.64
Y	35.17	10.86	-10.86	-35.17	-35.17	-6.99	6.99	35.17

Table 4-3: Locations of magnetic field base station instruments.

Instrument	Easting (ft.)	Northing (ft.)	UTM Zone
Magnetometer Base Station 1	2067151	15254064	14 N
Magnetometer Base Station 2	2065339	15255616	14 N
DGPS Base Station	2065311	15255605	14 N



Figure 4-5: Photos of the SkyTEM508 system.

4.4 Data Acquisition

All SkyTEM systems are calibrated to a ground test site in Lyngby, Denmark prior to being used for production work (HydroGeophysics Group Aarhus University, 2010; HydroGeophysics Group Aarhus University, 2011; Foged et al., 2013). The calibration process involves acquiring data with the system hovering at different altitudes from 16.4 to 164 ft (5 to 50 m) over the Lyngby site. Acquired data are processed and a scale factor (time and amplitude) is applied so that the inversion process produces the model that approximates the known geology at Lyngby.

For the LENRD survey, upon installation of the navigational instruments in the helicopter and assembly of the SkyTEM508 system, several test flights were flown in Nebraska to ensure that the equipment was operating within technical specifications. Initial survey set-up procedures included measurement of the transmitter waveforms, verification that the receiver was properly located in a null position, and verification that all positioning instruments were functioning properly. High altitude tests, used to verify system performance, were flown once at the beginning of the survey and repeated throughout the survey. In the field, visual quality control of the operational parameters for the EM and magnetic field

sensors including current levels, positioning sensor dropouts, acquisition speed, and system orientation were conducted with proprietary SkyTEM software following each flight.

Airborne data were collected over the survey grids across the project area from 11 – 19 October 2014 and approximately 1,471 line-miles (2368 line-kilometers) were acquired. Various airports and state parks were used as landing and refueling locations. These are shown in Table 4-4. Table 4-5 lists the locations, dates, and total line miles and corresponding line-kilometers flown for each block investigated in this project. A limited number of flight lines overlapped the daily flights lines are shown in Figure 4-6.

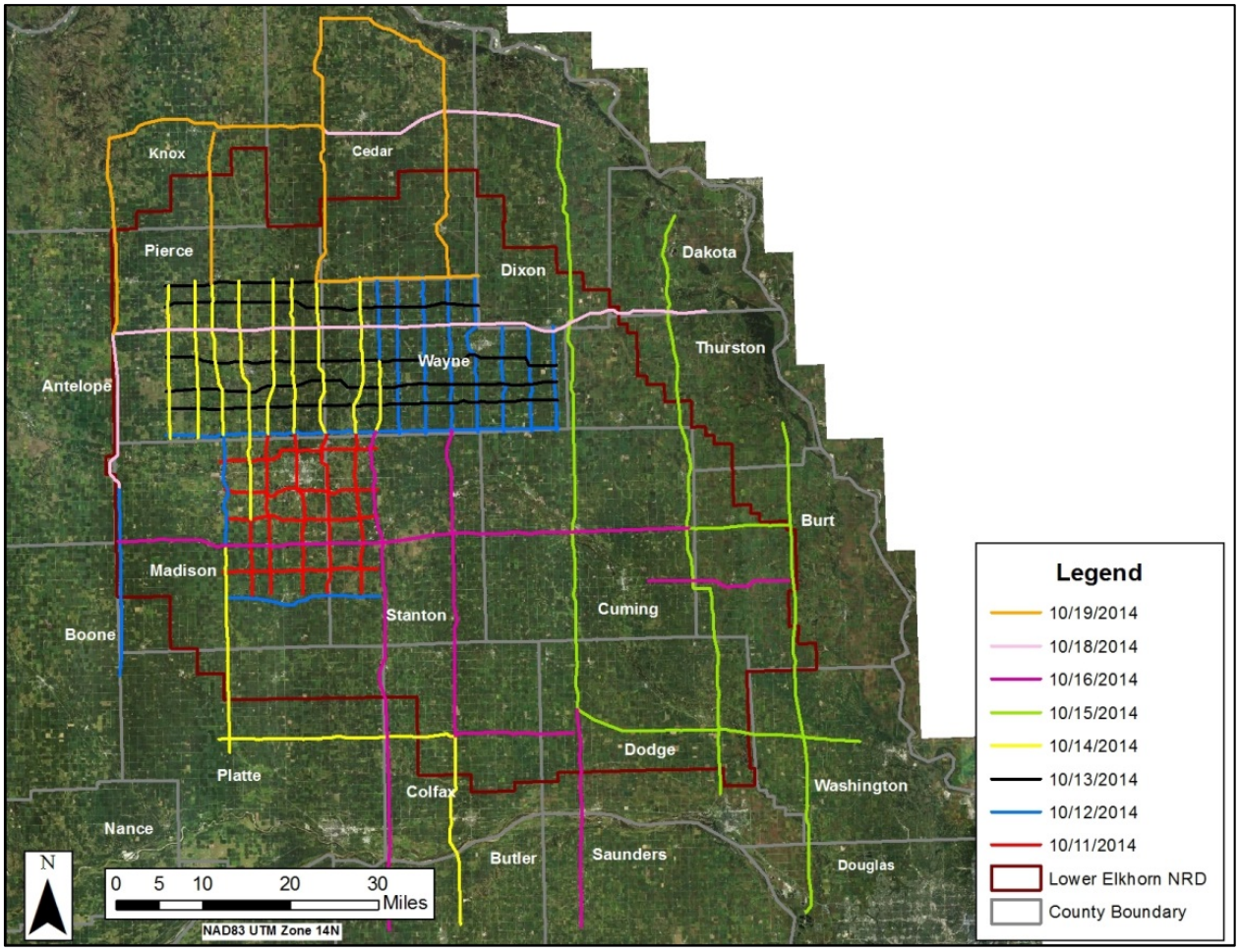


Figure 4-6: Flights lines as collected, organized by date.

Table 4-4: Airports and state parks used for landing and refueling by date of acquisition.

Date	Flight Number	Area Working
10/11/2014	1	Norfolk, NE
10/11/2014	2	Norfolk, NE
10/11/2014	3	Norfolk, NE
10/12/2014	1	Norfolk, NE
10/12/2014	2	Norfolk, NE and Wayne, NE
10/12/2014	3	Wayne, NE
10/13/2014	1	Wayne, NE
10/13/2014	2	Wayne, NE
10/14/2014	1	Wayne, Ne and Pierce, NE (Willow Creek State Park/Rec Area)
10/14/2014	2	Pierce, NE (Willow Creek State Park/Rec Area) and Norfolk, NE
10/14/2014	3	Norfolk, NE and Fremont, NE
10/15/2014	1	Fremont, NE and South Sioux City, NE (Powder Creek State Park/Rec Area)
10/15/2014	2	South Sioux City, NE (Powder Creek State Park/Rec Area) and Fremont, NE
10/15/2014	3	Fremont, NE and Tekamah, NE
10/16/2014	1	Tekemah, NE and Norfolk, NE
10/16/2014	2	Norfolk, NE and David City, NE
10/16/2014	3	Norfolk, NE and David City, NE
10/17/2014		
10/18/2014	2	Norfolk, NE and Martin Field, NE
10/18/2014	2	Martin Field, NE and Hartington, NE
10/19/2014	1	Hartington, NE
10/19/2014	1	Hartington, NE

Table 4-5: Production log displaying the number of production flights conducted on each day and total line miles and kilometers surveyed.

Date	Production Flights	Line-mi	Line-km
10/11/2014	3	154.2	248.2
10/12/2014	3	215.2	346.3
10/13/2014	2	193.3	311.1
10/14/2014	3	205.8	337.2
10/15/2014	3	139.7	224.8
10/16/2014	3	173.8	279.7
10/18/2014	1	76.7	123.4
10/19/2014	2	66.5	107.0
	Total:	1225.2	1977.7

4.5 Data Processing

4.5.1 Primary Field Compensations

A standard SkyTEM data acquisition procedure is that the acquired raw data are sent to SkyTEM in Denmark for Primary Field Compensations (PFC) prior to continued data processing by XRI (Schamper et al., 2014). The primary field of the transmitter affects the early recorded time gates, which in the case of the Low Moment, are helpful in resolving the near surface resistivity structure of the ground. The Low Moment uses a saw-tooth waveform which is calculated and then used in the PFC correction to correct the early time gates.

4.5.2 Automatic Processing

The AEM data collected by the 508 were processed using Aarhus Workbench version 4.2.7.2 (HydroGeophysics Group Aarhus University, 2011).

Automatic processing algorithms provided within the Workbench program are initially applied to the AEM data. GPS locations were filtered using a stepwise, second-order polynomial filter of 9 seconds with a beat time of 0.5 seconds, based on flight acquisition parameters. The AEM data are corrected for tilt deviations from level and so filters were also applied to both of the tilt meter readings with a median filter of 3 seconds and an average filter of 2 seconds. The altitude data were corrected using a series of two polynomial filters. The lengths of both eighth-order polynomial filters were set to 30 seconds with shift lengths of 6 seconds. The lower and upper thresholds were 1 and 100 meters, respectively.

Trapezoidal spatial averaging filters were next applied to the AEM data. The times used to define the trapezoidal filters for the Low Moment were 1e-5 sec, 1e-4 sec, and 1e-3 sec with widths of 5, 8 and 10 seconds. The times used to define the trapezoid for the High Moment were 1e-4 sec, 1e-3 sec, and 1e-2 sec with widths of 8, 10, and 20 seconds. The trapezoid sounding distance was set to 2.5 seconds and the left/right setting, which requires the trapezoid to be complete on both sides, was turned on. The spike factor and minimum number of gates were both set to 25% for both soundings. Lastly, the locations of the averaged soundings were synchronized between the two moments.

4.5.3 Manual Processing and Laterally-Constrained Inversions

After the implementation of the automatic filtering, the AEM data were manually examined using a sliding two minute time window. The data were examined for possible electromagnetic coupling with surface and buried utilities and metal, as well as for late time-gate noise. Data affected by these were removed. An example of locating areas of EM coupling with pipelines or power lines, and recognizing and removing coupled AEM data in Aarhus Workbench is shown in Figure 4-7 and Figure 4-8 respectively.

After manual processing, the AEM data were then inverted using a Laterally-Constrained Inversion (LCI) algorithm (HydroGeophysics Group Aarhus University, 2011). The profile and depth slices were

examined, and any remaining electromagnetic couplings were masked out of the data set. Examples of two inversions, one without EM coupling and the other with EM coupling, are shown in Figure 4-9.

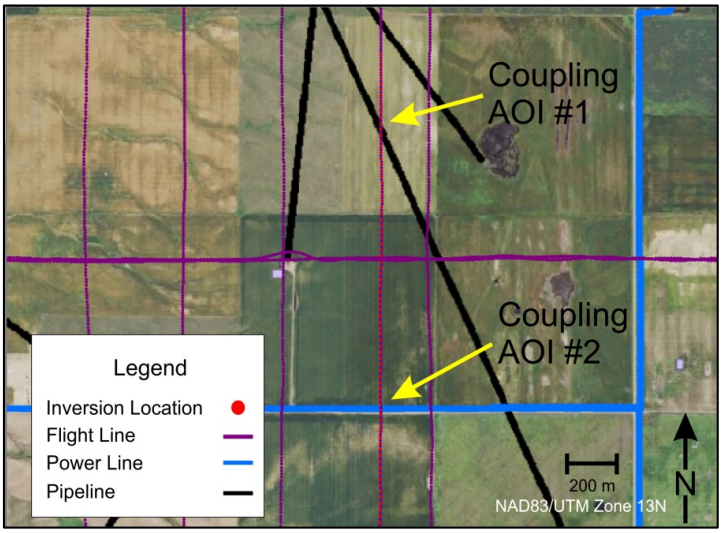


Figure 4-7: Example locations of EM coupling with pipelines or power lines.

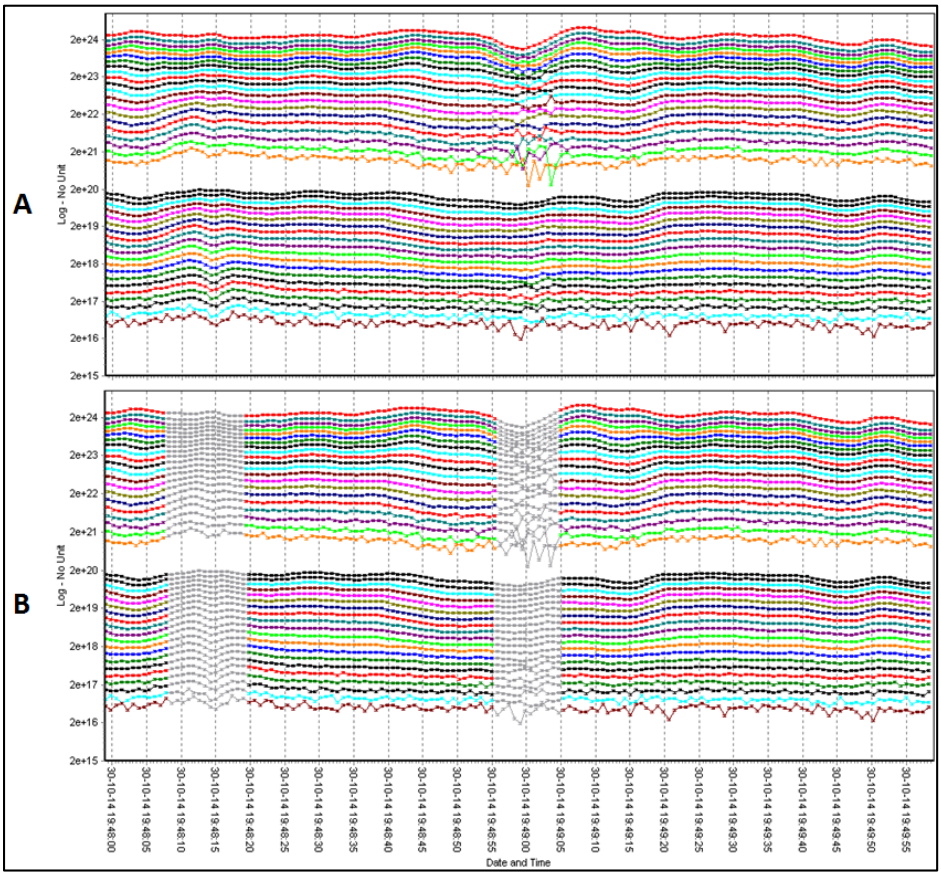


Figure 4-8: A) AEM data affected by coupling, shown in Figure 4-7, in Aarhus Workbench editor. The top group of lines is the Low Moment and the bottom is the High Moment. B) AEM data with area affected by coupling removed.

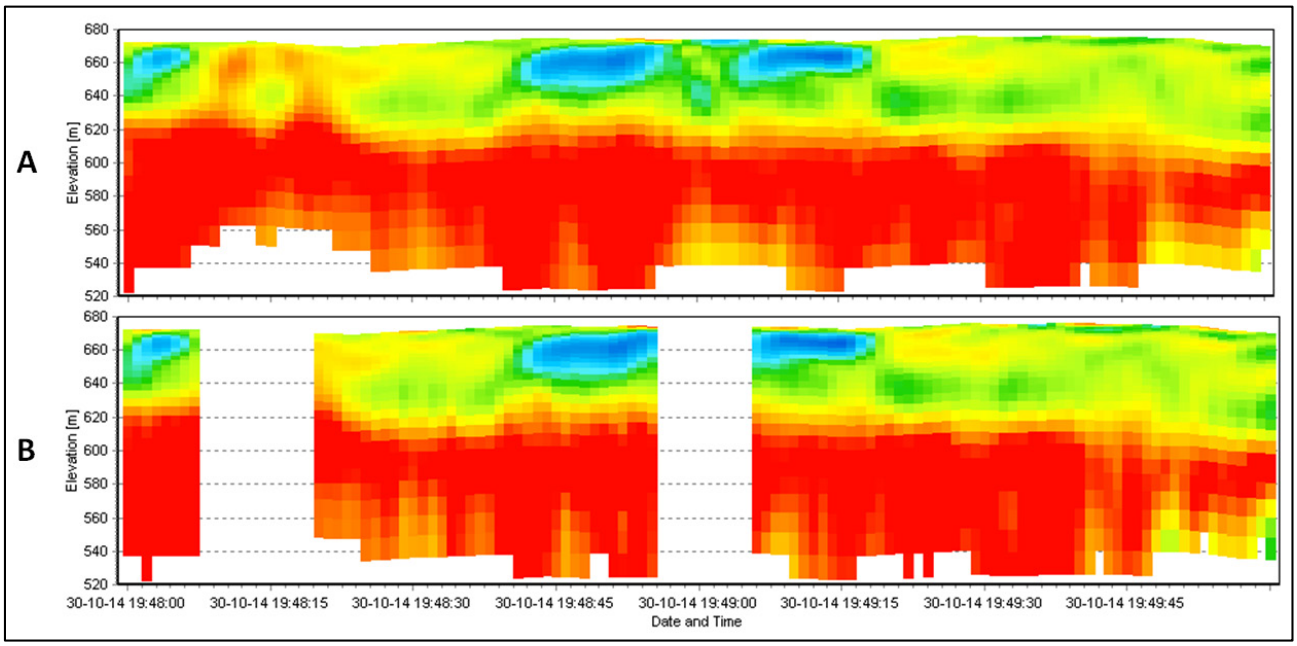


Figure 4-9: A) Inversion results where AEM data affected by coupling with pipelines and power lines were not removed. B) Inversion results where AEM data affected by coupling were removed.

4.5.4 Power Line Noise Intensity (PLNI)

The PLNI channel assists in identifying possible sources of noise from power lines. The PLNI is produced by performing a spectral frequency content analysis on the raw received Z-component SkyTEM data. For every Low Moment data block, a Fourier Transform (FT) is performed on the latest usable time gate data. The FT is evaluated at the local power line transmission frequency (60 Hz) yielding the amplitude spectral density of the local power line noise. The PLNI data for the LENRD survey area are presented in Figure 4-10. Pipelines, unless they are cathodically-protected, are not mapped by the PLNI.

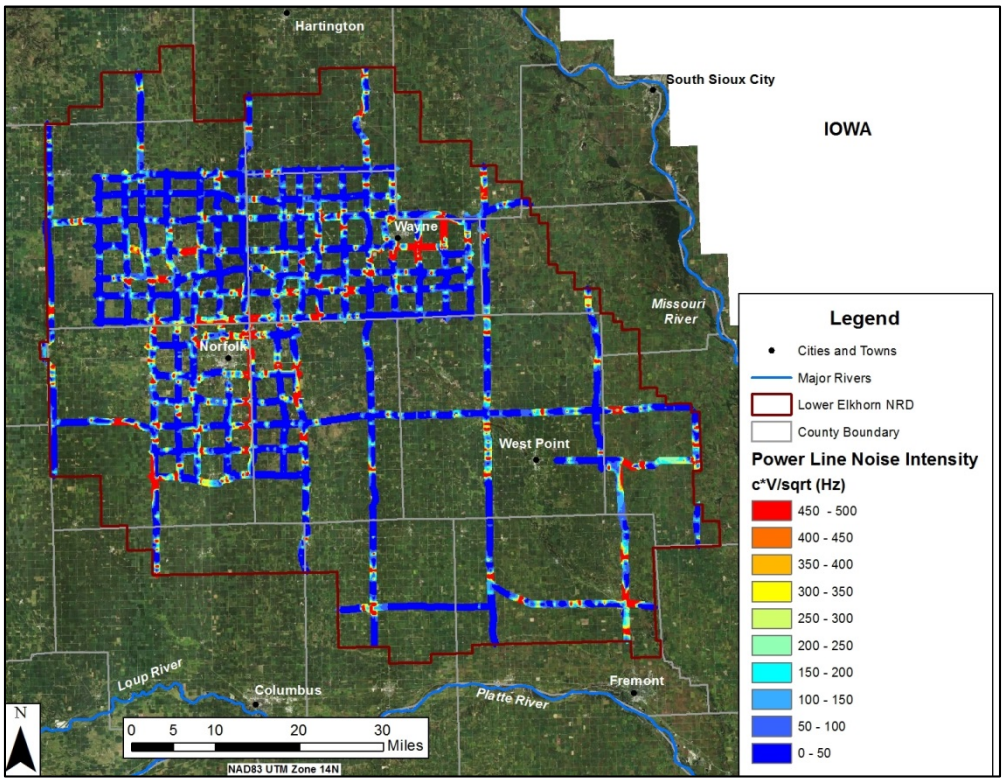


Figure 4-10: Power Line Noise Intensity (PLNI) map of the LENRD survey area.

4.5.5 Magnetic Field Data

As discussed above, the SkyTEM 508 includes a Total Field magnetometer. The magnetic field data can yield information about infrastructure as well as geology. Figure 4-11 shows the magnetic field data after correcting for diurnal drift and removing the International Geomagnetic Reference Field (IGRF). This data compares well with the regional magnetic data shown in Figure 4-12 (Bankey et al., 2002) with the exception of the high anomaly surrounding the city of Wayne, NE. The line spacing of the regional data is 5 miles that could explain the difference in magnitude in this area.

The 3D magnetic field analytic signal is presented in Figure 4-13. The analytic signal indicates areas of sharp changes in the magnetic field such as those caused by metallic infrastructure. This data is used in decoupling efforts.

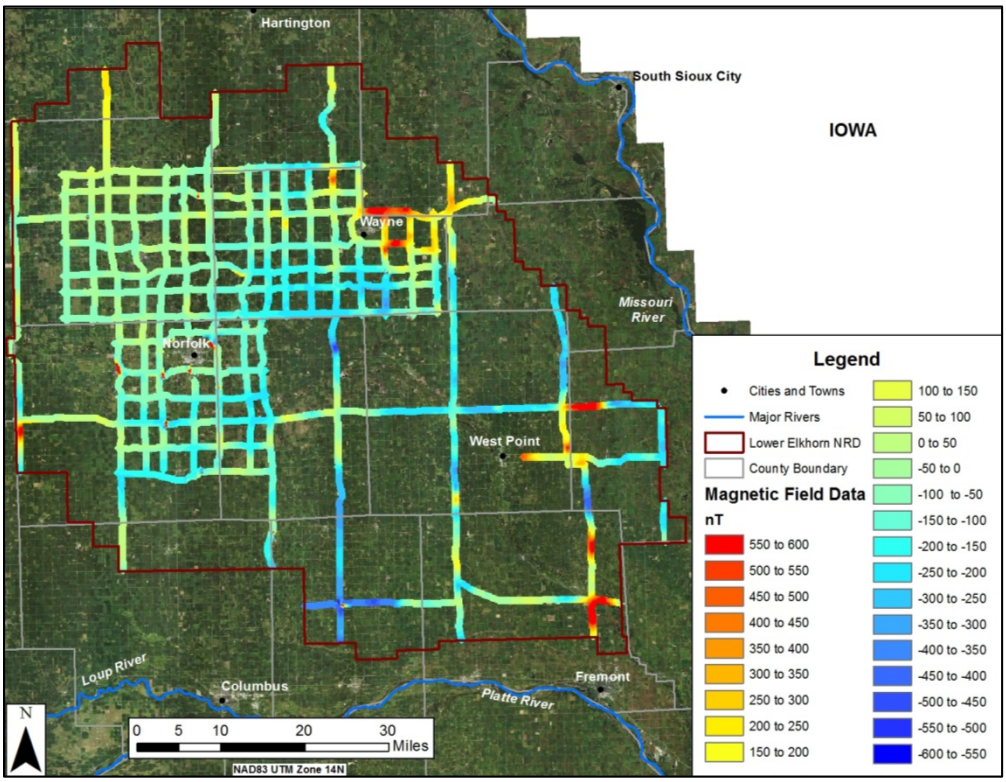


Figure 4-11: Magnetic field data corrected for diurnal drift, with IGRF removed.

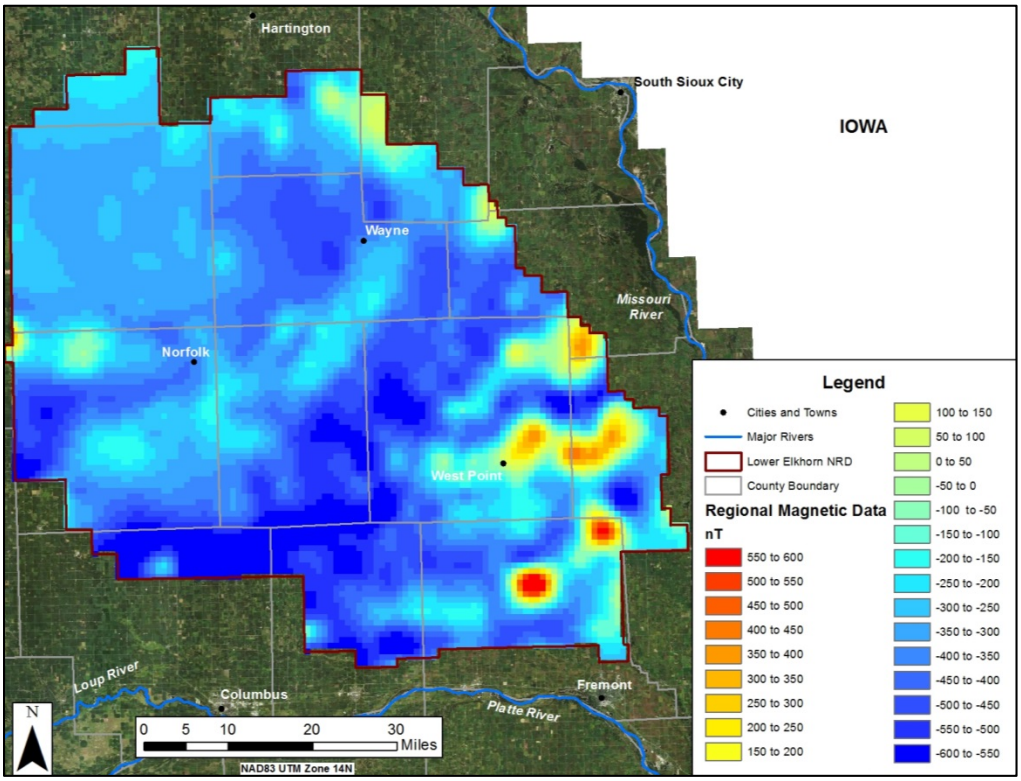


Figure 4-12: Regional magnetic field data within the LENRD boundary. Derived from Bankey et al. (2002).

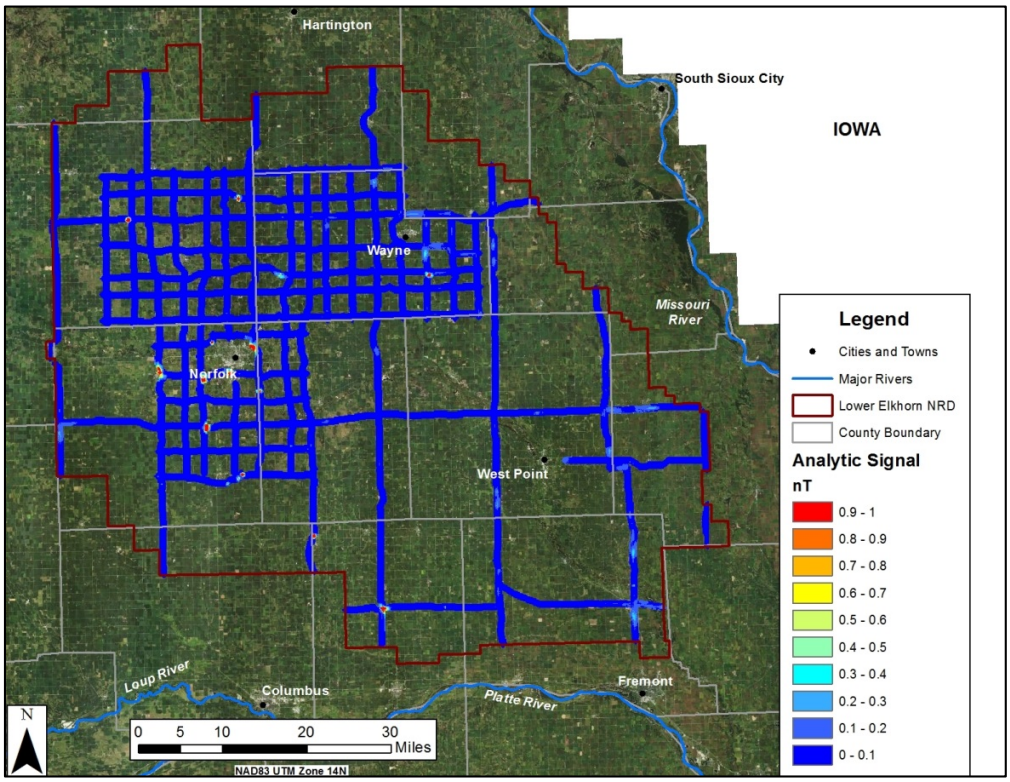


Figure 4-13: 3D magnetic field analytical signal calculated from the diurnal and IGRF corrected magnetic field data.

4.6 Spatially-Constrained Inversions

Following the initial decoupling and LCI analysis, Spatially-Constrained Inversions (SCI) were performed. SCI inversions use EM data along, and across, flight lines within user-specified distance criteria (Viezzoli et al., 2008).

A smooth model inversion of 30 layers, each with a starting resistivity of 10 ohm-m, was used (equivalent to a 10 ohm-m half space). The thickness of the first layer of the model was 5 m with the thickness of each consecutive layer increasing by a factor of 1.1. The bottom of the 29th layer was set to a depth of 1,640.4 ft (500 m), and it had a thickness of 133.5 ft (40.7 m). The thickness of the layers increases with depth (Table 4-6 and Figure 4-14) as the resolution of the technique decreases with depth. The reference distance was set to 100 m with a power law of 0.5. The constraint levels, ResVerSTD and ResLatStD, were set to 2 and 1.3, respectively, for all layers.

Table 4-6: Thickness and depth to bottom for each layer in the SCI inverted AEM models. The thickness of the model layers increase with depth as the resolution of the AEM system decreases with depth.

Layer	Depth to Bottom (ft)	Thickness (ft)	Layer	Depth to Bottom (ft)	Thickness (ft)
1	16	16	16	488	51
2	34	18	17	543	54
3	53	19	18	601	59
4	74	21	19	665	63
5	96	22	20	733	68
6	120	24	21	806	73
7	145	26	22	885	79
8	173	28	23	971	85
9	203	30	24	1062	92
10	235	32	25	1161	99
11	270	35	26	1268	107
12	307	37	27	1383	115
13	347	40	28	1507	124
14	391	43	29	1641	133
15	438	47			

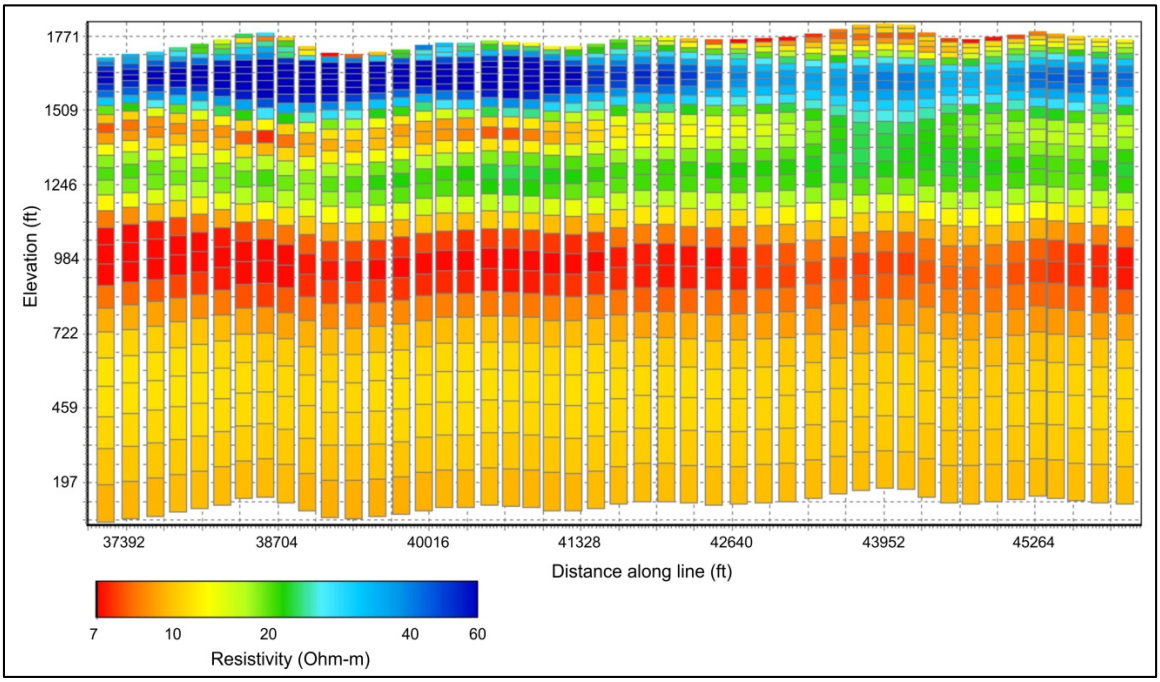


Figure 4-14: An example AEM profile illustrating the increase in model layer thickness with depth.

In addition to the recovered resistivity models the SCIs also produce data residual values (single sounding error residuals), total residual values (total model residual error values), and Depth of Investigation (DOI) estimates. The data residual compares the measured data with the response of the inverted model. The total residual is a weighted average of the data residual and the model residual (Christensen et al., 2009; SkyTEM Airborne Surveys Worldwide, 2012). The DOI estimates the depth to which the AEM data are sensitive to changes in the resistivity distribution at depth (Christiansen and Auken, 2012).

Lastly, 33 of the borehole conductivity logs, listed in Table 4-7, were used to constrain the inversions with a lateral standard deviation (STD) constraint of 2 and a reference distance of 3,280 ft (1000 m) (HydroGeophysics Group Aarhus University, 2011). A variety of a-priori STD values and reference distances were tested including STDs of 1.5 and 2, and reference distances of 3,280 ft (1000 m) and 9,840 ft (3000 m). Workbench resamples the geophysical logs to match the layer widths and depths set for the SCI results. Figures 4-15 and 4-16 compare the borehole logs with the starting model and the inverted model results for select boreholes. The green line shows the original borehole logs while the blue is that log resampled to match the layering used within the inversions. The purple line is the inverted model result without a-priori information while the red shows the result when the logs were used. In some instances the borehole logs did not greatly affect the inversion result, as shown in Figure 4-17. For these models there is possible error within the logs are the resistivity structure of the ground is varies significantly between the borehole locations and the AEM model location. Figure 4-18 shows a cross plot of the inverted resistivities compared with the resampled borehole resistivity for the 13 boreholes within the closer spaced flight lines.

The data residuals for each inversion result were compared to each other and to the inversion results where no logs were used. A STD value of 2 with a reference distance of 3,280 ft (1000 m) produced the best results with improved data residuals, shown in Figure 4-19. Their distribution became tighter and lower for the grid area (Figure 4-20). However, while a bulge in the distribution curve was produced around 0.7 for the recon lines (Figure 4-21), these residuals also became lower. Therefore, it was determined that including the resistivity logs in the inversion still produced better results than without the borehole logs.

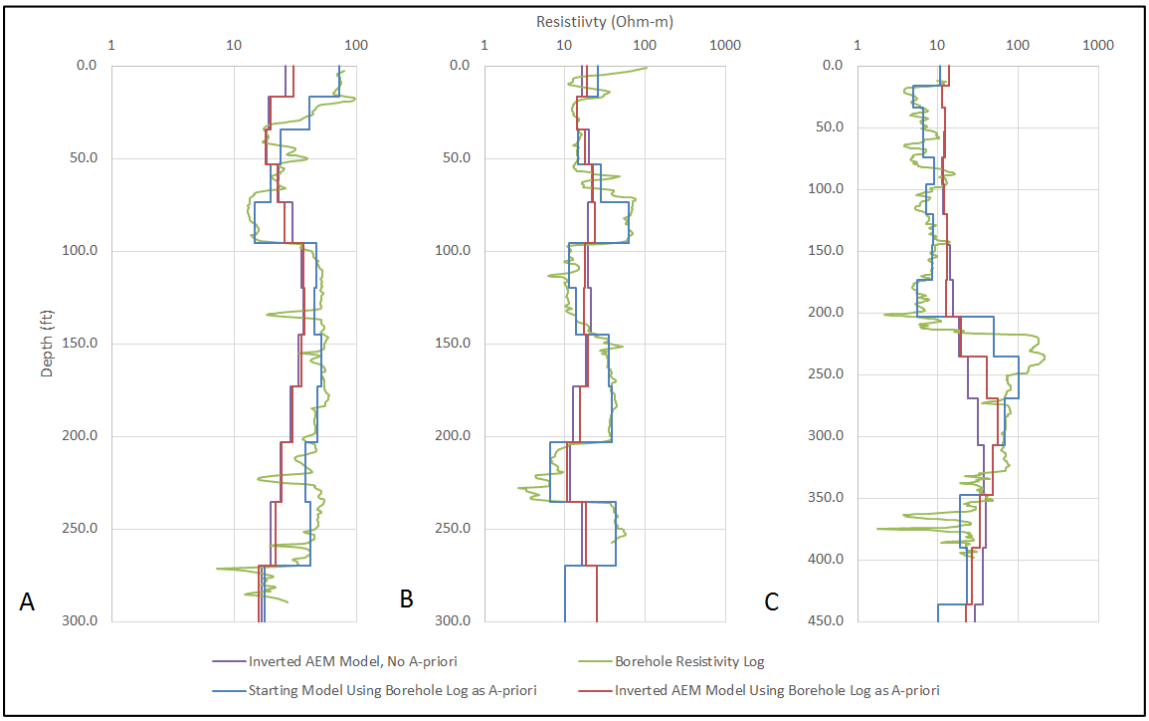


Figure 4-15: Borehole resistivity logs compared with inverted AEM models. A: Well 3-A-52, 1,700 ft from the AEM line. B: Well 3-A-53, 2,512 ft from AEM line. C: Well 4-A-52, 527 ft from AEM line.

Table 4-7: List of wells with borehole resistivity logs used as a-priori information for the SCI.

Well	Easting (ft)	Northing (ft)	Well	Easting (ft)	Northing (ft)
11-A-55	2083843	15230058	2-A-52	2206272	15232708
11-A-64	2262597	15365384	3-A-52	2082386	15306556
12-A-53	2017922	15432952	3-A-53	2038184	15353127
15-A-55	2021091	15239880	41-A-55	1958300	15257157
16-A-55	2024109	15221711	43-A-55	1957850	15289942
17-A-52	2159219	15388336	4-A-52	2082038	15324771
17-A-55	2021626	15207095	4-B-64	2162661	15235333
18-A-52	2159547	15373766	50-A-51	2081481	15353914
18-B-63	2304736	15217075	5-GT-80	2171033	15344869
19-A-55	2022160	15174314	6-A-63	2361917	15218772
1-B-53	2018581	15392880	6-GT-80	2332504	15199651
20-A-55	2022397	15159743	7-A-63	2364302	15229785
21-A-55	2022636	15145173	8-A-53	2018883	15374665
21-A-62	2373117	15033154	13-LE-99	2084122	15215488
22-B-63	2306209	15260868	1-LE-99	2052429	15313291
26-A-52	2229477	15390033	8-LE-03	2087189	15197325
29-A-52	2155121	15450209			

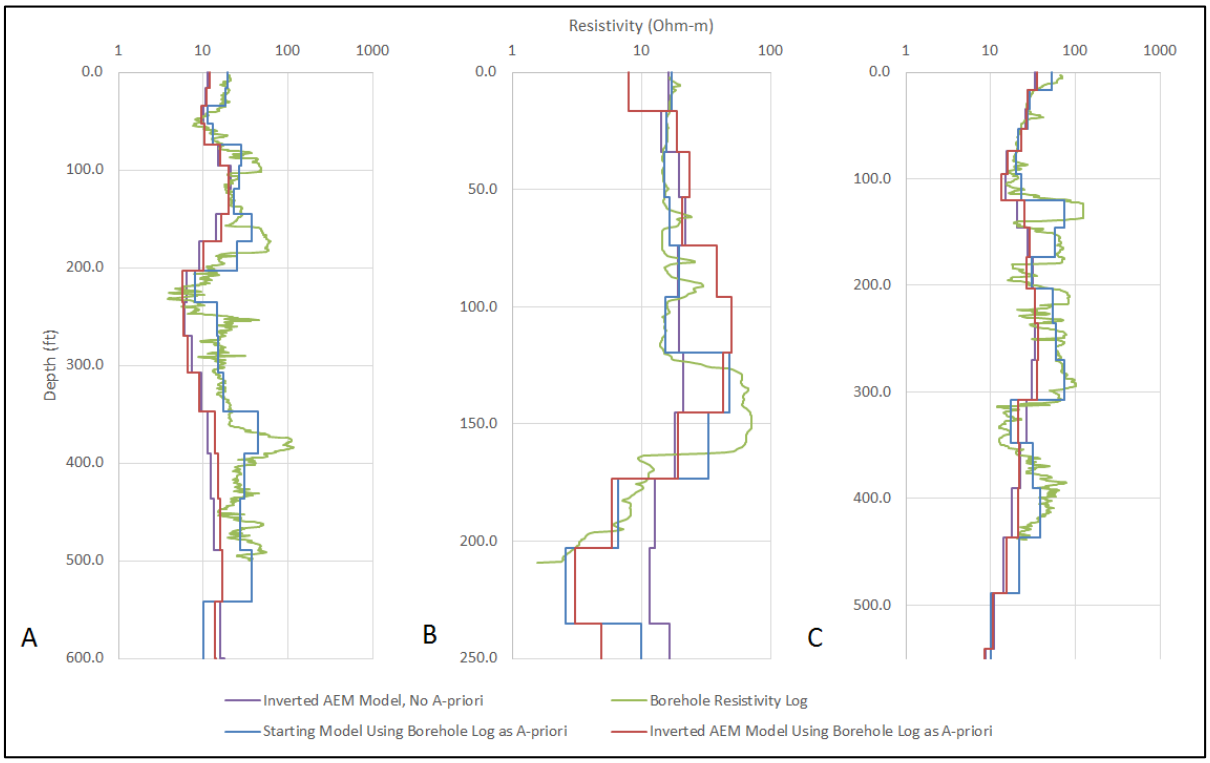


Figure 4-16: Borehole resistivity logs compared with inverted AEM models. A: Well 5-GT-80, 721 ft from the AEM line. B: Well 8-A-53, 1,768 ft from AEM line. C: Well 15-A-55, 3,132 ft from AEM line.

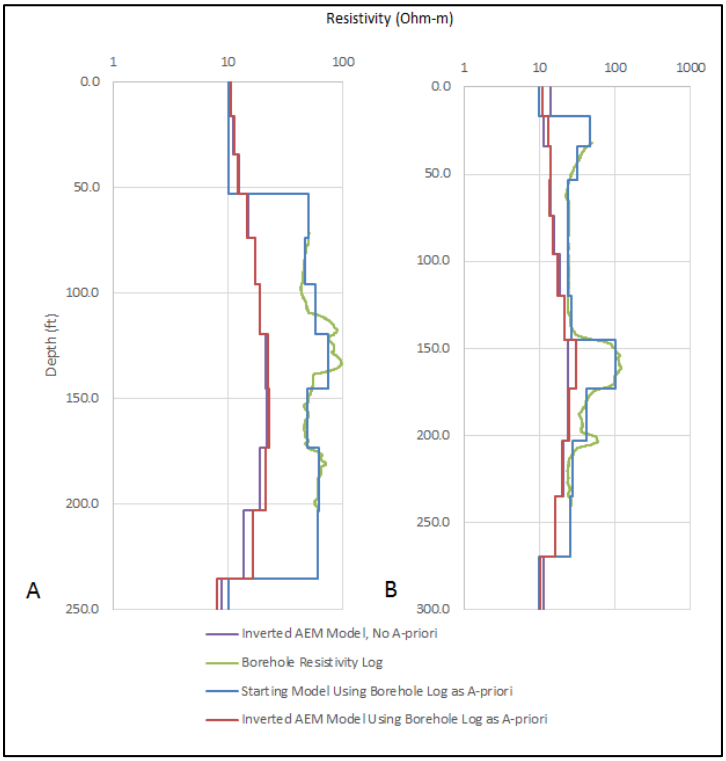


Figure 4-17: Borehole resistivity logs compared with inverted AEM models. A: Well 8-LE-03, 1,540 ft from AEM line. A: Well 13-LS-99, 2,349 ft from AEM line.

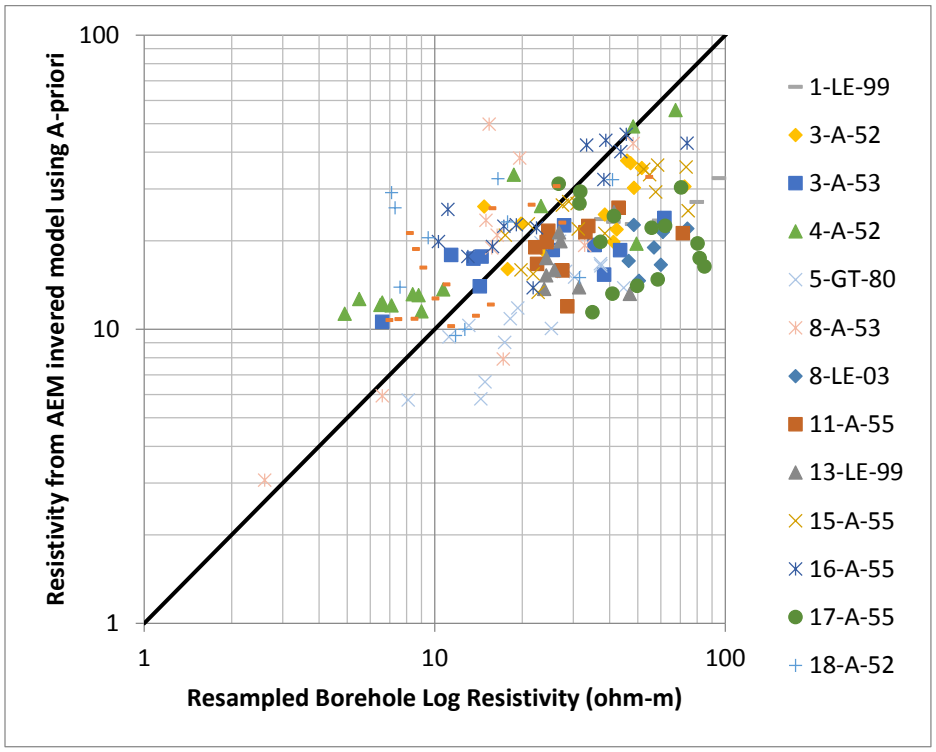


Figure 4-18: Cross-plot resistivities compared with the resampled borehole resistivity for the 13 boreholes within the closer spaced flight lines.

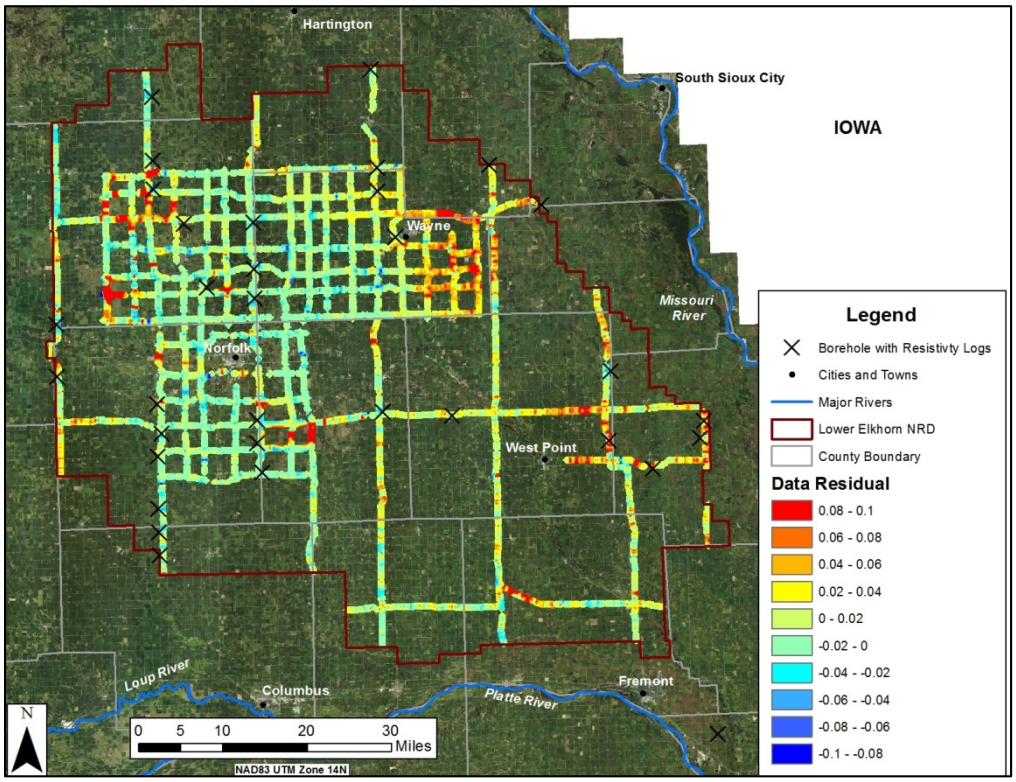


Figure 4-19: Difference between data point residuals produced by SCIs with and without using the borehole conductivity data as a-priori information. Red indicates an improvement in the residuals by greater than 0.1.

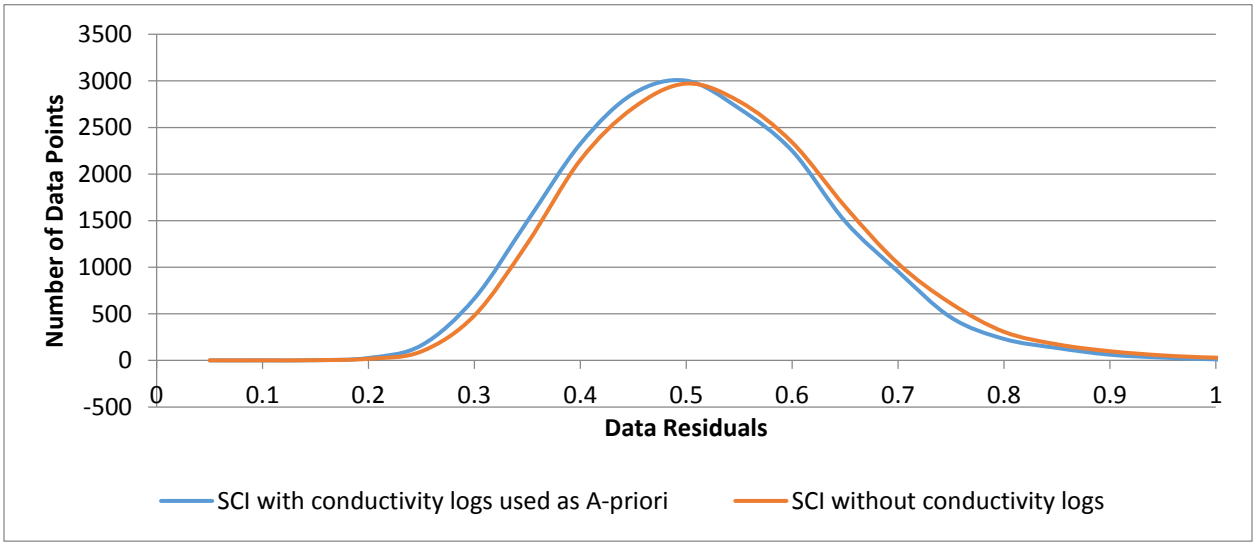


Figure 4-20: Data residuals distribution produced by the SCIs in the three-mile grid area with and without use of resistivity logs as a-priori information.

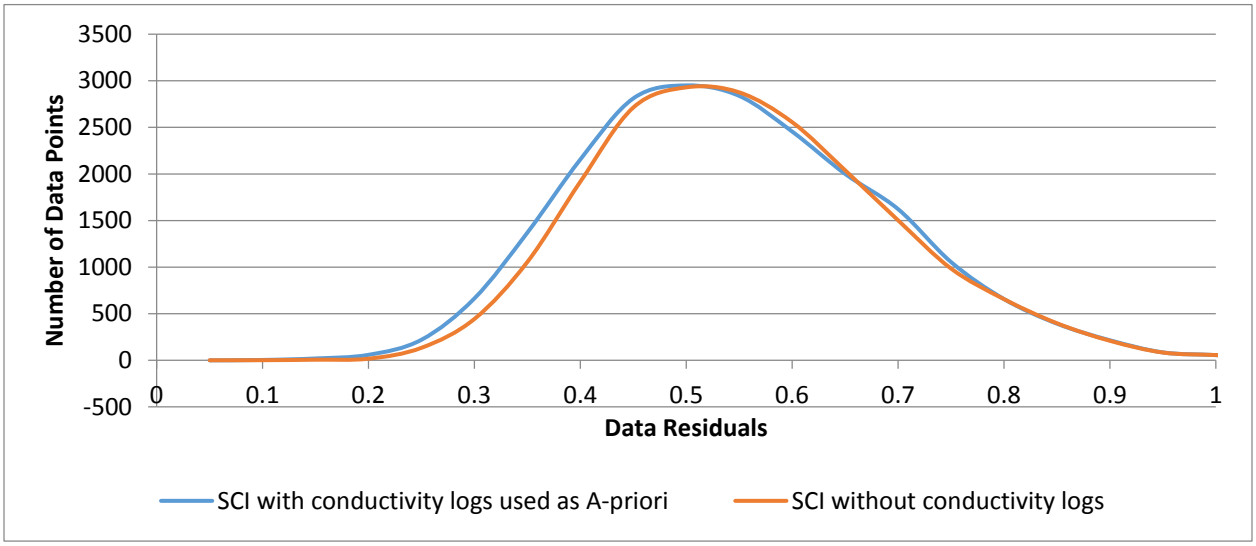


Figure 4-21: Data residuals distribution produced by the SCIs in the 10-mile recon lines with and without the resistivity logs as a-priori information.

4.6.1 Determination of the DOI

The Depth of Investigation (DOI) plays a critical role in data interpretation. The DOI is a numerical estimation of the depth below which the resolution of a model, resulting from a numerical inversion, diminishes. This depth develops primarily due to the limitations of the TDEM method including: the equipment and methodology used for data acquisition, the noise in the data, and the resistivity structure (the geology) being investigated (Christiansen and Auken, 2012).

In addition to inverting the AEM data, Aarhus Workbench also calculates depths of investigation (DOI) for each inverted sounding, both a DOI Upper and a DOI Lower. 'Upper' refers to a shallower DOI

estimate while 'Lower' refers to a deeper one. The derivation of these depths is presented in Christiansen and Auken (2012) and discussed in more detail in Appendix 3.

The Aarhus Workbench uses inverted model sensitivities (the Jacobian) determined during the last inversion step, along with an estimate of data uncertainty to calculate the DOI's. The Jacobian matrix is the sensitivity of the data to perturbations at the current location in model-space. As such, the Jacobian is also a representation of the sensitivity of changes in the model to the observed data.

The last step is to calculate the cumulative sensitivities, S, by summing up the individual thickness-normalized sensitivities starting with the bottom layer. That is, for a 30-layer model (which is usually used in all the XRI Workbench inversions) the cumulative sensitivity for the 30th layer is the thickness-normalized sensitivity for the 30th layer. Then the cumulative sensitivity for the 29th layer is the sum of the cumulative sensitivity for the 30th and the thickness-normalized sensitivity for the 29th layer. The cumulative sensitivity for the 28th layer would be the sum of the cumulative sensitivity for the 29th layer and the thickness-normalized sensitivity for the 28th layer.

However, there is a difference between *resolution* of a property and *detection* of a property. Resolution means that the properties of interest are accurately recovered through inversion. Detection indicates that while the true value of a property may not be accurately resolved, there is still some sensitivity, in the data, to changes in that property. The DOI is generally the line of demarcation between resolution and detection.

Christiansen and Auken (2012) define the global threshold value as that cumulative sensitivity which indicates "*the miminum amount of sensitivity needed for indicative information*". They further state that "*setting the threshold value is very much a question of fine-tuning based on experience, intuition, and comparing different models with different methods. The threshold value suggested here is purely empiric…. Setting a higher threshold value will decrease the DOI, and a lower value will increase the DOI.*"

The upper and lower DOIs typically exported by the Aarhus Workbench are for cumulative sensitivities 1.2 (upper DOI) and 0.6 (lower DOI). However, additional cumulative sensitivity values can also be developed and exported including 0.4, 0.2, and 0.1. Variations in the character of the DOI's are functions of the resistivity of the sounding for which the DOI is calculated. The DOI contours for the cumulative sensitivity thresholds are going to be much deeper under resistive zones and shallower under conductive zones. An example of a DOI produced using a 0.1 cumulative sensitive is shown on the profiles in Figure 4-22 and in Appendix 3.

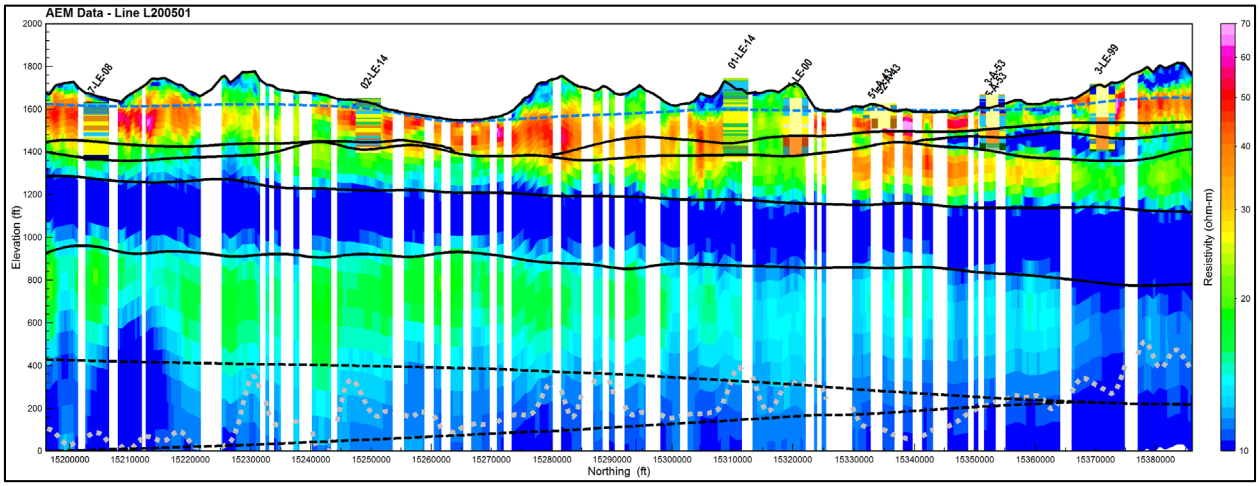


Figure 4-22: Sample of AEM resistivity inversion model with the DOI marked as grey boxes at the bottom of the image.

5 Results and Interpretation

A total of 1,197 line miles (1,926 line km) of airborne EM were collected. Of that total, 254 lines miles (409 line km), or 21%, were removed due to electromagnetic coupling with infrastructure leaving a total of 942 line miles (1,516 line km) for inversion and interpretation. Had the flights line paths not been optimized prior to data collection, the expected data retention would have been 35% instead of 79% (using an approximate 656 ft (200 m) radius of interference). Figure 5-1 shows the locations of the inverted resistivity models. Figure 5-2 displays the flight line numbers.

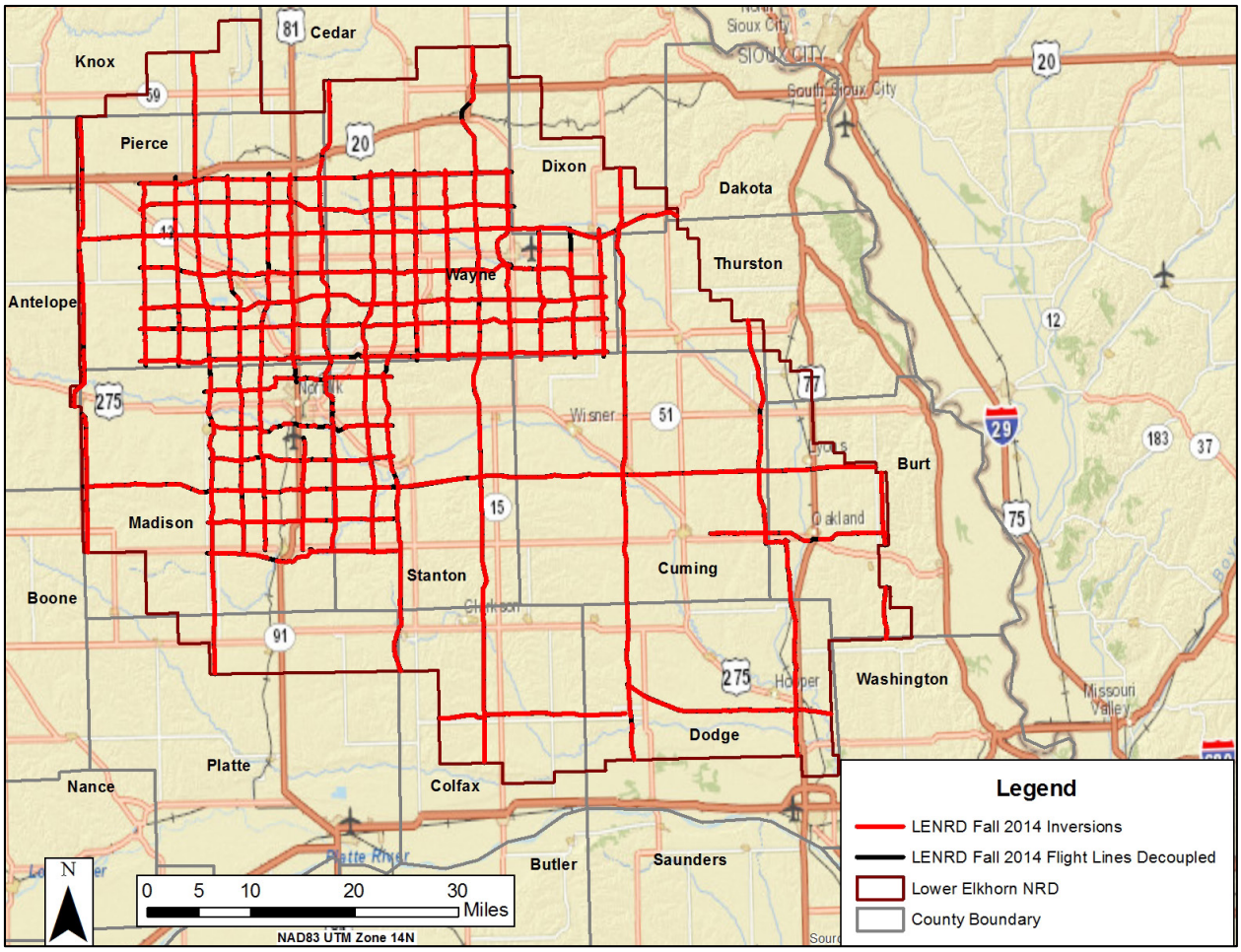


Figure 5-1: Locations of inverted data along the AEM flight lines.

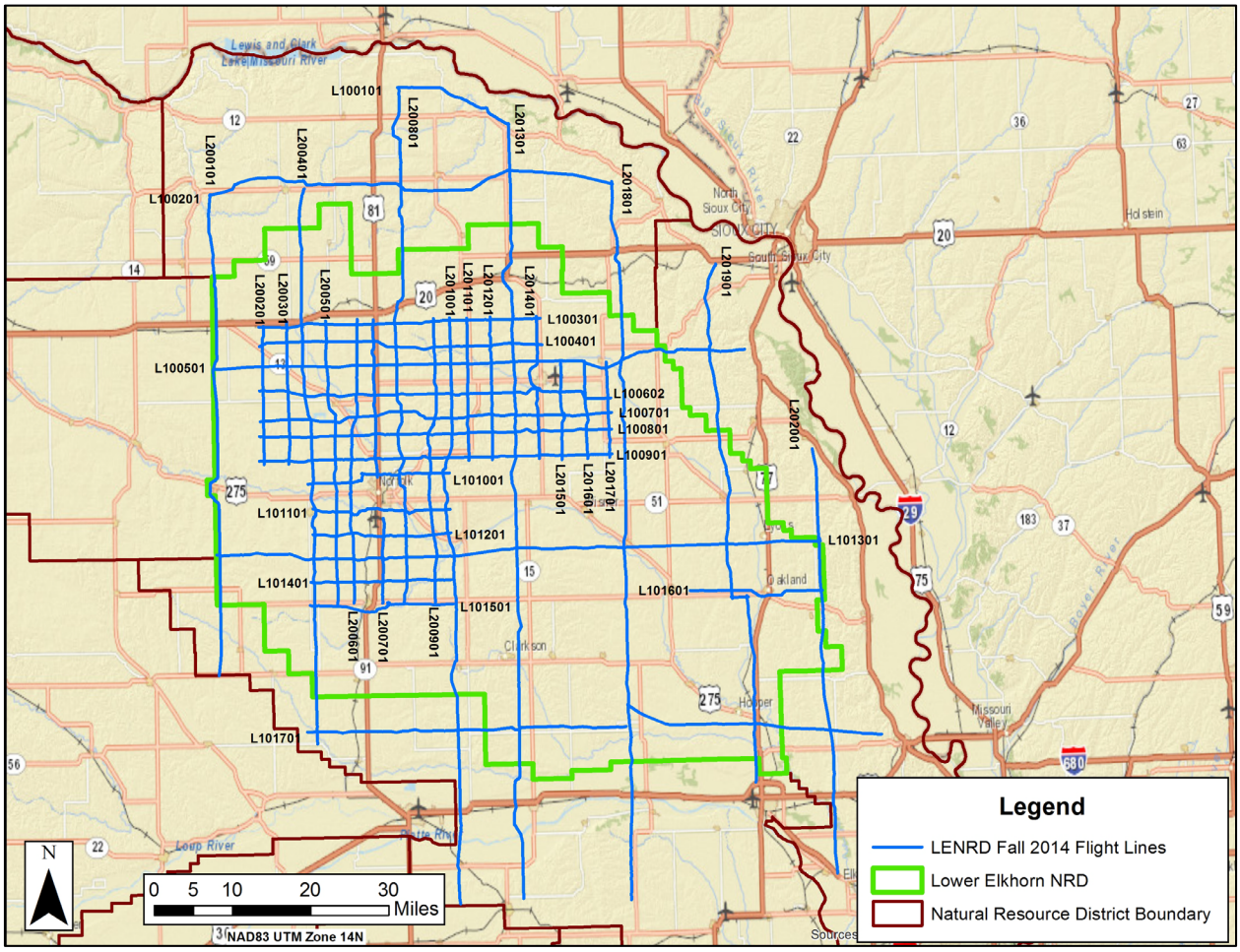


Figure 5-2: AEM flight lines with line numbers.

5.1 AEM Results and Interpretation

After final processing of the AEM data, characterization of the subsurface was performed in cross-section format using Encom PA. In this step, contacts between the bedrock (Paleozoic and Cretaceous), Tertiary, and Quaternary deposits were selected for every flight line in the project area. The interpreted geological units included the *To*, *Kp, Kn, Kc, Kgg, Kd, [P,* and *M* as well as older, undifferentiated Paleozoic strata (Korus and Joeckel, 2011). The Greenhorn Limestone and Graneros Shale (*Kgg*) were not geophysically distinct from the *Kc* at all locations. Since these units function as aquicludes over much of the area, it was determined that keeping the units undifferentiated was the best approach to represent the AEM data and the hydrogeologic framework of the project area. This process was aided by the use of CSD and NOGCC borehole logs, which provided lithologic, stratigraphic, and geophysical information. The historical CSD cross-sections (University of Nebraska-Lincoln School of Natural Resources, 2014) were projected in Encom PA to aid in interpreting the AEM data. The interpretations were simultaneously checked against the CSD's Nebraska bedrock geology map (Burchett, 1986) and other geological maps in the northern portion of the project area. After the cross-section interpretations of the geological contacts were completed, the interpreted points were inspected in 3D with the NOGCC

boreholes, CSD boreholes, CSD historic bedrock surface, and CSD cross-sections (Korus et al., 2012; Divine et al., 2010).

Areas of offsets between intersecting AEM flight lines were minimized by reinterpreting the information based on visualization of the AEM data in a 3D display. During the interpretation process, a limited number of CSD stratigraphic assignments were determined to be in disagreement with the AEM results. These discrepancies can be categorized as follows: 1) incorrect stratigraphic selections of *Kd* versus *Kp*; 2) AEM-enhanced stratigraphic selections that provided additional data to indicate *Kp* and not Quaternary deposits; 3) incorrect calls of Tertiary (Oligocene) White River Group that were confirmed as *Kp* from the AEM; and 4) picks that indicated *To* but were interpreted as Quaternary from the AEM. It was also determined that the NOGCC stratigraphic assignments contained inaccurate indications of the depth of the bedrock. These data were omitted. The NOGCC stratigraphic selections in the boreholes within the Cretaceous and Paleozoic units were utilized in the interpretation.

In addition to the geologic profiles, historic bedrock geology maps were also used to assist in the interpretation of the AEM inversion results (Korus et al., 2012; Divine et al., 2010). These maps were georeferenced and the interpreted contour lines were digitized using ESRI's ArcMap. The digitized contour lines were gridded to create either surfaces or thickness maps.

Regional surface grids of geologic formation were produced during this process. To produce these grids the elevations of the interpreted top of the formation as well as data from CSD and NOGCC holes were imported into a Geosoft Oasis Montaj (OM) database. The interpreted elevation data were then gridded for each formation independently using the OM minimum curvature gridding (MCG) algorithm with a 1500-ft cell size, a blanking distance of 50,000 ft, and the cells to extend beyond set to 50. All other parameters were either left as the default or blank. The large blanking distance was required to fill in between the largely spaced recon lines, where 15 miles or more separated adjacent flight lines. CSD and NOGCC holes were used to provide additional formation elevation data throughout the surveyed area. The 1500-ft cell size preserved most of the spatial resolution obtained from the AEM data but minimized artifacts from the MCG routine. While the MCG routine does a good job at honoring the data, in areas where the spatial density of data points is low the MCG routine may trend towards an overall average data value. This may cause artifacts in the final grid, grid values that are not supported by data in the general vicinity. A smaller cell size resulted in these gridding artifacts on the boundary of the project area and where only recon lines were available (no CSD or NOGCC holes available). A 9-point convolution filter was applied to each grid using the pre-defined Hanning filter under GRIDFILT GX within OM. This type of filter is common in image processing and was used to reduce high-frequency noise in the grid.

The gridding parameters used resulted in grids that were continuous across the project area but also extended outside the project area or beyond the areal extent of the interpreted feature in the AEM data. Once the grids were generated, each individual grid was masked to remove gridded data that was either outside the project area or in areas where that geologic surface was not identified. The mask was generated from the AEM interpretation, CSD and NOGCC holes, and the LENRD bedrock geology map. In

areas where no AEM data or drill holes were available, the contours for each geologic unit were followed as depicted on the bedrock geology map.

Once masked, the grids were then sampled to the location of the AEM data within OM and visually inspected for consistency. In areas of sparse data, grid surfaces may not meet or overlap (e.g. the gridded bedrock surface exceeded the DEM elevation by a small interval (< 5 ft) in a minor number of instances). In areas of incongruity, data were manually adjusted to ensure geologic surfaces met appropriately or did not overlap. This manual editing was only conducted on the geologic surface data that coincided with the location of the AEM data and used to generate the cross section plots presented in this report. The digital regional grids provided with this report will show discontinuities throughout the project area where different geologic surfaces meet or pinch out. In most cases, this is typically less than 30 feet, but some areas exist where the elevation offset of successive geologic units is 75 ft or more.

Following construction of the bedrock surface, the consolidated and unconsolidated deposits were isolated within the AEM data. A voxel resistivity grid was made of the AEM data using a 1,000 ft square horizontal cell with the thickness related to the model cell thickness (Section 4.6). The voxel was then sliced at the bedrock surface. This surface was the top of the *To, Kp, Kn, Kc_Kgg*, or the *Kd,* depending on location in the project area. The voxel values were then sampled on the AEM flight path cross-sections to indicate the location of the resistive intervals that are interpreted as unconsolidated Quaternary aquifer materials. The aquifer and non-aquifer materials in the Quaternary system were separated by four major resistivity thresholds selected in Encom PA. These ranges include 1-12 ohm-m representing non-aquifer materials (glacial till, loess), 12-20 ohm-m representing marginal aquifer deposits with potential for interlayered silt and clay, 20-50 ohm-m range indicating the Quaternary system's principal aquifer, and the interval of 50 ohm-m or greater, indicating the coarsest, sand-rich intervals within the principal aquifer (further discussion on the basis of these ranges is provided in Section 5.1.5). To assist in the determination of the saturated materials, the 1995 CSD statewide water table was mapped into the cross-sections. These surfaces were then gridded to provide a formation or geologic material top and bottom along the flight line. The *To* resistive material was coupled with the overlying Quaternary resistive material, as it is assumed the aquifers in these units commonly act as one, or are in close hydraulic communication in the western half of the project area. The *Kd* resistors were also sampled from a sliced voxel model at a resistivity range of 16 ohm-m or greater.

It should be noted that care must be exerted not to use the voxel information beyond the flight lines, as the voxels are not constrained and thus will not provide information due to the large interpolation distances between flight lines. In some areas on the interpretation profiles, there are slight differences at the land surface and the underlying geologic interpretation. This is an artifact of displaying a 3D model along a line profile feature.

5.1.1 Interpretation of the Quaternary and Tertiary Hydrogeologic Framework

The interpreted AEM sections along all lines are included in Appendix 1. These results are compared to the CSD test holes in Appendix 2.

The AEM reveals considerable variability in the Quaternary and Tertiary deposits across the LENRD project area. Although the *To*, the primary host strata of the High Plains aquifer, is known to contain consolidated and semi-consolidated intervals of sandstone and siltstone, it is included in the discussion of the principal aquifer where it exists beneath the project area. This approach to characterizing the hydrostratigraphy is based on the connection of the separate units and the behavior of the coarse, unconsolidated Quaternary materials acting as one aquifer with the underlying *To*. The *To* exceeds 150 ft in thickness along flight line 200301 near the west boundary of the district. The easternmost extent of the *To* is less than 20 miles east of this flight line, where the unit terminates near the north-south flight line 200901. This eastward thinning of the *To* (indicated as the area beneath the orange line) is also clearly indicated in the 3D framework and 2D profiles included in this report.

To assist in the characterization of the aquifer underlying the district, the 1995 Nebraska regional water table surface (CSD) was converted to a grid dataset and incorporated into the hydrostratigraphic interpretive profiles of the LENRD project area (blue dashed line in the profile figures). Overall, the regional water level surface conforms closely with the subsurface character revealed in the AEM profiles. In the drainage valleys, the surface matches closely with the land surface elevation, which would be expected where shallow groundwater conditions typically persist. Beneath the upland areas, the regional water level surface is typically found within the till deposits, indicating confined or semi-confined aquifer conditions, which are typical in the principal Quaternary aquifer in eastern Nebraska where thick till and loess sequences are present.

As described in section 2.1.1, loess and glacial till comprise the uppermost geologic materials at the land surface to depths exceeding two hundred feet in some places. These deposits, along with other low-permeability materials (mixtures of clay-rich sediments) are shown as light blue in the AEM interpretive profiles and 3D framework images in this section and Appendix 1. These intervals are considered “non-aquifer material.” The AEM data reveals the combined thickness of these deposits in detail, with the intervals of greatest thickness present along a region trending northwest-southeast through the middle of the district that also continue southward beyond the district’s southern boundary. This area is associated with a moraine complex that extends from the Nebraska-South Dakota border to northern Kansas (Reed and Dreezen, 1965). The till deposits become discontinuous west of the North Fork of the Elkhorn River near the edge of the glaciated region of Nebraska. In this area, loess is the predominant surficial material that overlies older Plio-Pleistocene and Tertiary deposits.

The aquifer materials in the project area, including Quaternary and Tertiary deposits (where present), are identified with the colors tan (representing marginal aquifer materials), yellow (representing principal aquifer materials), and brown (representing the coarsest, sand-rich intervals of the principal aquifer). These colors correspond to the resistivity ranges described at the beginning of this section. As

displayed in Figure 5-3, considerable variability exists in the aquifer resources that underlie the project area. The principal aquifer material (yellow) is found primarily in the western half of the project area as well as in the northern half of Wayne County, where some of the thickest primary aquifer intervals exist beneath the district. The most extensive area underlain by principal aquifer material extends from just east of the north-south flight line no. 200801 westward to the district boundary and primarily north of the Elkhorn River. Much of this area includes Quaternary materials directly overlying the *To*. Within the principal aquifer (yellow shading in the profiles), seven distinct areas of sand-rich deposits (50 ohm-m or greater) are identified and displayed in Figure 5-3. Area 1, situated in eastern Pierce County, extends northwest of Norfolk along the North Fork of the Elkhorn River and eastward to an area between flight lines 200801 and 200901. In this area, aquifer material with resistivities exceeding 50 ohm-m range from less than 10 ft to approximately 150 ft in thickness and are present at shallow depths in the subsurface, indicating the potential for high recharge rates to the aquifer. The resistive intervals of 50 ohm-m or greater in Area 2 are present along the North Fork of the Elkhorn River near the northern project area boundary as well as in an apparent northwest trending body of coarse material with characteristics of an ancestral fluvial system (Figure 5-4). In these areas, the highly resistive material approaches 100 ft in thickness.

The presence of this productive aquifer material in the area surrounding the North Fork of the Elkhorn River valley is further substantiated by the density of irrigation wells within an area bounded by flight lines 200801, 200201, 100501, and 100901. In this area, the density of irrigation wells is 3.6 per square mile, with an average registered pumping rate (for wells with non-zero registered pumping rates) of 866 gallons per minute (gpm). It should be noted that it is unclear as to which of these geologic units (the Quaternary materials, the *To*, or both) are tapped by irrigation wells in this area. The principal aquifer in Areas 1 and 2 also includes underlying *To* material. It is assumed that the principal Quaternary aquifer in this area and the *To* act as one aquifer unit. However, the specific degree of connection locally is unknown, and further, localized information on discrepancies in permeability, storage, and vertical flow gradients between these units is required to fully ascertain this connection and behavior of the aquifer that consists of materials from different geologic sequences.

Several highly resistive zones exceeding 50 ohm-m and approaching 200 ft in thickness are present beneath the Elkhorn River valley west of the city of Norfolk near flight lines 101001 and 101101 (Area 3) and along the western project area boundary approximately 13 miles west/northwest of Norfolk near the intersection of flight lines 100901 and 200201 (Area 4). In Area 3, several resistive bodies are interlayered within principal aquifer material, ranging in thickness from less than 20 ft to approximately 100 ft, with isolated intervals ranging from 175 to 200 ft in thickness (flight line 200501). North of the present-day river channel, the resistivity data possibly indicates the location of the former Elkhorn River channel, which has appeared to migrate southward in recent time. Area 3 is underlain by the *Kn*.

In Area 4 (Figure 5-3), a large body of material exceeding 40 ohm-m is present along flight line 200201 that exceeds 200 ft in thickness. A considerable extent of this coarse interval of the principal aquifer is present at a shallow depth below the land surface with very little conductive, non-aquifer material above it. This condition would indicate high recharge potential to the aquifer in this area. Although the

extent of this thick, resistive body of sediments westward beyond the district is unclear, recon line 200101 west of the project boundary indicates an upper surficial resistor that could be associated with the large body of coarse deposits found at the intersection of flight lines 100901 and 200201. The principal aquifer in this area also includes approximately 50 to 75 ft of *To* materials.

Area 5 (Figure 5-3) is a smaller, more isolated body of resistive material located in the southwest corner of the district, it is contained within a more extensive zone of principal aquifer material between 20 and 50 ohm. The thickest portion of the principal aquifer exceeding 50 ohm-m exceeds 150 ft in places, but overall is less extensive than the coarse deposits found beneath the river valleys to the north. The principal aquifer in this area includes a thin interval of *To* that terminates just east of this area.

Area 6 (Figure 5-3), located near the intersection of flight lines 101301 and 201001 in central Stanton County, is an additional smaller body of material exceeding 50 ohm-m that appears to extend eastward beyond the district boundary along ENWRA reconnaissance flight line 101301. The resistive material is located immediately south of an area where the Elkhorn River shifts its course northeastward from its southeastward direction below its confluence with the North Fork of the Elkhorn River. The thickness of this interval of highly resistive material approaches 150 ft. Area 6 is deposited atop a thin sequence of *Kn* and a thicker interval of *Kc*.

The seventh area, exceeding 50 ohm-m, is a west to east trending linear featured located along the northern boundary of the project area. A portion of this interval along the northernmost district flight line east of reconnaissance flight line 200801 is one of the thickest resistive features in the district, approaching 200 ft. Area 7 transitions into marginal aquifer approximately 6-8 miles south of fight line 100301 and does not extend to the eastern district boundary. The principal aquifer materials in this area are deposited on *Kn*, with a small extent sitting above *Kc* on the far eastern extent of the resistive body. The *To* terminates beneath the far western edge of Area 7 (flight lines 100301 and 100401), and is not an aquifer resource beneath this body of the aquifer.

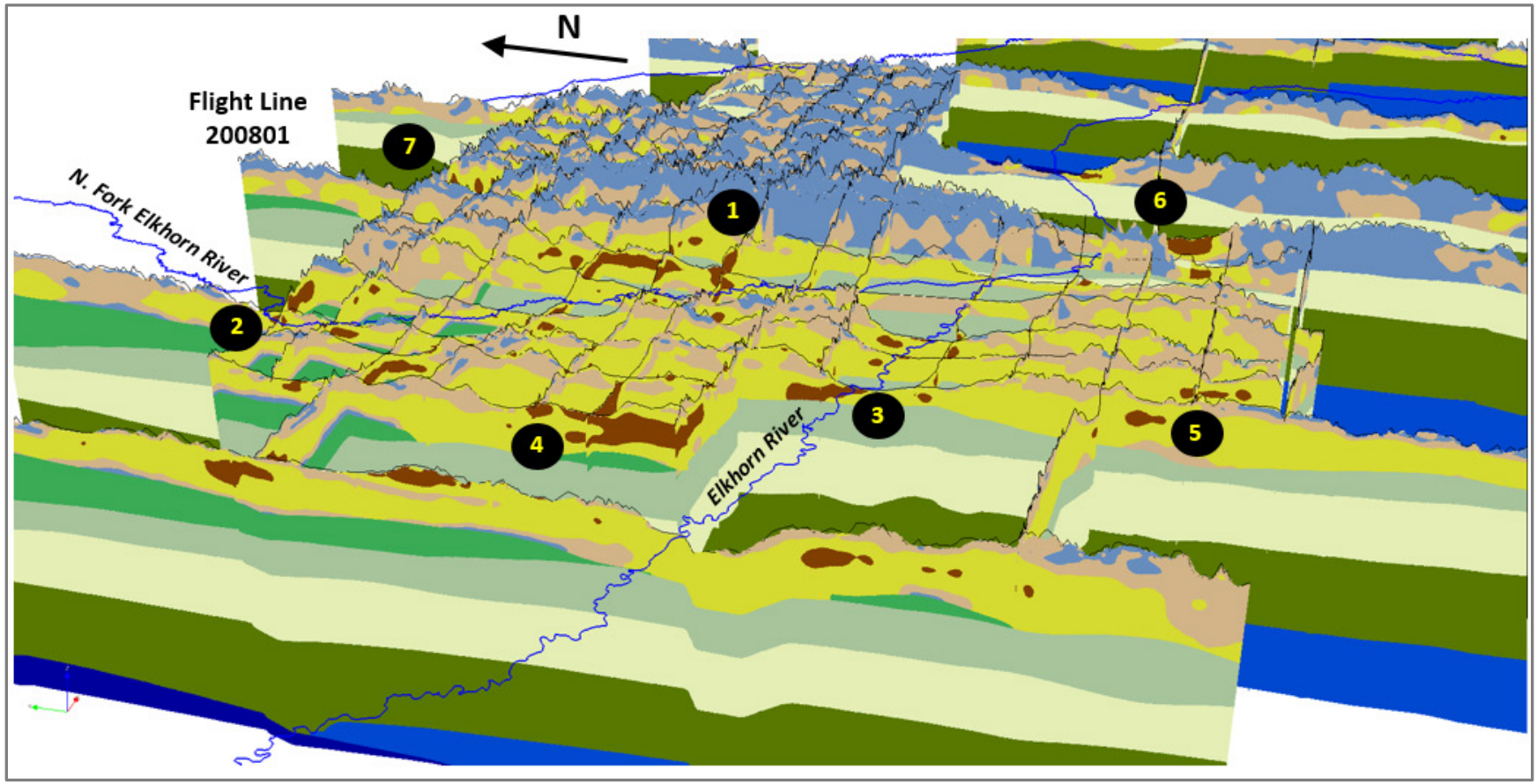


Figure 5-3: A northeastward view of the 3D hydrostratigraphic framework of the LENRD project area, including geologic materials ranging from Quaternary deposits to Paleozoic bedrock. The image includes the seven labeled areas of sand-rich, coarse principal aquifer materials (brown colored zones). The Elkhorn and North Fork of the Elkhorn Rivers are also displayed on the framework, and some of the ENWRA reconnaissance lines are displayed beyond the district flight block.

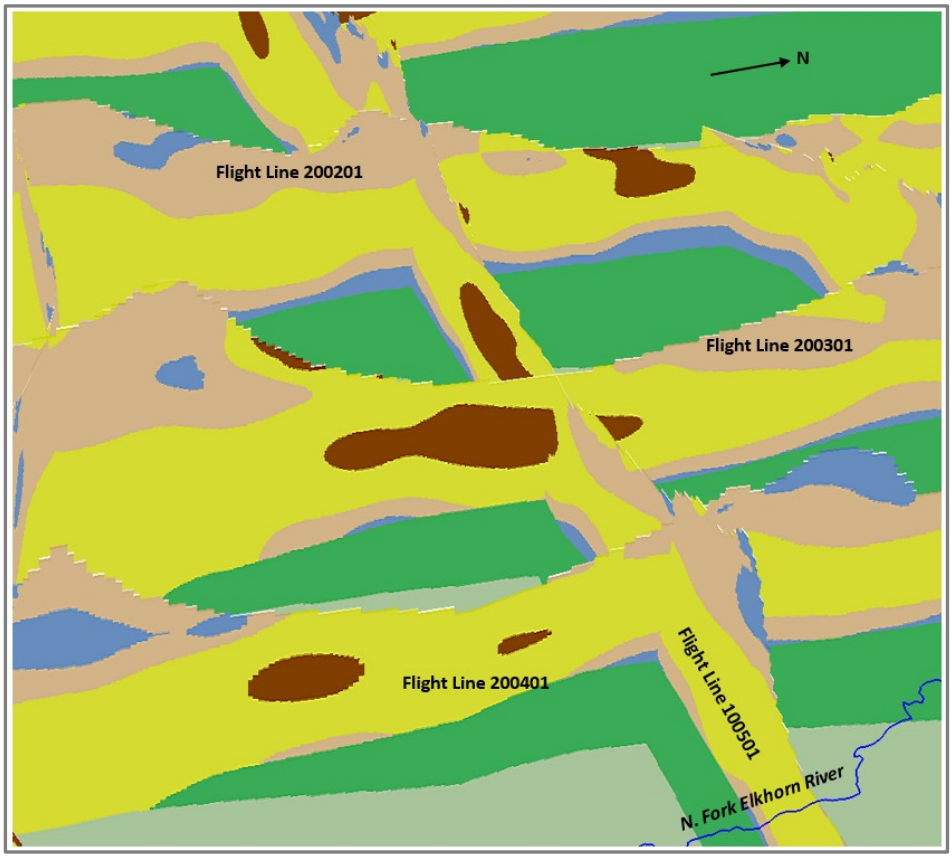


Figure 5-4: A 3D view of the northwest-trending buried channel in the sand-rich area 2 of the principal aquifer (brown intervals).

Material considered marginal aquifer is present throughout much of the project area and is variable in extent and thickness. In places, it is also present above the 1995 Nebraska regional water level surface. It is most extensive south of Norfolk and the Elkhorn River, where thicknesses approach 200 ft. In this area, the aquifer is primarily composed of marginal material, with isolated intervals of primary aquifer material mantled by thin non-aquifer deposits. North of the Elkhorn River, marginal aquifer deposits are more dispersed among principal and sand-rich principal aquifer and non-aquifer deposits, with the exception of the area along flight lines 100801 and 100901. The eastern one-third of the project area is underlain primarily by marginal aquifer deposits overlain by thick sequences of non-aquifer materials. The marginal aquifer in this area shows a dispersed southeastward trend, with layered aquifer and non-aquifer materials. This pattern is exemplified in flight lines 100701 and 100901, where the AEM profile reveals mostly non-aquifer materials containing isolated bodies of marginal aquifer material. The distribution of irrigation wells in this area further substantiates the presence of mostly marginal aquifer. Low density of high-yield wells is considered an indicator of either low transmissivity, lack of areal extent of productive aquifer, or both. In a rectangular area between flight lines 200901, 100501, 201601, and 100901, the density of irrigation wells is 0.6 per square mile, with an average registered pumping rate of 734 gallons per minute. This indicates that in the area underlain by marginal aquifer in the eastern one-third of the project area, there is generally less than one irrigation well per square mile, whereas in the area west of flight line 200801 (northwest of Norfolk) previously described, there is nearly one irrigation

well per 160 acres. Of the wells that are used for irrigation in the area underlain by marginal aquifer, registered pumping rates in the eastern one-third of the district, on average, pump over 100 gpm less than irrigation wells found west of Flight Line 200801.

Non-aquifer material (aquitard), composed primarily of glacial till, loess, and clay-rich mixes of silt and fine sand, is predominately found east of flight line 200801, where the extensive moraine complex in eastern Nebraska trends northwest to southeast across the district. The thickest intervals are found in western Wayne and Stanton Counties along west-east flight lines 100602, 100701, 100801, and 100901 and north-south flight lines 200901 and 201001 in western and south-central Wayne County. The thickness of this aquitard ranges from less than 100 ft to over 300 ft in places. Most of the hummocky, upland hills region of Wayne and Stanton Counties are composed primarily of non-aquifer material from the land surface to depths exceeding 200 ft, beneath which is underlain typically by marginal aquifer or principal aquifer in isolated intervals. The aquitard extends from this area with varying thickness to the eastern border of the district and is interlayered with marginal aquifer. Along the north-south flight line 201301, particularly where this line intersects with flight line 100901, the subsurface is comprised entirely of aquitard. In this area, the non-aquifer deposits ranges from 250 to 300 ft in thickness. Some areas have a basal aquitard deposited on top of Cretaceous bedrock. This aquitard is likely remnant ground moraine till from the initial glaciation that entered Nebraska from the northeast during the early Pleistocene. This material was presumably reworked during subsequent retreat and advancements of the ice sheet during pre-Illinoian time of the Pleistocene.

It should be noted that the separate body of *To* identified in the bedrock geology map of the state (Burchett, 1986) was not revealed by the AEM data. This separate *To* feature is located partially in the same area underlain by the sand-rich Area 6 of the principal aquifer discussed in the previous section. It is possible that these coarse Quaternary deposits were originally mapped as *To* during the creation of the statewide geologic map in the 1970s (Burchett, 1986). Examination of the CSD test holes in this area did not reveal any consolidated or semi-consolidated material in the subsurface at depths where the *To* would be expected. Along with this evidence from the CSD boreholes, there is no evidence of this *To* feature in the project area flight line block or the nearby recon lines to the southeast of Area 6 discussed in the prior section.

5.1.2 Interpretation of Bedrock Geology

Underlying the *To* and the Quaternary deposits is a sequence of Cretaceous and Paleozoic bedrock strata approaching 2000 ft thick in places. Although no major structural features are evident within the AEM project area, a subtle dip in the bedrock underlying the *To* and Quaternary deposits is revealed in the resistivity data. The most pronounced dip in the bedrock strata is observed in the AEM survey's west-east profiles, where the Cretaceous and Paleozoic units dip westward towards the Central Nebraska Basin (Miller et al., 1964). This trend is particularly evident in flight lines 100201, 100501, and 101301. The north-south profiles also reveal northward dipping strata from near the southern border of the project area towards the Missouri River. Although less pronounced than the westward dip, examples of northward dip are apparent in AEM profiles 200410 and 200801. The strata appear to dip towards a

trough on the south limb of the Siouxia Uplift/Transcontinental Arch located in southeastern South Dakota (J. A. Peterson, 1984).

5.1.3 Cretaceous Stratigraphic Sequence

The uppermost Cretaceous unit present beneath the project area is the regionally ubiquitous Pierre Shale *(Kp)*, which subcrops in the northwest portion of the project area in Pierce County. Overall, the resistivity of the *Kp* is generally consistent in the 10-12 ohm-m or less range. The *Kp* in this area approaches 200 ft in thickness, as indicated in flight lines 200201 and 200301. The easternmost extent of the *Kp* is near north-south flight line 200601 and along east-west flight line 100501 in east-central Pierce County. South of this location, the *Kp* subcrop shifts westward to where it is present beneath only a small portion of the project area beneath the sand-rich Quaternary material coupled with *To* in Area 4 of the principal aquifer. This unit is not known to produce water in eastern Nebraska, and serves as a basal aquiclude beneath the High Plains aquifer (*To*).

Beneath the *Kp* are the chalk, limestone, and shale deposits of the *Kn*. The *Kn* is the uppermost bedrock unit immediately below the Quaternary deposits across parts of the eastern and southern halves of the project area. The thickness of the formation ranges from upwards of 350 ft in the western half of the project area to less than 20 feet near its terminus in the eastern half of the LENRD. The resistivity profile reveals the lithologic variability in the formation, as resistivities range from around 12 ohm-m to nearly 40 ohm-m. The lower resistivities likely indicate shale and marl, the mid-range resistivities indicate chalk, and the highest resistivities are likely limestone. The *Kn* is not considered a widespread aquifer source in eastern Nebraska, however, beneath the major river valleys of the project area, the uppermost interval of the *Kn* can contain fractures holding groundwater that is in hydraulic connection with the overlying Quaternary aquifer. This condition is evident in flight line 101001 (personal comm. with Sue Lackey, CSD, October 2013).

Underlying the *Kn* stratigraphically is the *Kc*, which consists of interlayered shale, limestone, and sandstone. The maximum documented thickness of this unit is approximately 300 ft (Burchett, 1986). Like the overlying *Kn*, variability in resistivity is present throughout the *Kc*, as well as in the underlying *Kgg*. The variability in resistivity across each of these units created no clear contacts in the AEM data at all locations in the subsurface, thus, test hole data and 2D historic cross sections were relied on to guide the selection of the stratigraphic contacts of these units. Ultimately, these three units were grouped as one unit in the interpretation of the AEM data (light green color associated with *Kc* in the color legend). Collectively, these three units range in thickness from 50 ft near the eastern edge of the project area to nearly 450 ft beneath the western half of the project area. Hydrogeologically, the combined units of the *Kc*, and *Kgg* act as an aquitard locally to the underlying *Kd*.

The lowermost strata in the Cretaceous sequence is the *Kd*, which hosts the Maha aquifer in eastern Nebraska. The *Kd* is present beneath the entire project area with a thickness ranging from 400 to nearly 500 ft on the western edge of the project area to less than 200 ft east of the project area boundary. The formation has pronounced dip westward along profiles 100201 and 100501. The *Kd* has variable

resistivity, ranging from approximately 12 to over 40 ohm-m. The resistive zones in the *Kd* are thicker and more extensive than the overlying units of the *Kc* and *Kgg* and provide potential targets for groundwater development. The area with the highest resistivity levels (40 ohm-m) is found in the eastern half of the district (flight line 201401) at depths ranging from 600 to 700 ft bgl, and an additional area of intermediate resistivity (approximately 16-27 ohm-m) is present beneath the southern half of the district at depths ranging from 750 to 900 ft bgl. An area of less resistive material (10-15 ohm-m) is present in the northwest quarter of the project area and beyond as revealed in the ENWRA flight lines. Due to the lack of geologic test hole or geophysical borehole log control, it is not clear as to whether these more conductive intervals are porous sandstones containing brackish water, shale, or ironstone, all conditions that would cause a lower resistivities to be detected in the survey. This area of the *Kd* is known to have brackish water with total dissolved solids ranging from 1,000 to 5,000 milligrams per liter (Helgesen et al., 1993). With extended intervals of less resistive material, it is possible that the TDS levels are causing the change in the geophysical signature of the *Kd* in this area of the survey.

The bedrock surface topography that underlies the Quaternary materials varies across the project area, from generally flat to pronounced undulation where paleovalleys are filled with glacial outwash, till, or fluvial deposits from drainages existing prior to or during the glaciation of North America during the Pleistocene. Along the northern three flight lines in the district, a ridge in the *Kn* with an eastwardly thinning *To* draped upon this Cretaceous bedrock. The location of this *Kn* ridge also coincides with the western edge of the moraine complex that exists across the district, as well as where some of the thickest intervals of non-aquifer (till and loess) material exists in the northern extent of the project area. Overall, areas of undulating topography in the Cretaceous bedrock occur typically where the *Kn* is the uppermost unit beneath the Quaternary and Tertiary units. In the southern and eastern areas of the district, the Cretaceous-Quaternary contact becomes generally flat.

5.1.4 Paleozoic Stratigraphic Sequence

The depth of investigation for the AEM survey discussed in this report allowed for detection of the Paleozoic strata that underlies eastern Nebraska. As indicated in the geologic time scale and lithostratigraphic sequence (Figure 2-2), Paleozoic units from Permian through Cambrian age are present, primarily consisting of carbonates, evaporites, and clastic material indicative of cyclical transgressions and regressions of shallow seas inundating the region during the Paleozoic Era. Although test hole information was adequate for selection of individual Cretaceous units in the AEM data, sparse information at the depths these units were encountered did not allow for the selection of individual strata. Thus, these units are differentiated by geologic period only (i.e. “undifferentiated Pennsylvanian, Mississippian”), and not by stratigraphic nomenclature.

Undifferentiated *[P* units are the uppermost Paleozoic unit detected by the AEM in the project area. It is present under most of the project area but thins considerably northward from a thickness exceeding 400 ft in the southern half of the district to less than 50 ft in the northeast corner of the district. Resistivities of the *[P* strata are typically 15 ohm-m or below in the project area. Underlying the undifferentiated *[P* strata are *M* units, within thickness of the detected interval ranging from less than

100 ft to over 300 ft in the eastern half of the project area. Resistivities in the *M* strata show more variation than the overlying *[P* materials, with levels ranging from over 40 ohm-m to 10 ohm-m. However, in other areas of eastern Nebraska, resistivity can range higher, exceeding 100 ohm-m in some locations beyond the district bounds in the ENWRA recon lines. The Paleozoic beds detected in the AEM survey beneath the project area show similar westward structural trends as the overlying Cretaceous strata, with a pronounced dip along the west-east profiles. No discernable northward dip is evident in the Paleozoic units beneath the project area. Flight lines 200201 and 200401 display the northernmost extent of the *[P* strata, as these units pinch out near the northern boundary of the district. These units are not widely used as aquifer resources in eastern Nebraska, and further investigations would be required to assess the potential from groundwater development in the Paleozoic units underlying the project area, particularly in the resistive features of the *M* interval.

5.1.5 Resistivity-Lithology Relationship

A critical aspect of a geophysical survey, for whatever purpose, is assessing the nature of the material detected by the geophysical method applied in the investigation. In regards to the LENRD project area survey, assessment of the sediment character, in both the Quaternary deposits and the consolidated strata was conducted to determine the overall composition of the major categories used to define the aquifer and aquitards. A numerically robust assessment of the resistivity thresholds used to characterize non-aquifer, marginal and principal aquifer, including sand-rich intervals in the principal aquifer was calculated. This allows for the characterization of the ranges of resistivities present in the major geologic units described in this report.

It should be noted that many of the e-logs used in this analysis are located beyond the project area bounds, but within the ENWRA reconnaissance line area. These additional points were required to create a population of data points large enough to perform the statistical calculations. The relationship between resistivity and lithology type was assessed by performing an association function that linked nine lithologic descriptor codes for Quaternary sediments used in the CSD test hole lithologic characterization with the resistivity values across that depth interval as indicated in the 33 high-graded resistivity logs utilized in the inversion modeling of the AEM data. With this approach, several thousand points became available for each lithologic description in the test holes used in this analysis. From this list of associated resistivity levels and pre-categorized lithologies, statistical analyses were performed to aide in defining the various thresholds used to determine the aquifer material type in the project area subsurface. The following paragraphs contain descriptions of each analysis performed.

Figure 5-5 displays what is known as a “box and whiskers” plot of the resistivity range for each of the nine unconsolidated materials in the Quaternary system. These plots indicate the spread of the range of resistivities for each of the materials, including the 75^{th} and 25^{th} quartiles, median values, and the maximum and minimum values (whiskers). Included in the background of the plot are the divisions in resistivity between the aquitard and the three aquifer designations in the AEM interpretations. Glacial till (blue) has an interquartile range of resistivities from approximately 17 to 45 ohm-m, with a median value of 25 ohm-m and maximum and minimum values of around 90 and 11 ohm-m, respectively. This

plot indicates that for glacial till, there is a wide spread of resistivity. This should not be unexpected, as glacial till can be composed of a wide variety of unsorted sediment sizes, including gravel and sand intermixed with fines. The spread of resistivities for the lithologies displayed in Figure 5-5 could be an artifact of drilling and sampling methods implemented, the drilling fluid used, or the calibration of the geophysical instrument implemented during the logging.

Silt/loess has a similar resistivity distribution of as glacial till, but with a higher median near 29 ohm-m, and a lower minimum value near 2 ohm-m. This wide range could be a result of silt and loess being combined in one category, where silts from different horizons that are intermixed with other fines such as fine sand or clay could create the wide range in values for this material.

For the lithologic category clay, the median value is close to that for glacial till category, but with a lower maximum value (approximately 40 ohm-m) and lower minimum value (3 ohm-m). These differences should be expected, as glacial till is typically composed of more resistive materials in comparison to clay materials alone.

Silty clay has the lowest median value of the 9 categories displayed in Figure 5-5 (approximately 14 ohm-m). Silty sand and sandy clay each have very similar characteristics in this plot, which should be expected as these lithologic categories are similar.

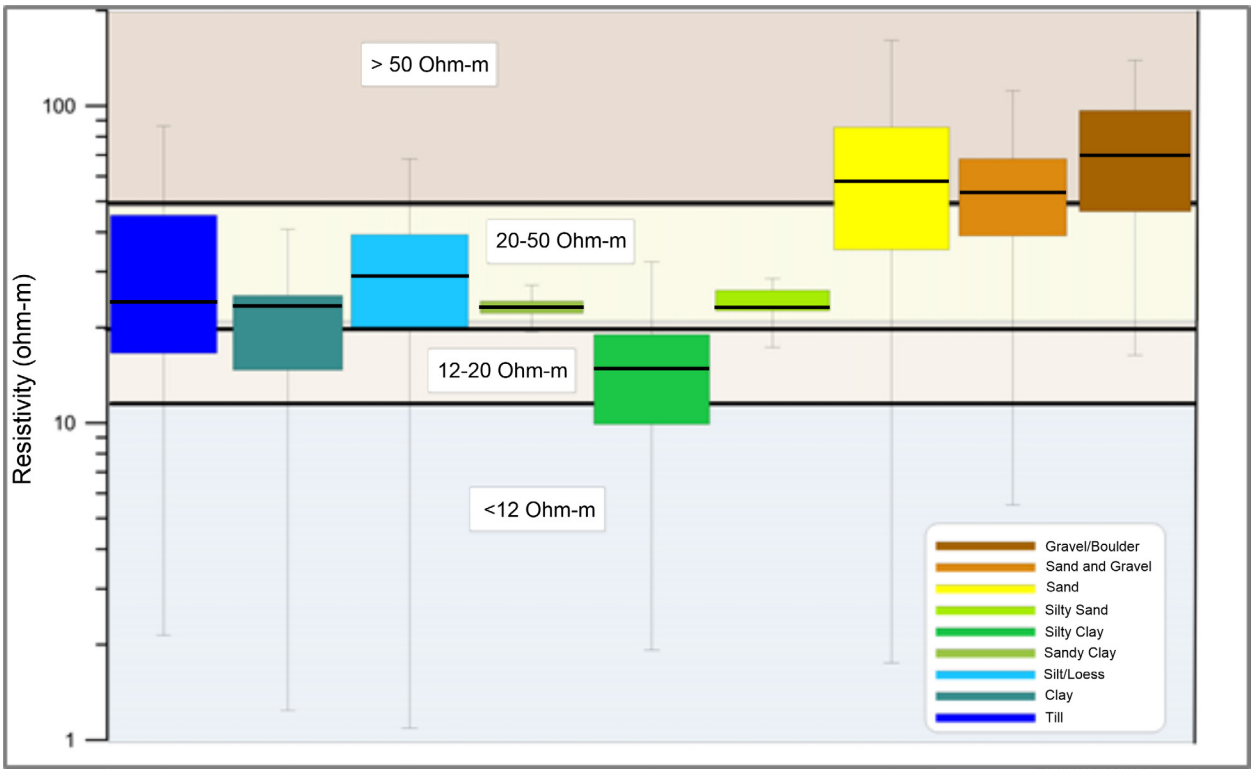


Figure 5-5: Box and whisker plots for the resistivity ranges for the nine most common unconsolidated materials encountered in the Quaternary system.

The distribution of sand, sand and gravel, and gravel and boulder categories are considerably higher than the median and interquartile ranges of the fine materials displayed on the Figure 5-5. The median resistivity of the three coarse sediment ranges is 55 ohm-m or higher, and the lowest 25th quartile (sand) is 35 ohm-m, indicating that 75 percent of the resistivity values for each of these three coarse categories is 35 ohm-m or higher. Sand also has the maximum (117 ohm-m) and the minimum (7 ohm-m) values of the three coarse sediment categories.

Figure 5-6 displays a histogram of the unconsolidated material distribution by frequency count of materials associated with resistivities from the 33 borehole geophysical logs assessed from across the LENRD and ENWRA area. The color-defined bins of the histogram show the thresholds for resistivity used to define the major aquifer material type in the interpretation of the AEM data. Non-aquifer material (blue), shows a distribution on the log-scale x-axis from 1 to 12 ohm-m. This material range corresponds primarily to intervals of resistivity associated with silty clay, clay, silt/loess, and till. The tan area, between 12 and 20 ohm-m, is defined by a mix of fine to coarse sediments, with abundant silty clay still present. The principal aquifer (yellow), is defined by materials ranging from 20 to 50 ohm-m. This interval has a considerable peak of material with a resistivity approximately in the 22-27 ohm-m range and a secondary peak in the 45 to 50 ohm-m range. The fourth category on the histogram represents materials 50 ohm-m and greater, which corresponds to the coarse, sand-rich intervals of the principal aquifer. This interval is considerably lower in the frequency count than the primary aquifer, but by highlighting this interval, discreet sections of the aquifer are revealed showing possible depositional trends in the Quaternary deposits as well as identifying areas where the potential for high-yield wells is the greatest.

Figure 5-7 and Figure 5-8 display pie charts that indicate the distribution of sediment type within each aquifer material range (0-12, 12-20, 20-50, >50 ohm-m). As would be expected, fine materials (silt/loess, clay, till) are the predominant material types for the non-aquifer material (0-12 ohm-m). For marginal aquifer material (12-20 ohm-m), slightly over 14% of the material in this range has a component of sand, with silt/loess, till, and clay comprising over 75% of this range. For principal aquifer material, over 37% of the material consists of coarse materials, and for the coarse portion of the principal aquifer at 50 ohm-m or greater, over 85% of the lithology consists of coarse material.

Figure 5-9 contains the overall distribution of sediment type as indicated in the 39 e-logs used to assess the lithology-resistivity relationship across in the project area (note: data includes e-logs from beyond the project area boundary). Over 48% of the lithologies indicated by the e-logs were categorized as sand, sand and gravel, or gravel and boulders. Silt/loess was the second highest category at 27.2%. This should be expected, considering the presence of silt within the many of the major depositional features in the project area (loess, till, outwash, alluvium). Glacial till is the second most abundant non-coarse material at over 13%. The remaining categories containing some component of clay is just over 10% of the overall distribution.

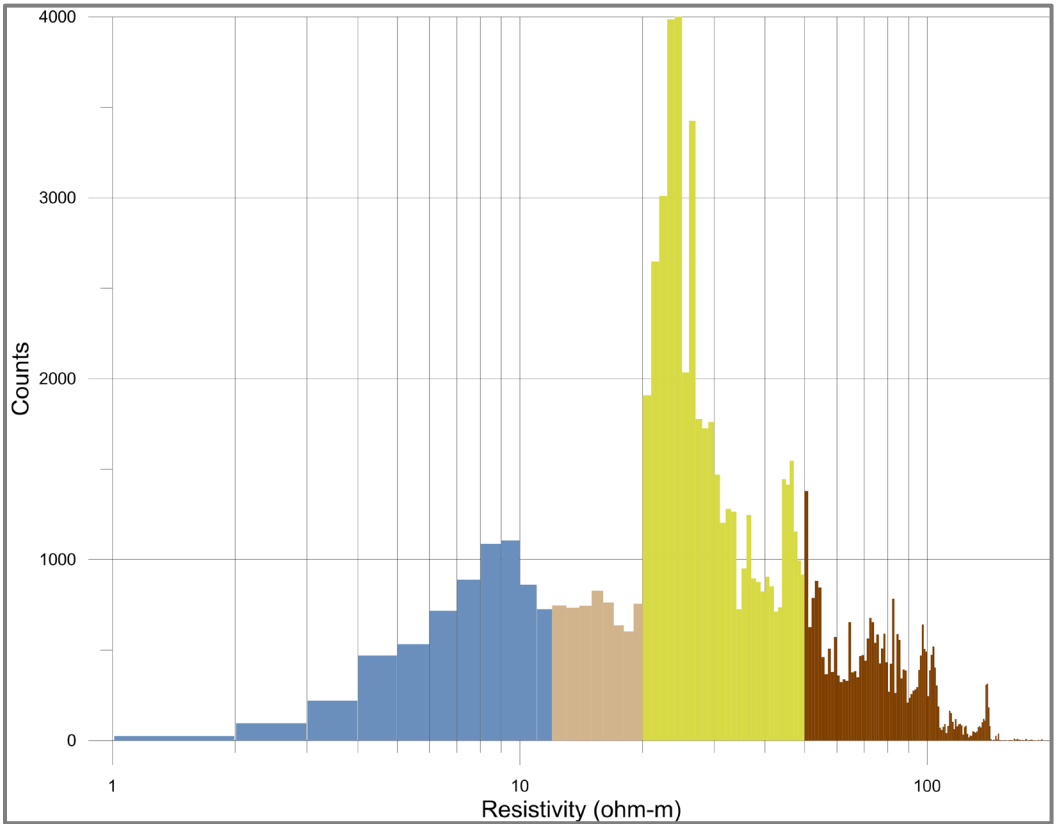


Figure 5-6: Histogram plot displaying the distribution of resistivities by major aquifer material color categories (blue- non-aquifer material, tan- marginal aquifer, yellow- principal aquifer, brown- sand-rich, coarse intervals of the principal aquifer).

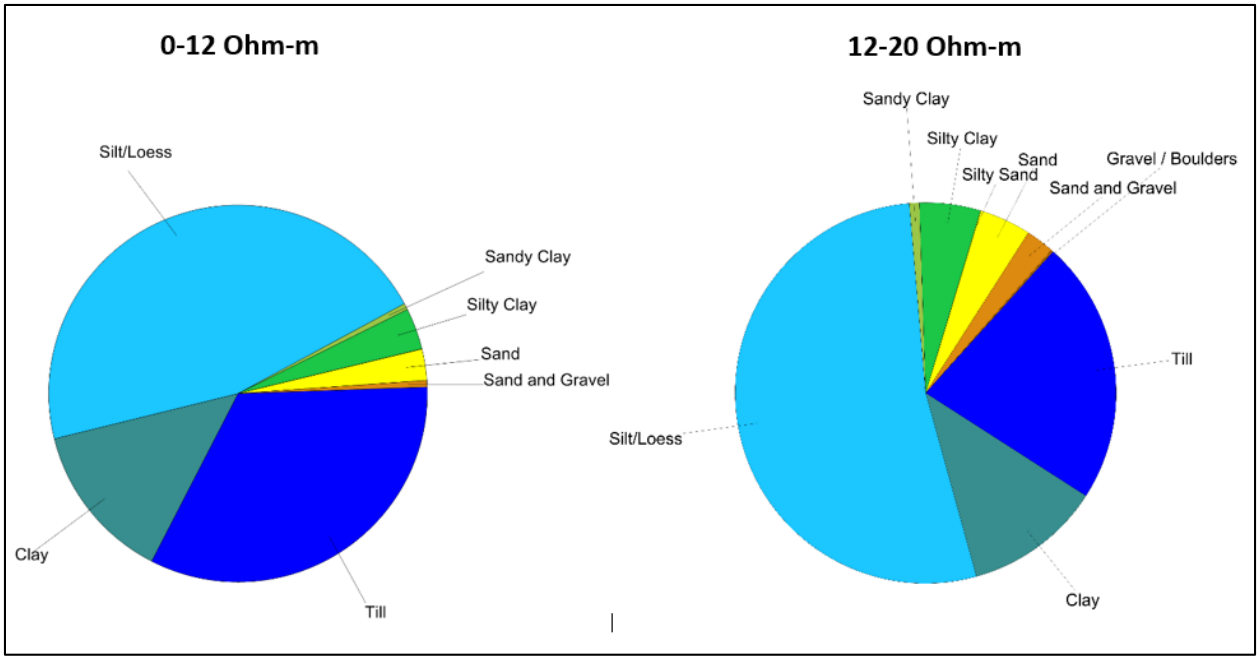


Figure 5-7: Pie charts of the distribution of material within each resistivity range for the four aquifer materials used in the interpretation of the AEM data- 0-12 ohm-m and 12-20 ohm-m.

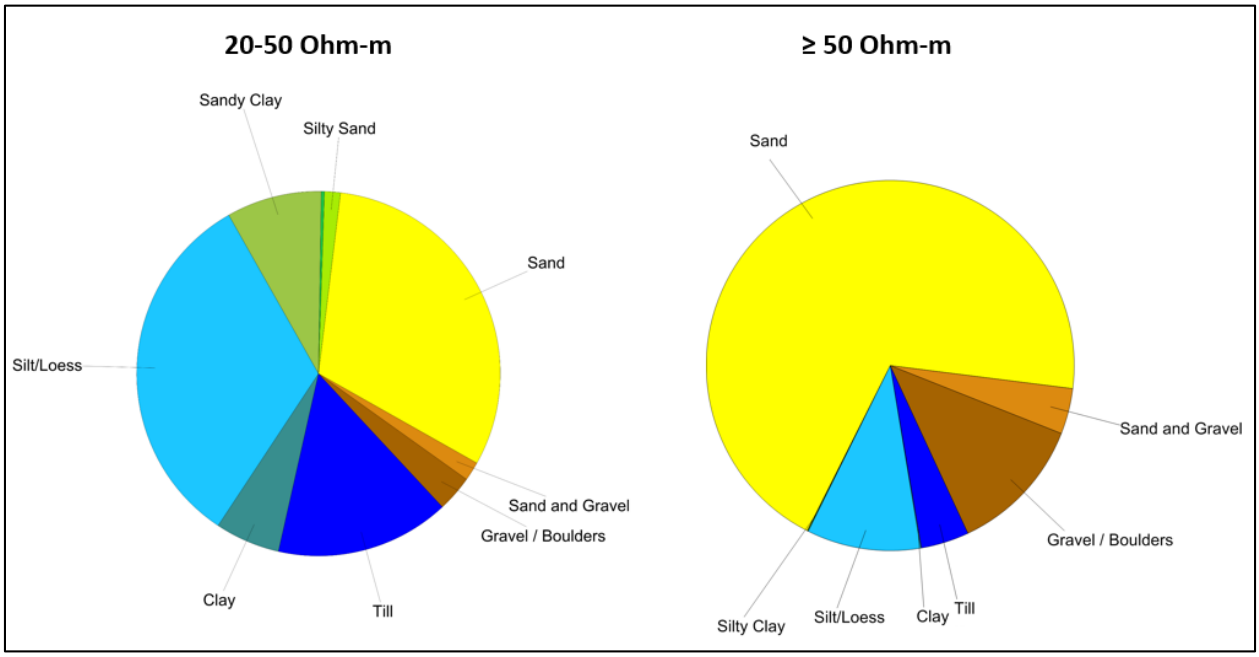


Figure 5-8: Pie charts of the distribution of material within each resistivity range for the four aquifer materials used in the interpretation of the AEM data- 20-50 ohm-m, and 50 ohm-m and above.

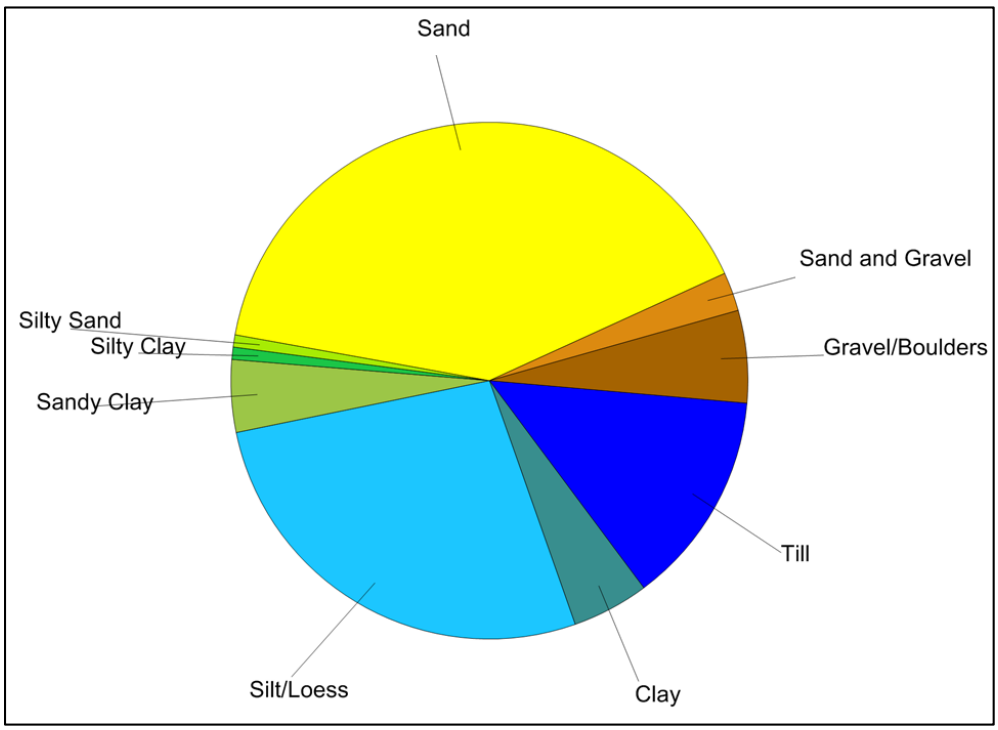


Figure 5-9: Pie chart of the overall lithology indicated in the 33 e-logs used to characterize the relationship of lithology and resistivity in the project area.

Figure 5-10 displays four pie charts showing overall percentage of lithologies in selected CSD test holes located within the project area. These charts are displayed with the CSD glacial till thickness map set in semi-transparent shading to demonstrate the relationship of the percentage of each major material

with the extent and thickness of the till within the district. At CSD test holes 8-A-53 and 4-A-52, the glacial till component in the holes are the largest of the four locations analyzed, with nearly two-thirds of 8-A-53 consisting of glacial till. Test hole 4-A-52 has a larger sand component, which is likely a result of this hole being located above the 50 ohm-m or greater, sand-rich zone of the principal aquifer north of Norfolk. Each of these locations are situated where the CSD map indicates till to be present. At test hole 16-A-55, which sits at the western edge of the extent of glaciated region of eastern Nebraska, till is absent, with sand and sand and gravel comprising nearly half of the borehole's lithologic content. The remaining half is predominately silt/loess with minor amounts of clay and silty clay. This hole is located near the sand-rich Area 5 of the principal aquifer defined in Figure 5-3. Finally, test hole 5-GT-80, located just west of the city of Wayne and in the area defined as primarily marginal aquifer or non-aquifer material, the pie chart reveals the predominant material in the hole was silt/loess (two-thirds), with the remaining one-third characterized as sand. This hole is located within an area demarcated with an absence of glacial till. In AEM profile 201401, the distribution of material in this hole is predominately silt/loess, with only minor intervals of sand, which matches closely with the pie-chart distribution. The hole sits on the edge of a body of marginal aquifer that contains small intervals of principal aquifer material. This hole thus demonstrates that silt-sized particles can still be considered part of the marginal aquifer in the AEM interpretation if sand intervals are also present.

Figure 5-11 displays a box and whiskers plot of the resistivity distribution for the bedrock strata described in the interpretation section, including the *To*. Analysis of the bedrock data was conducted on CSD test holes that penetrated into the bedrock. It also included oil and gas wells with data on Paleozoic strata. The median resistivity values for each unit in Figure 5-11 are 40 ohm-m or less, with the exception of the undifferentiated *M* strata, which has a considerably higher distribution than the other formations, with 75% of the data greater than 100 ohm-m. *Kp* has the lowest median (9 ohm-m) and lowest overall value of resistivity, as would be expected for a unit predominately composed of shale. *Kn* and *Kd* have similar distributions and maximum/minimum ranges, with one exception being the *Kd* having a lower median resistivity (approximately 20 ohm-m). The similarities in these two units on this plot exemplify how the *Kn*, which is predominately a shale and chalk, can contain resistive material, and the *Kd*, predominately a sandstone, can contain shale and other more conductive material. The *KcKgg*, and the undifferentiated Paleozoic strata also have similar resistivity characteristics, with median values around 16 ohm-m. The *To* has the narrowest distribution band of the formations displayed in Figure 5-11, with maximum and minimum resistivities (whiskers) of 45 and 12 ohm-m, respectively. The median value in the *To* is 30 ohm-m, a value that would be expected of interlayered sandstone, siltstone, sand, gravel, and silt. This narrow distribution for the *To* could be a result of the distal location of these sediments from their source area along the Rocky Mountain front in Colorado and Wyoming.

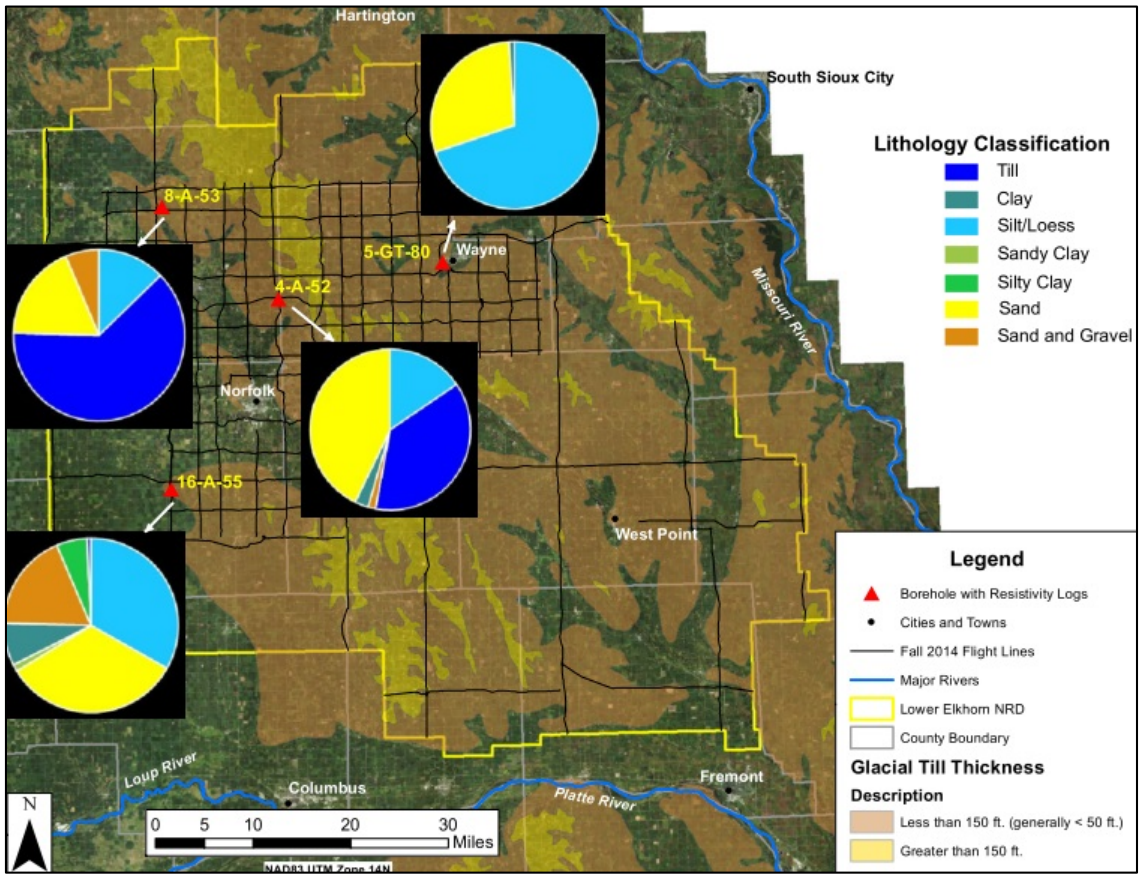


Figure 5-10: Pie charts showing overall percentage of lithologies in selected CSD test holes.

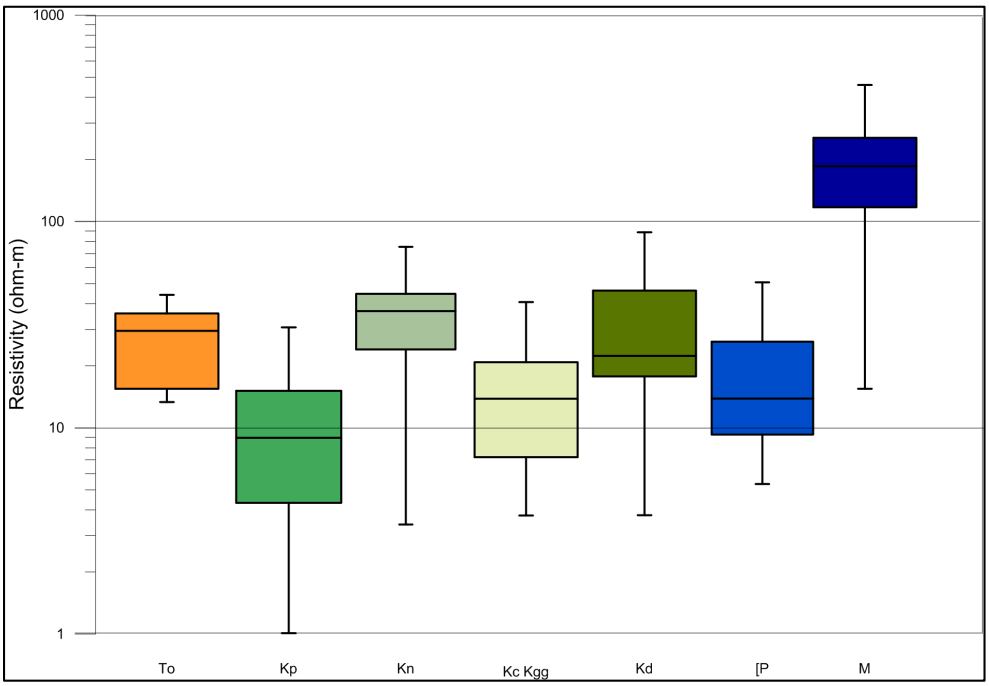


Figure 5-11: Box and whiskers plot of the resistivity distribution of the Cretaceous and Paleozoic bedrock units discussed in the interpretation of the AEM data.

Review of the NOGCC database provided two holes with electrical logs within three miles of a flight line. These were wells 2616718000API and 2616721003API that were 5186.2 ft and 12828 ft, respectfully, from the flight lines. These allow comparison of the AEM inversion model to some NOGCC resistivity logs. Figure 5-12 displays the electrical resistivity logs compared with the closest AEM sounding. It is important to note that the resistivity logs started well into the Cretaceous strata. However, there is a good match to the AEM resistivities at depths in excess of 1000 ft. It is also important to note that the averaging effect of the AEM models to smooth out the thin resistive units around 600 ft in 261671900 and 500 ft in 2616721003. The logs compared to the AEM clearly indicate the inflection in the resistivity logs at 400 ft. This further provides assurance that the AEM is mapping the resistivity structure of the bedrock within the survey area of the LENRD.

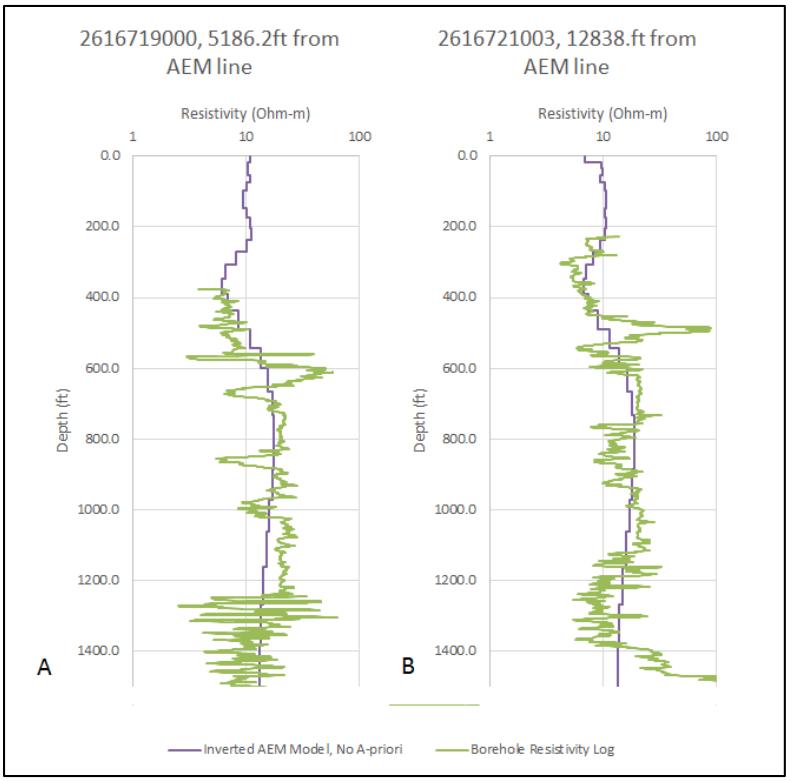


Figure 5-12: Deep Oil and Gas borehole resistivity logs compared with inverted AEM models. A: Well 2616719000, 5,186 ft from the AEM line, B: Well 2616721003, 12,838 ft from AEM line.

The statistical plots presented in this section for the Quaternary deposits might reveal possible bias for a higher resistivity than expected, particularly for glacial till, as well as the category for sand having such a wide range in resistivities (Figure 5-5). As mentioned above, the spread of resistivities for glacial till in Figure 5-5 could be an artifact of drilling and sampling methods implemented, the drilling fluid used, or the calibration of the geophysical instrument implemented during the logging.

The region north of Norfolk and the Elkhorn River and west of Flight Line 200801 is underlain by the most prolific aquifer material in the district. This area appears to have a combination of depositional environments providing potential for optimal groundwater development including the presence of *To*,

the presence of glacial outwash deposits that are sourced from the glacial margin to the east. Recent deposition of alluvium from eastward meandering drainages, including former channels of the North Fork of the Elkhorn and Elkhorn Rivers contribute to the overall aquifer resources in the western half of the district.

5.1.5.1 Sensitivity Evaluation of the Lower Principal Aquifer Material Thresholds

Based on the discussion above in Section 5.1.5, the Quaternary and Tertiary material were separated into four characteristic aquifer materials including non-aquifer (aquitard), marginal, principal, and coarse aquifer material. These breaks were determined based on the distribution of the resistivities (Figure 5-6) and the lithology (Figure 5-7 and Figure 5-8). However, the question can arise as to the sensitivity of the selection of the thresholds, specifically the lower threshold for the principal aquifer material (20 ohm-m). In order to assess this sensitivity, a test was conducted by analyzing the data set with thresholds of 20 and 21 ohm-m. The change in the percent thickness of the principle aquifer material was then calculated over the complete data set. It is important to note that the thickness was evaluated as being greater than or equal to both 20 and 21 ohm-m. For each of the thresholds (20 and 21 ohm-m), the materials were calculated based on the methodology outlined in Section 5.0. The thicknesses of the principal aquifer material were then compared using the following:

$$T_{Diff} = \frac{abs(T_{20} - T_{21})}{T_{20}}$$

where T_{Diff} is the fractional difference in thickness, T_{20} is thickness of the principle aquifer material with resistivities greater than or equal to 20 ohm-m, and T_{21} is the thickness of the principal aquifer material with resistivities greater than or equal to 21 ohm-m.

This calculation was carried out for all data points within the 2014 flight area, including the ENWRA and the LENRD flight areas (Figure 5-13). The statistics of this change in thickness analysis indicate that the median fractional difference is at 0.04, or 4%, and a first quartile of 0.01 (1 percent), and a third quartile of 0.10 (10%). This means that 75% of the data indicates a thickness change of the principal aquifer materials of less than 10% when comparing thicknesses derived from both 20 ohm-m and 21 ohm-m thresholds. Thus Figure 5-13 displays a histogram of the distribution of the variation in interpreted thickness of the principal aquifer material using 20 and 21 ohm-m thresholds.

This analysis indicates that the sensitivity of picking 20 or 21 ohm-m is relatively insignificant for the overall interpretation of the thickness of the principal aquifer materials. Figure 5-14 demonstrates the impact on the interpreted cross sections with an example cross section showing both 20 and 21 ohm-m thresholds.

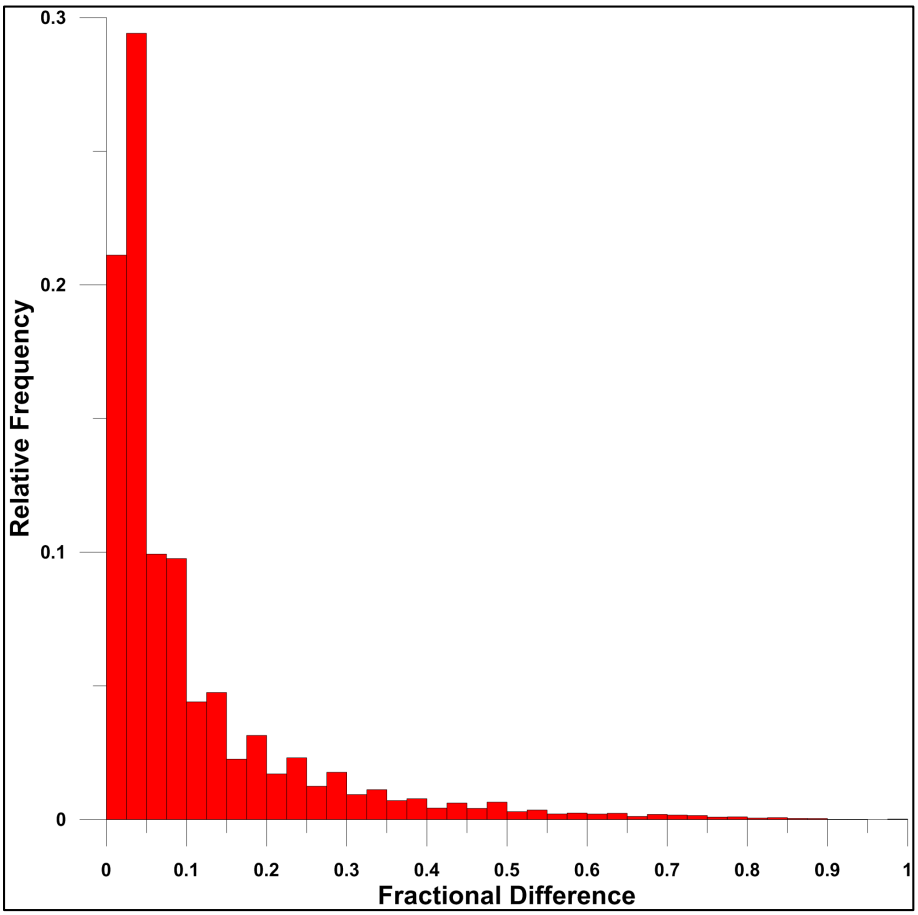


Figure 5-13: Histogram of the distribution of the fractional difference in the thickness of the principal aquifer materials using 20 and 21 ohm-m resistivity thresholds.

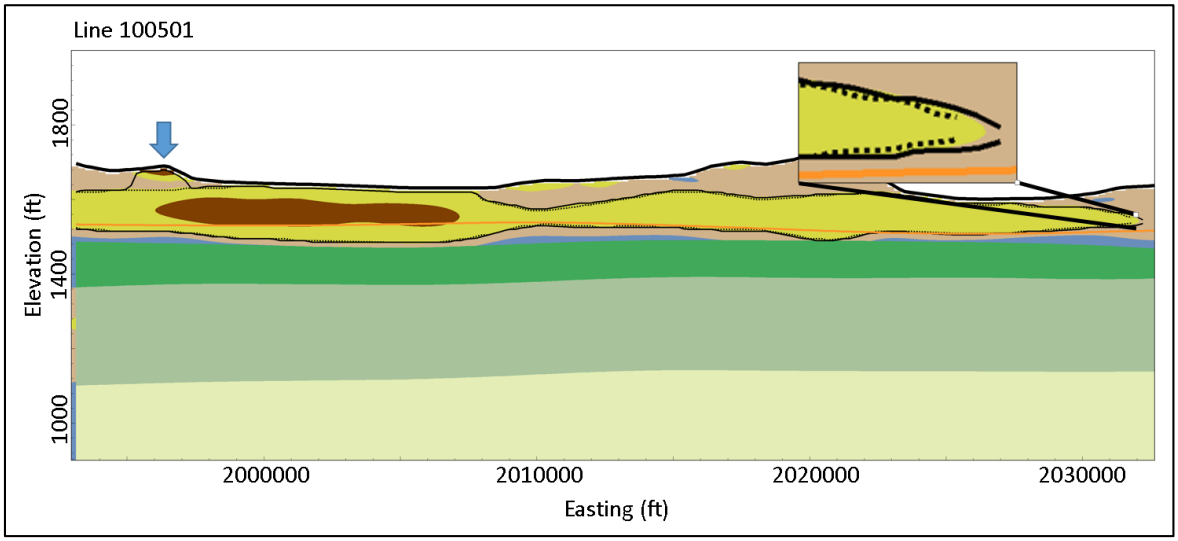


Figure 5-14: Example cross section illustrating the small difference between selecting a 20 ohm-m threshold or a 21 ohm-m threshold to define the principal aquifer. The solid black line enclosing the yellow (principal aquifer material) represents the 20 ohm-m threshold and the dotted black line enclosing the principal aquifer material represents the 21 ohm-m threshold.

Figure 5-14 shows that the area encompassed by the 20 ohm-m threshold (solid black line) is slightly greater than the 21 ohm-m aquifer extent (dotted black line), which results in a thicker estimation of the principal aquifer material. This result is not unexpected as the lower resistivity value should encompass a larger range of resistivities of greater than or equal to 20 ohm-m. However, it can also be observed that the change in the interpretation is generally insignificant (see zoomed-in view in Figure 5-14), as the change in overall extent, when viewing the principal aquifer materials on a regional basis, is negligible when considering overall volume of the aquifer. It should be noted that in some areas where principal aquifer material is present at the land surface (indicated by blue arrow in Figure 5-14), but separate from the underlying main body of principal aquifer material, these intervals were included in the interpretation even if these features were separated by marginal aquifer material. This approach was warranted since this interpretation is a discussion on the major aquifer features in the subsurface of the LENRD. Surficial resistive materials are considered critical in assessing areas of aquifer recharge and, thus, are included in the principal aquifer zone even where separation from the main principal aquifer materials can occur.

In summary, the results of this sensitivity analysis indicate that for 75% of the data, a thickness change of less than 10% occurred between a threshold change of 20 to 21 ohm-m. Overall, the interpreted principal aquifer materials show a stable solution that is not sensitive to a 1 ohm-m change in the principal aquifer material threshold.

5.1.6 Comparison with CSD Geologic Cross Sections and Test holes

Overall, the AEM profiles generally match the historic and contemporary (Divine et al., 2010; Korus et al., 2012) used in the AEM interpretive analysis. The multiple cross sections (Figure 5-15 and Figure 5-16) provided an additional background information dataset in the geologic interpretation process, which proved particularly useful in areas of the Cretaceous strata where units showed similar resistivities. The AEM profiles provide a resource for refinement of geologic cross sections previously created in eastern Nebraska, particularly in areas where formation contacts were estimated due to lack of test hole control.

AEM has an averaging impact on the imaging of the subsurface, such that, sometimes, the inverted geophysical data cannot identify fine lithologic details that can be gleaned from test hole logs such as thin laminae within thicker deposits or interbedded layers of a single formation. An example of this condition exists near the city of Wayne, NE. In this area, the Quaternary material is considered marginal aquifer to aquitard. When the AEM is compared to the CSD test hole and cross section information, it is clear that the details of the interbedded nature of fines and sands beneath this area cannot be identified from the AEM inversion results. Figure 5-17 shows the AEM model inversion fit to the data near CSD test hole 5-GT-80 (just west of Wayne). This plot exemplifies the nature of the aquifer throughout much of the eastern half of the project where isolated bodies of aquifer material, either marginal or principal, are interlayered with aquitard material. The lithology profile in Figure 5-17 displays the limited vertical intervals of coarse materials available for designing screen intervals in wells where these geologic conditions persist.

Registered wells in this area of the LENRD are capable of producing upwards of 200 gpm. Thus, the screened intervals in these wells include enough thin layers of sand interbedded with clay and silt that they can yield suitable flow rates for productive wells (e.g. near CSD test holes 9-A-64, 10-A-64, 30-A-51 of flight line 100501 (Figure 5-18)). Figure 5-19 includes a zoomed in view of flight line 100501 demonstrating this condition. The important consideration in this example is that the regional nature of the grids flown in the project area does not have the additional supporting data of closely spaced flight lines to assist in resolving the finer nature of some of these thinner aquifer materials. Even with additional flight lines, it is still possible that the thin beds could not be resolved. The AEM data and analysis have the ability to provide a view of the subsurface that provides a more scale-appropriate view of the aquifer materials for inclusion into groundwater models. This is due to the difficulty, due to averaging, in developing models for the NRD that could include all the fine details of interlayered deposits. A bulk average aquifer property would need to be used.

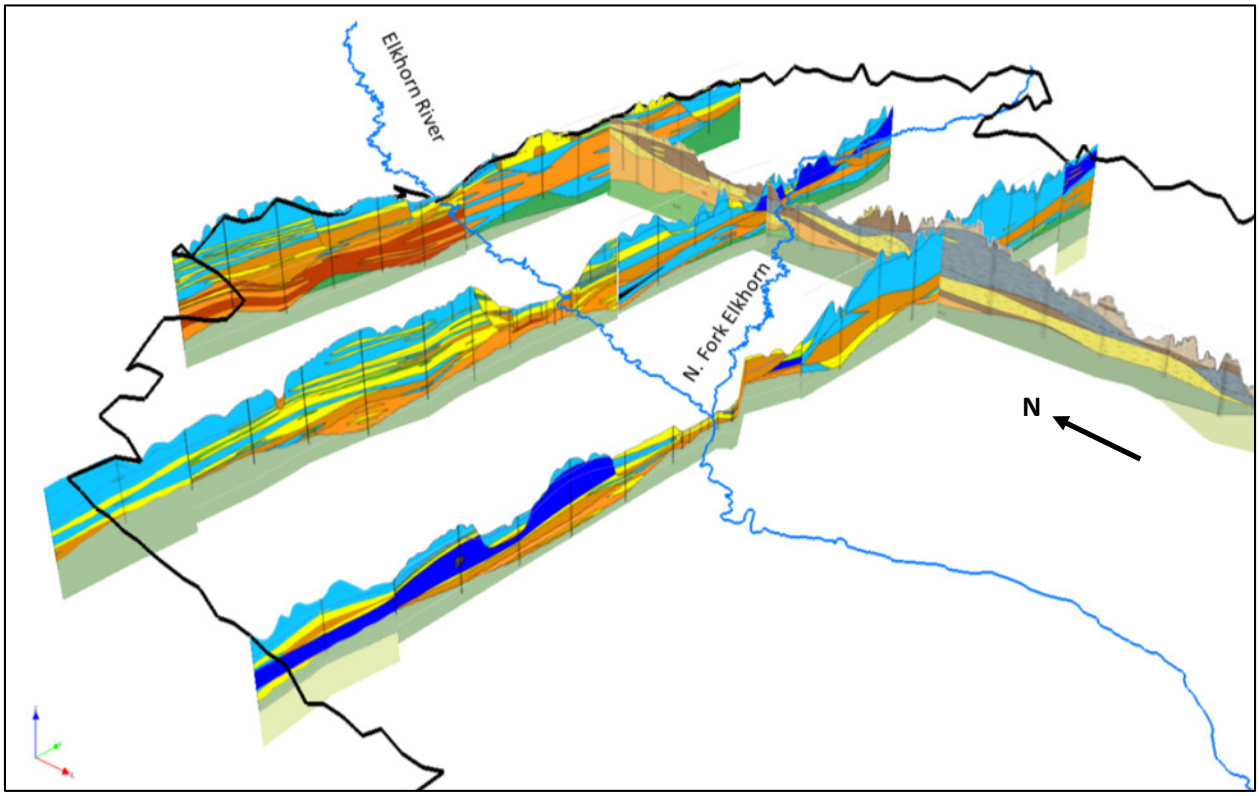


Figure 5-15: Northwestward view of LENRD project area displaying the locations of historic and contemporary CSD geologic cross sections.

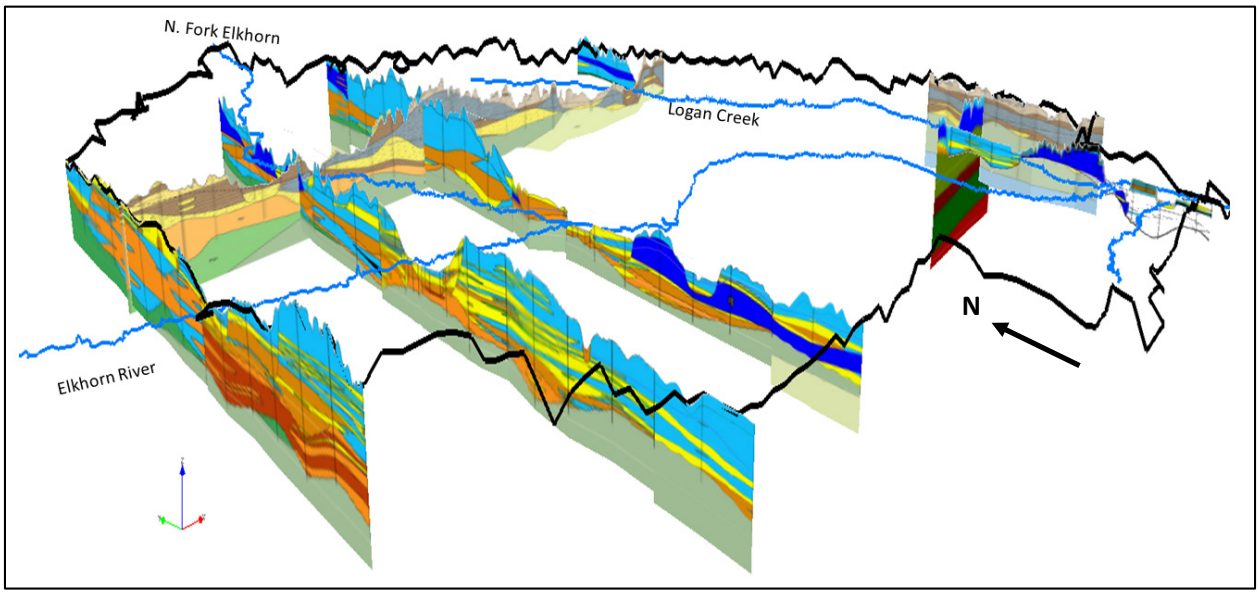


Figure 5-16: Northeastward view of LENRD project area displaying the locations of historic and contemporary CSD geologic cross sections.

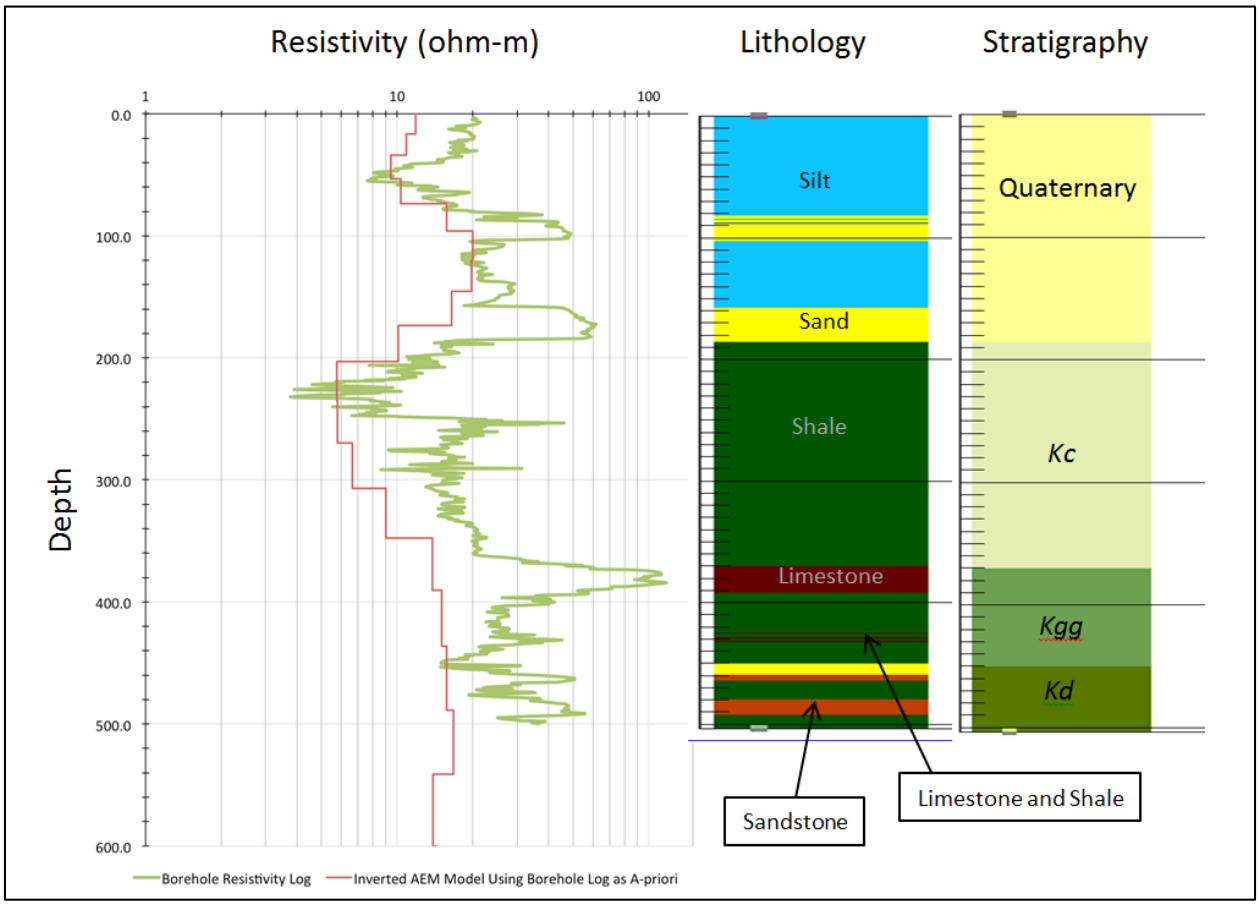


Figure 5-17: Comparison of the TEM inversion model, borehole log, lithology, and stratigraphy at CSD test hole 5-GT-80.

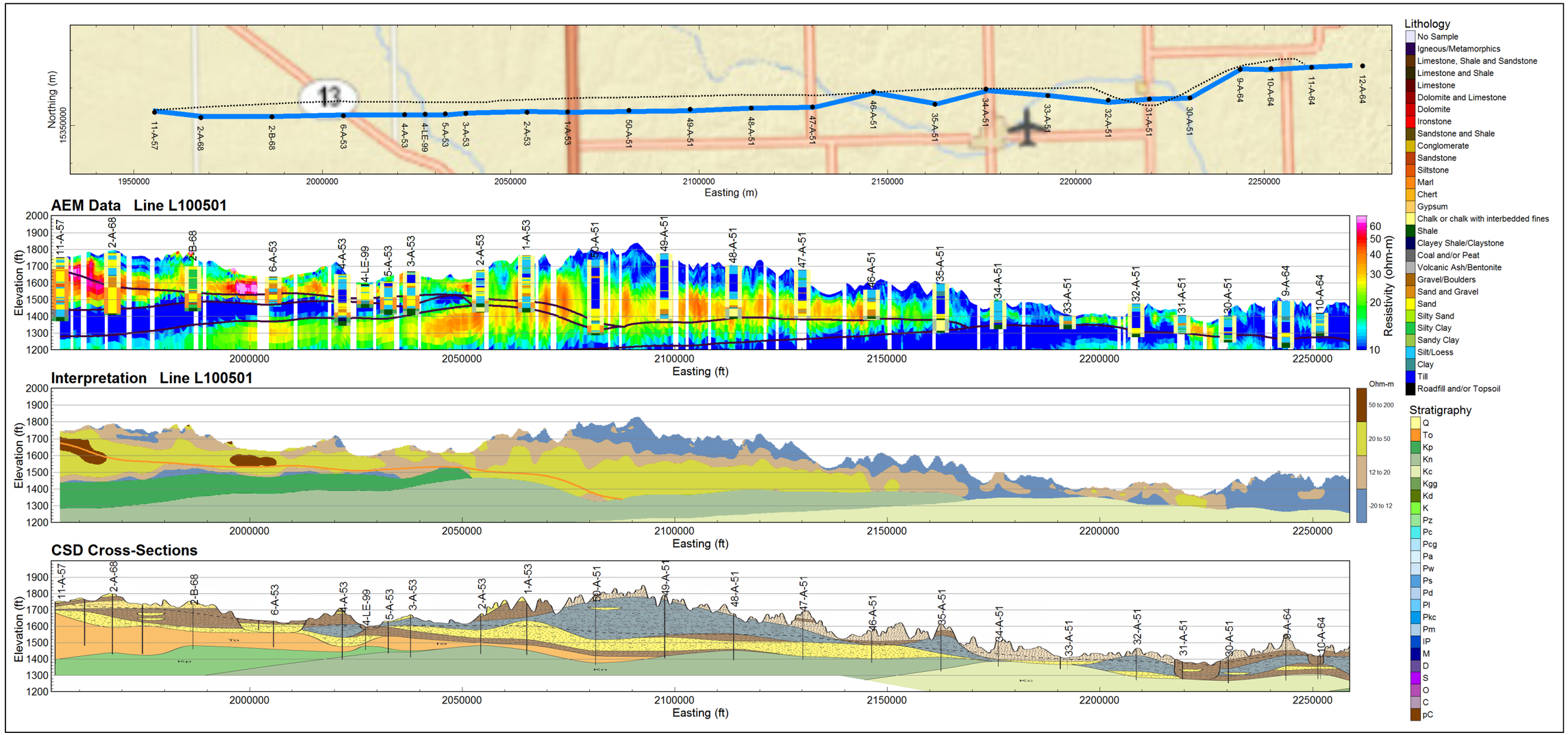


Figure 5-18: Combined display of AEM data (second panel), hydrostratigraphic interpretation (third panel), and CSD cross section (bottom panel) for flight line 100501 near Wayne, NE. The locations of the AEM flight line and CSD cross section are displayed in the top panel.

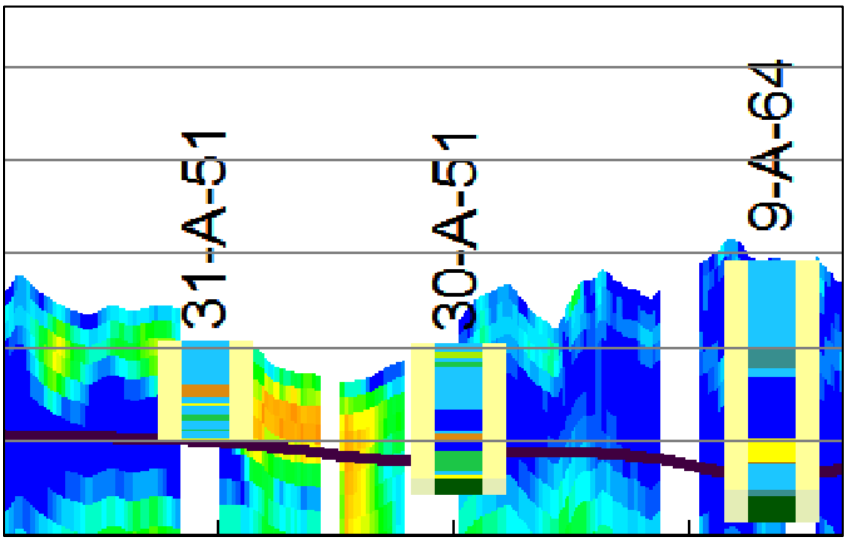


Figure 5-19: Zoomed-in view along the eastern extent of AEM flight line 100501, demonstrating the thin intervals of material indicated in the test hole logs that correspond to only the averaged resistivity data across intervals of greater thickness. This is particularly evident in 31-A-51 and 9-A-64.

Along AEM flight line 100501, near wells 11-A-57, 2-A-68 and 2-B-68, the CSD test holes and cross sections are closely matched. The nature of the AEM, acquiring a TEM sounding approximately every 250 ft apart, allows for additional information to be applied for refining cross sections between test holes. The comparison between the Quaternary materials and the *To* shows similar contacts in the cross sections between AEM interpretation and CSD cross sections. Each of the three profiles displayed in comparative figures mutually support and lend strength to the final interpretation of the hydrogeologic section. The CSD cross sections are particularly useful in that they provide information that fills in gaps in the AEM survey where data was missing (blank vertical lines) to produce the interpretative cross sections.

Line 101601 (Figure 5-20) was flown across the Oakland, NE area. This flight line was included in a 2007 AEM survey (Abraham et al., 2011) during the first project year of ENWRA. The Oakland area was chosen in 2007 to be the test area for using AEM to image heavy glacial sediments at depth to map the underlying aquifer material. The system used was an airborne frequency domain AEM system with a limited depth of penetration in these sediments due to large amounts of electrically conductive clay and silt. Near test holes 50-A-50, 2-EN-06, and TH-01-OAKLAND, a paleochannel is known to exist that was not imaged in 2007. Using the 2014 AEM time domain system, this subsurface feature was indeed imaged. The AEM matches the test holes and the CSD cross sections closely in this area. From this assessment, the paleochannel is considerably wider than previously thought, information that can assist LENRD managers in better understanding the availability of groundwater in this area.

Note the profiles displayed in Figure 5-18 and Figure 5-20 are included in larger, 11x17 inch, landscape page format, in Appendix 2 along with the remainder of the AEM profile-interpretive section-CSD cross section figures in Appendix 2.

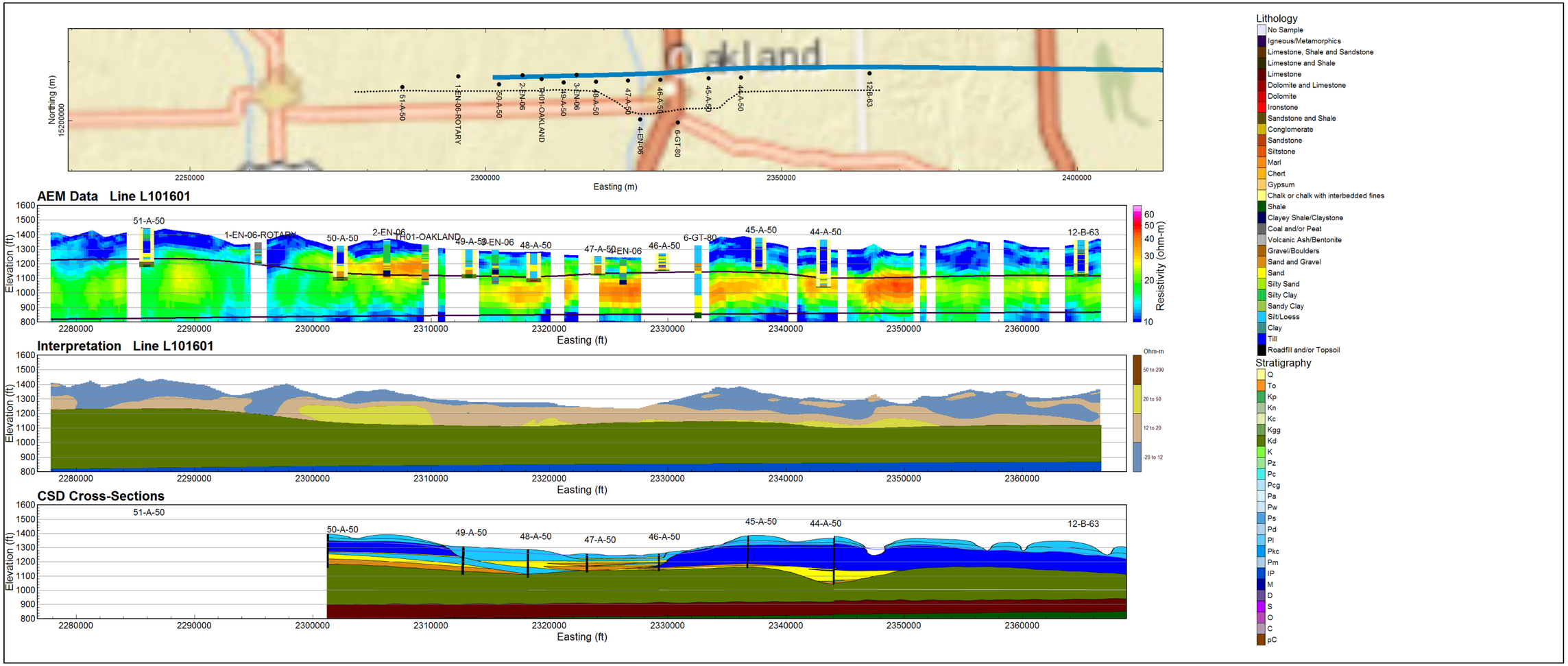


Figure 5-20: Combined display of AEM data (second panel), hydrostratigraphic interpretation (third panel), and CSD cross section (bottom pane) for flight line 101601 near Oakland, NE. The locations of the AEM flight line and CSD cross section are displayed in the top panel.

5.2 Summary and Recommendations

5.2.1 Key AEM Survey Findings

The AEM survey of the project area provided a wealth of information of the subsurface at the three mile flight line spacing implemented for this project. The hydrostratigraphic model was able to detect strata as deep as the Paleozoic units beneath northeastern Nebraska, with the depth of investigation exceeding 1200 ft in places. The following bulleted list of items summarizes the key findings resulting from this survey:

- Aquifer resources beneath the survey area vary considerably within the Quaternary and Tertiary system, with most of the principal aquifer located in the western and southern thirds of the project area. Within the principal aquifer, seven distinct bodies of sand-rich principal aquifer (>50 ohm-m) were identified, with most of these areas being at least 100 ft thick and located close to the land surface. Some of these areas were nearly 200 ft thick. Two of these sand-rich areas are crossed by the North Fork of the Elkhorn and the Elkhorn Rivers, which indicates the potential for hydraulically connected conditions between the principal aquifer and these surface water features. Marginal aquifer is the predominant groundwater source in the eastern one-third of the project area, with other smaller zones of this material in the southern half of the area surveyed. This aquifer material typically underlies thick sequences of till and loess, and in many places, the materials are disconnected. This condition is reflected in the irrigation well density in this area, where there are approximately six times fewer irrigation wells per square mile than in the western one-third of the project area.

- The Quaternary system component of the principal aquifer is underlain by Tertiary *To* material under much of the western half of the project area. The thicknesses vary from 150 ft on the westernmost flight lines to near zero near flight line 200801. It is likely that these separate material types (Quaternary and Tertiary) act as one aquifer unit or are in close hydraulic communication. It is possible that some siltstone layers common in the *To* could create local varying conditions in the vertical gradient between the two systems.

- Non-aquifer (aquitard) materials are most abundant in the central and eastern portions of the survey area, with till and loess sequences exceeding 200 ft in some locations. Basal till is also present in much of this area of the survey, and fine deposits are interlayered throughout the marginal aquifer area of the eastern one-third of the survey area. West of this area, the thinner intervals of non-aquifer material are predominately loess deposits.

- The full sequence of Cretaceous strata present in eastern Nebraska was detected by the AEM system. Most units displayed unique resistivities that allowed for identification of the individual formations with the use of test hole information. One exception to this was the similarity

between the *Kc* and the *Kgg*. Thus, these units were lumped as one stratigraphic unit in the hydrostratigraphic interpretation, which was considered appropriate since these units are not known aquifer resources in eastern Nebraska and act as confining units to the underlying *Kd*.

- The full thickness of the *Kd* is revealed in the AEM survey. The AEM data captured the variability in resistivity in this formation, which provides an inventory of potential drill targets in this formation for possible bedrock aquifer development. The most extensive areas of the *Kd* with resistivities 16 ohm-m or greater are in the eastern and southern thirds of the survey area. The *Kd*, which hosts the Maha aquifer in eastern Nebraska, is a viable groundwater resource where the sandstone has suitable permeability and porosity.

Underlying the Cretaceous strata are *P* and *M* strata. The *P* material have resistivities similar to the overlying Cretaceous deposits, whereas the *M* deposits have a considerable variation in resistivity that are typically higher than the younger formations sitting above. Neither of these Paleozoic intervals are utilized for groundwater over widespread areas in eastern Nebraska.

5.2.2 AEM Survey Gridline Spacing

One of the primary objectives from the evaluation of the processed AEM data was to assess the appropriate AEM flight line spacing distance for evaluating hydrogeologic resources over areas of various extents, particularly in the glaciated terrain found in eastern Nebraska and much of the upper Midwest. The original project area survey grid layout was spaced at 3 miles between flight lines. Final line spacing, however, ranged from two to five miles due to infrastructure across the district (the spacing for this survey will still be referred to as a spacing of three miles in this report). Evaluation of the hydrostratigraphy detail revealed in the AEM survey, from the three mile spacing for the project area, or the 10 mile spacing applied in the ENWRA reconnaissance flights, indicates that no “one size fits all” spacing plan is applicable for all areas. Rather, this evaluation reveals that overall project objective and geology of interest dictates the flight line density required to complete a successful AEM survey of an area.

The three mile line spacing utilized in this survey is deemed appropriate to characterize the overall general hydrostratigraphic framework of a glaciated landscape covering an area on the order of 1000 to 2000 mi^2 (the areal extent of many NRDs in eastern Nebraska). As indicated in Figure 5-3 (3-D view from south), the major characteristics and trends of the Quaternary system that hosts the principal aquifer are clearly evident. The framework defined by the three-mile flight line arrangement allows LENRD management to visualize and understand the extent, thickness, and transmissive character of the principal aquifer across the district. At any location of interest within the district, an exploratory well would be on average no more than 1.5 miles from a flight line. Additionally, the framework based on the three-mile flight line spacing reveals other key characteristics of the project area’s hydrogeology, including the extent of confining materials, potential recharge areas, aquifer connectivity with surface water, and the relationship of the principal Quaternary aquifer materials with underlying bedrock units. This level of framework detail provides the LENRD with a digital inventory of key hydrogeologic

characteristics of the district and provides a basis for identifying initial hydrogeologic conditions where more local, detailed characterization is required. It is recommended that for a district-scale survey of Quaternary deposits as presented in this report, the spacing of flight lines does not exceed three miles. This is particularly important in locations such as in the eastern half of the district where principal aquifer deposits are considerably more dispersed than in other parts of the district. A spacing of flight lines greater than three miles could further limit the survey's ability to detect these features.

Although the three-mile grid is considered appropriate for district-scale surveys, a denser grid spacing is required for smaller, specific water supply projects such as the survey conducted for the towns of Clarkson and Howells, NE in the southern portion of the LENRD in 2013 (Abraham et al., 2013). This density is necessary to capture local-scale detail and changes in the subsurface character, conditions that typically occur in glaciated settings. With the three-mile grid spacing, small glacial outwash deposits such as what was revealed in the AEM survey near Clarkson would not have been detected (Figure 5-21).

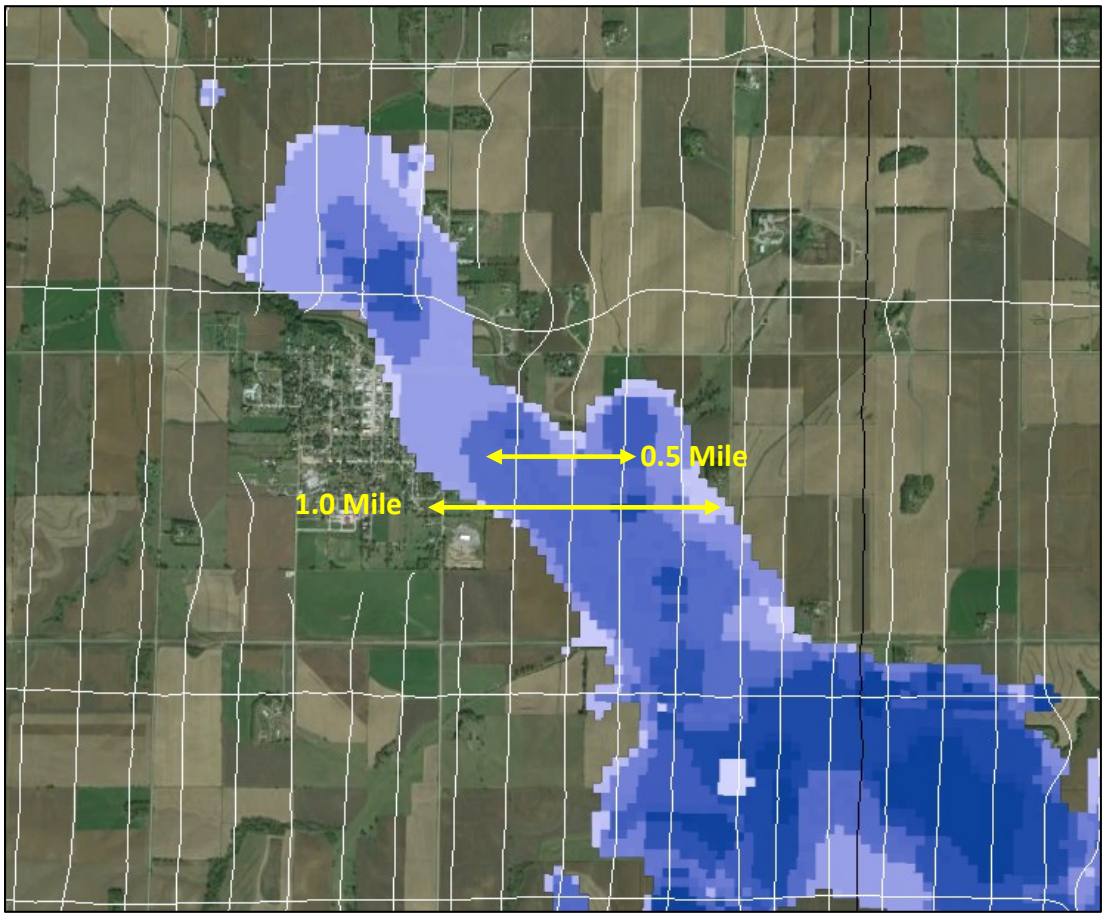


Figure 5-21: Display of aquifer material near Clarkson, NE with a 700 ft grid line spacing. The yellow lines demonstrate how some portion of the aquifer would have been missed if the AEM flight line spacing were set at 0.5 or 1.0 miles.

These features are critical for supplying small municipal systems. Thus, it is recommended that for surveys smaller than 100 mi^2, flight-line spacing should be in the range of 600 to 1500 ft distance to capture local features in the subsurface that could be critical to groundwater development and management.

The flight line spacing necessary, in eastern Nebraska, for characterization of the bedrock strata is less stringent than the recommended spacing for delineating the Quaternary system. Review of the stratigraphic detail in the AEM data indicates that the character of the bedrock units in the project area has less variability than the overlying Quaternary deposits. At a spacing of 3 miles, the AEM survey reveals bedrock structure and features in detail. The features detailed in the subsurface profiles, however, are only true for locations in close proximity to the flight lines, as remnant bodies of strata disconnected from the main extent of the unit may be missed with this three mile spacing distance. Evaluation of AEM data at the recon line spacing density (10 miles) also reveals the general trend in stratigraphic character (thickness, extent, structure) of the bedrock units beneath the project area. Although minor remnant or "pinch-out" features could be missed at flight line spacing of 10 miles, this spacing is still considered adequate for district-scale surveys intended to characterize general trends in bedrock units that may host aquifers. Just as recommended with smaller scale issues in the Quaternary system, closer grid spacing is required to map local bedrock features for water supply studies, particularly with identifying and characterizing resistive intervals within bedrock units such as the *To*, *Kd* (Maha aquifer), and in limited areas of fractured *Kn* shale. Because of the similarity in the lithologic character of the Quaternary system and the *To*, the three mile line spacing is appropriate for the Tertiary deposits as well.

At the three mile grid spacing, the detail in the subsurface information is not suitable to create 3D voxel models of aquifer features. The previous example from the Clarkson, NE area demonstrates how densely collected data provides the ability to estimate the aquifer material volume and estimates of groundwater in storage. Without closely spaced flight lines providing fine detail of the subsurface, it is not recommended that these volume and storage calculation be made.

5.2.3 Applicability and Recommendations Regarding Future Groundwater Investigations

The hydrostratigraphic framework resulting from this AEM survey provides a database of information on the structure of the groundwater resources available beneath the surveyed portion of the LENRD. As noted, the flight line spacing implemented in this survey proved to be appropriate to assess the overall character of groundwater resources in the district. The resulting datasets from this survey provide readily useable information that can be immediately applied to future or current groundwater investigations.

The current grid arrangement provides detailed representation of the various Quaternary, Tertiary, and Cretaceous aquifer and aquitard materials present in the subsurface at three mile spacing within the district. Although this spacing is not adequate for creation of 3D voxel models of the subsurface across the entire district, users are able to have a general understanding of the subsurface materials likely to be

encountered in an area of interest, as AEM data will be available typically less than 1.5 miles from any location. Such info can include the type of aquifer material present (if any), the depths to the aquifer top and base, as well as the thickness of the intervals of interest. Conversely, the extent and thickness of non-aquifer materials is also available, data that can assist in planning managed groundwater recharge projects or developing groundwater quality protection plans (i.e.- wellhead protection plans, best management practices for application of agri-chemicals). Additionally, for non-water development needs, the AEM survey data can be utilized to assess current or locate future sand and gravel mining operations within the district.

The AEM flight line profiles can also provide a guide as to where future data collection is necessary for proper assessment of groundwater resources. As mentioned, the current spacing provides an initial, baseline starting point to the character of the hydrostratigraphy. However, changes in the distribution of subsurface features can occur within short distances in the glaciated terrain of eastern Nebraska. For example, in an AEM survey conducted in the southern LENRD between the towns of Clarkson and Howells (Abraham et al., 2013), a line spacing of just under 1000 ft was used during data acquisition. This closely spaced flight path layout allowed for detection of the extent of the limited glacial outwash deposits surrounding these towns. Had a spacing of a one-half mile or one mile been used in this study, a considerable portion of the aquifer resources near Clarkson, NE would not have been detected (Figure 5-21). Thus, the current framework provides a base starting point of hydrogeologic information available beneath the district, and it can also provide guidance as to the possible line spacing required for future, localized investigations. For example, if acquisition of data is required in one of the seven sand-rich principal aquifer areas where the bodies are continuous, a survey could be conducted with slightly less dense grid spacing than for a survey conducted in the eastern half of the project area where the marginal aquifer is interlayered with aquitard material and very isolated principal aquifer deposits.

The hydrostratigraphic framework data produced from this survey is also readily applicable for numerical groundwater model investigations. The most straightforward application of the processed AEM data is the delineation of grid surfaces that represent geologic material contacts that can be directly utilized to define groundwater model layer and boundary elevations, as well as to identify where geologic units terminate and the character of that boundary. This information can be especially useful for a groundwater model, especially for areas where a particular unit pinch out, like the *To* beneath the project area. Recent enhancement to groundwater modeling codes, such as MODFLOW-USG (Panday et al., 2013) has the ability to simulate discontinuous geologic layers. However, this capability is only useful if the data for the model appropriately represents the natural system.

In addition to providing model-ready datasets of geologic layer elevations, the AEM framework can provide additional information that can be applied to developing more robust initial conceptual models of groundwater flow systems, or improving upon pre-existing groundwater flow-system conceptualizations. For example, the hydrostratigraphic framework described in this report clearly indicates areas of higher probability of groundwater recharge as compared to other areas. This information can allow for more precise spatial assignment of recharge to a groundwater model. Also, in regards to stream depletion concerns, the AEM framework clearly demonstrates where the major

drainages in the Elkhorn River watershed are most closely in communication with the sand-rich portions of the principal aquifer, or where principal aquifer materials have some degree of disconnect from these surface water features. This information could impact both the groundwater model calibration, as well as the estimates of impacts on the streams by extraction wells over time, which affects how the LENRD manages its groundwater. The distribution of materials can also aid in groundwater model calibration efforts as well. Resistivities are generally associated with the degree of permeability and storage capacity in the aquifer. Further investigation into the resistivity can provide estimates of hydraulic conductivity with the appropriate methodologies, information of which can be used as initial hydraulic conductivity values in a groundwater model. Also, the distinct areas of permeability, for example the coarse, sand-rich areas identified in Figure 5-3, can be assigned as unique zones or interpolation point data within the conceptualization and calibration of a groundwater model.

The lithologic character distributions based on resistivity as indicated in Figure 5-7and Figure 5-8 can also provide preliminary estimated ranges of hydraulic conductivity (*k*) for each of the aquifer materials. For the non-aquifer/aquitard category, which is predominately till, silt/loess, and clay, *k* values could range from 2.8×10^{-6} feet per day (ft/d) to 2.8×10^{-1} ft/d. For the marginal aquifer materials, much of the material distribution is similar to the aquitard material, with the exception of a larger interval of coarse material (nearly 15 percent). Thus, *k* values could be expected to increase in these areas toward the range of 1-3 ft/d where coarse materials are present. For the principal aquifer, more expanded areas of *k* values ranging from 30 to nearly 300 ft/d could be present. For areas of the principal aquifer with resistivity over 50 ohm-m, especially where well-sorted gravel is present, *k* values could exceed 1000 ft/d. For this condition to occur, however, the gravel would need to be angular and well-sorted with a minimal component of sand or silt in the matrix (Fetter, 1994). Specific yield values in the sand-rich portion of the principal aquifer could range from 0.21 to 0.27, with values of the parameter ranging from 0.02 to 0.18 in clay, silt, and sandy clay deposits that are predominant in the marginal aquifer and aquitard materials (Johnson 1967). For the *To* portion of the principal aquifer, *k* values can range from 1 to 50 ft/d, with specific yield values ranging from less than 0.01 to 0.3 (Gutentag et al., 1984).

Helgesen, et al. (1993) report transmissivity within the Maha aquifer beneath the project area ranging from approximately 7,500 to 75,000 gpd/ft (converted from reported values of 1,000 to 10,000 ft^2/d). With an assumed thickness of 500 ft, these transmissivity values would equate to a *k* range of 2 to 20 ft/d, with the higher values of this range likely occurring in the more resistive intervals of the *Kd* identified in the interpretive profiles of Appendix 1. These reported values are only estimates of the *k* that could be encountered in the *Kd*, and it is advised that aquifer tests or other geophysical methods be implemented to specifically characterize local conditions in this bedrock aquifer source.

To more accurately characterize the physical parameters of the aquifer, as well as for further verification of the lithologic-resistivity relationship described, it is recommended that sonic cores are implemented to obtain specific lithologic samples undisturbed by drill bits or drilling mud. This would provide undisturbed core of the subsurface with only minimal disturbance of fine material that is normally lost during mud-rotary drilling. Following retrieval of the core, implementation of a calibrated, full-suite geophysical log would be recommended. The resulting data would provide specific resistivity and

gamma log data that could be more reliably correlated with the lithology present at that interval. Additionally, nuclear magnetic resonance (NMR) technology could be utilized to characterize porosity and permeability of the materials encountered at the location of interest. It is possible that a sonic core could provide tighter constraints on the resistivity ranges, particularly with the maximum and minimum ranges for glacial till and sand. If the fines are lost in the mud rotary-based drill hole, it would be nearly impossible to assess the quantity of fines in these intervals identified as till or sand, which would thus result in erroneous lithologic characterization, even if those intervals resulted in lower than expected resistivities from the geophysical log for that lithology type.

To further characterize the similarities and differences in the areas where Quaternary principal aquifer materials overlie *To* deposits, piezometer networks with short screened intervals (10 ft maximum) should be installed with several piezometers set and various depths to capture vertical flow gradients in the aquifer. Based on the density of irrigation wells in the western half of the project area, particularly north of the Elkhorn River, it is likely that both stratigraphic intervals are tapped. However, there is little understanding as to the specific connection of these two units and their productive capacities.

It is also recommended that sonic coring efforts focus on a location where bedrock resistors are present, particularly in the *Kd*, ideally with one in the northwest portion of the project area where less resistive intervals were detected in the AEM as well as higher resistive areas in the eastern half of the district. A core would provide beneficial insight into the understanding of the cause of the higher conductive areas in the *Kd*, which could be caused by lithologic or pore water characteristics. Sonic core data can also provide insight into the nature of the resistive intervals revealed in the *M* strata.

Based on the experience and knowledge gained from this effort, the following summarized recommendations are presented to guide future investigations in support of groundwater management in the LENRD. They are as follows:

- Additional AEM surveys should be extended contiguous to the current project area providing seamless 3x3 mile grid of flight lines across the LENRD. This work will allow the staff and board of the LENRD the ability to assess the hydrogeology of the area at a scale suitable for characterization of the major aquifer and aquitard features beneath the district, allowing for consideration of any additional work that might be needed for management purposes.

- The connectivity between groundwater and surface water features along the streams and rivers within the district is not well understood. The addition of a near-surface, high resolution AEM streambed mapping program of the riparian area is recommended. This data would provide finer detail of the lithology of this critical area, and more precisely characterize the extent and shape of the aquifers and aquitards that affect hydrologic connection to streams.

- For locations where the topic of investigation involves localized aquifer features, a tighter grid spacing is recommended, on the order of 600 to 1500 ft separation. Surveys of this scale will allow for creation of 3D voxel models of aquifer materials, from which calculations of aquifer

volume and groundwater in storage can be made, which can provide LENRD management greater insight into the quantity of groundwater available in the area of interest.

- A CSD test hole program that includes penetration through the *Kd*, ideally in the areas where the most extensive resistors were detected in the AEM survey. Following drilling and lithologic analysis, water quality testing and assessment of potential well yield via aquifer tests is recommended. It is suggested that future test hole sites be selected with knowledge gained from the AEM survey.

- The AEM survey identified areas along the flight lines where a greater probability of groundwater recharge is likely to occur. A high resolution AEM survey of these areas would quantify the geographic extent of these areas and the hydrologic connection to the subsurface. This information could then be used to specifically site recharge studies in known locations that provide the greatest benefit to understanding the meteoric contribution to the water balance of the LENRD.

Utilize aquifer characterization techniques in conjunction with the AEM survey flight lines to improve the understanding of important changes in hydraulic conductivity, storage, and yield. This information can then be used directly with future groundwater modeling endeavors to improve model calibration and predictive capability.

6 Description of Data Delivered

The geophysical and borehole electronic data are included as Appendix 4. Electronic interpretation results are also included.

Table 6-1 describes the data columns in the .xyz file 20141126_345_Nebraska_XRI.xyz. This file contains the raw geophysical data, including magnetic, as supplied directly from SkyTEM. The results of the two SCIs are included in xyz files Gridlines_SCIresults.xyz and Reconlines_SCIresults.xyz and the data columns of these databases are described in Table 6-2. The borehole data used to constrain the SCI inversions and to assist in the interpretation of the inversion results are included in the files listed in Table 6-3. Each type of borehole information has both a collar file containing the location of each of the wells, and a second file containing the borehole data for the individual wells. The data column descriptions for the collar files are listed in Table 6-4. Table 6-5 describes the channels in all of the borehole data files as well as indicates which type of data contains each channel. The various interpretation results are included in data files Reconlines_AEMData_InterpSurfaces.xyz and Grid_AEMData_InterpSurfaces.xyz. Table 6-6 describes the data columns of those files.

In addition to the data delivered in .xyz format Google Earth .kmz files were created to view the geophysical AEM flight line locations, geophysical data, and interpreted geologic data. Within the .kmz file, the AEM flight line is shown, as well as place marks at each location where there are AEM inversion results. The attribute data for each unique place mark contains information including the top elevations of various geologic units, as well as the presence of aquifer material. These .kmz files are delivered within the “LENRD_2014” folder, the file “read_me.txt” provides instructions in regards to how to use the .kmz files in Google Earth.

Table 6-1: Channel name, description, and units for 20141126_345_Nebraska_XRI.xyz with EM, mag, DGPS, Inclinometer, altitude, and associated data.

Parameter	Description	Unit
FID	Unique Fiducial Number	Seconds
LINE	Line Number	LLLLLL
FLIGHT	Name of Flight	yyyymmdd.ff
DATETIME	DateTime Format	Decimal days
DATE	DateTime Format	yyyymmdd
TIME	Time	hhmmss.sss
ANGLEX	Angle (in flight direction)	Degrees
ANGLEY	Angle (perpendicular to flight direction)	Degrees
HEIGHT	Filtered Height Measurement	Meters [m]
LON	Longitude, WGS84	Decimal Degrees
LAT	Latitude, WGS84	Decimal Degrees
E	Easting, NAD83 UTM Zone 13N	Meters [m]
N	Northing, NAD83 UTM Zone 13N	Meters [m]
DEM	Digital Elevation	Meters [m]
ALT	DGPS Altitude	Meters above sea level
GDSPEED	Ground Speed	Kilometers/hour [km/h]
CURR_2	Current, Low Moment	Amps
CURR_1	Current, High Moment	Amps
LMZ_G01	Normalized (PFC-Corrected) Low Moment Z-RxCoil value	$pV/(m^4*A)$
HMZ_G01	Normalized (PFC-Corrected) High Moment Z-RxCoil value	$pV/(m^4*A)$
LMX_G01	Normalized (PFC-Corrected) Low Moment X-RxCoil value	$pV/(m^4*A)$
HMX_G01	Normalized (PFC-Corrected) High Moment X-RxCoil value	$pV/(m^4*A)$
BMAG_RAW	Raw Base Station Mag Data	nanoTesla [nT]
DIURNAL	Diurnal Mag Data	nanoTesla [nT]
MAG_RAW	Raw Mag Data	nanoTesla [nT]
MAG_COR	Mag Data Corrected for Dirurnal Drift	nanoTesla [nT]
PLNI	Power Line Noise Intensity monitor	C*V/sqrt(Hz)
X_ft	Easting, NAD83 UTM Zone 13N	Feet [ft]
Y_ft	Northing, NAD83 UTM Zone 13N	Feet [ft]

Table 6-2: Channel name, description, and units for Gridlines_SCIresults.xyz and Reconlines_SCIresults.xyz with EM inversion results.

Parameter	Description	Unit
X_ft	Easting NAD83, UTM Zone 14	Feet [ft]
Y_ft	Northing NAD83, UTM Zone 14	Feet [ft]
X_m	Easting NAD83, UTM Zone 14	Meters [m]
Y_m	Northing NAD83, UTM Zone 14	Meters [m]
TOPO	Topography	Feet [ft]
FID	Unique Fiducial Number	
LINE	Line Number	
ALT	Altitude	Feet [ft]
INVALT	Inverted Altitude	Feet [ft]
INVALTSTD	Inverted Altitude Standard Deviation	
DELTAALT	Change in Altitude	Feet [ft]
NUMDATA	Number of data points	
RESDATA	Residual of individual sounding	
RESTOTAL	Total residual for inverted section	
DOI_LOWER	Less conservative estimate of DOI	Feet [ft]
DOI_UPPER	More conservative estimate of DOI	Feet [ft]
RHO_I_1 THROUGH RHO_I_30	Inverted resistivity of each later	Ohm-m
RHO_I_STD1 THROUGH RHO_I_STD2	Standard deviation of inverted resistivity	
SIGMA_I_1 THROUGH SIGMA_I_30	Conductivity	mS/m
DEP_BOT_1 THROUGH DEP_BOT_29	Depth to the bottom of individual layers	Feet [ft]
DEP_TOP_1 THROUGH DEP_TOP_30	Depth to the top of individual layers	Feet [ft]
THK_1 THROUGH THK_30	Thickness of individual layers	Feet [ft]

Table 6-3: Files containing borehole information.

Database	Description
CSD-E-logs_Collar.gdb	Electrical logs from CSD wells
CSD-E-logs_data.gdb	
CSD-GEO-logs_Collar.gdb	Geophysical logs from CSD wells
CSD-GEO-logs_data.gdb	
CSD-LITH_Collar.gdb	Lithology logs from CSD wells
CSD-LITH_from_to.gdb	
CSD-STRAT_Collar.gdb	Stratigraphy logs from CSD wells
CSD-STRAT_from_to.gdb	
GP-logs-inv-constrain_Collar.gdb	Geophysical logs used to constrain the SCIs
GP-logs-inv-constrain_data.gdb	
OandG-GP-logs_Collar.gdb	Geophysical logs from the Oil and Gas wells
OandG-GP-logs_data.gdb	
OandG-LITH_Collar.gdb	Lithology logs from the Oil and Gas wells
OandG-LITH_from_to.gdb	
OandG-STRAT_Collar.gdb	Stratigraphy logs from the Oil and Gas wells
OandG-STRAT_from_to.gdb	

Table 6-4: Channel name, description, and units for collar files

Parameter	Description	Unit
DH_Hole	Name of individual boreholes	
DH_East	Easting of boreholes, NAD83, UTM Zone 14	Feet [ft]
DH_North	Northing of boreholes, NAD83, UTM Zone 14	Feet [ft]
DH_RL	Elevation of top of borehole	Feet [ft]
DH_Dip	Dip of borehole	Degrees
DH_Azimuth	Azimuth of borehole	Degrees
DH_Top	Depth to top of borehole	Feet [ft]
DH_Bottom	Depth to bottom of borehole	Feet [ft]
DH_ZMin	Minimum elevation in borehole	Feet [ft]
DH_ZMax	Maximum elevation in borehole	Feet [ft]

Table 6-5: Channel name description and units for borehole data

Parameter	Description	Unit	Type of Log
DH_East	Easting of boreholes, NAD83, UTM Zone 14	Feet [ft]	All
DH_North	Northing of boreholes, NAD83, UTM Zone 14	Feet [ft]	All
DH_RL	Elevation of top of borehole	Feet [ft]	All
DH_From	End of interval	Feet[ft]	Strat, Lith
DH_To	Start of interval	Feet [ft]	Strat, Lith
DH_Strat_Code	Code used to indicate type of stratigraphy		Strat
DH_Soil_Code	Code used to indicate type of lithology		Lith
DH_Description	Description of stratigraphy or lithology		Strat, Lith
DH_Depth	Depth	Feet [ft]	GP
DH_SP	Self Potential	milliVolt [mV]	GP, E, Geo
DH_SN	Short Normal Resistivity	Ohm-m	GP
DH_SFL	Spherically Focus Log	Ohm-m]	GP
DH_ILD	Induction Log Deep	Siemens/m [S/m]	GP
DH_ILM	Induction Log Medium	Siemens/m [S/m]	GP
DH_LAT	Laterolog	Ohm-m	GP
DH_Res	Resistivity	Ohm-m	Constrain, E
DH_Nat_Gam	Natural Gamma	Counts	Geo
DH_Res_SnglPt	Resistivity Single Point	Ohm-m	Geo
DH_Res_16	Resistivity 16in	Ohm-m	Geo
DH_Res_64	Resistivity 65in	Ohm-m	Geo
DH_Res_Lat	Res Laterolog	Ohm-m	Geo
DH_SP_Cond	Self Potential Induction	milliVolt [mV]	Geo
DH_Res_FL	Resistivity of the fluid	Ohm-m	Geo
DH_Tmp_FL	Temperature of the fluid	Degrees F	Geo
DH_Del_Tmp	Change in temperature of the fluid	Degrees F	Geo

Table 6-6: Channel name description and units for the interpretation results file.

Parameter	Description	Unit
X_ft	Easting NAD83, UTM Zone 14	Feet [ft]
Y_ft	Northing NAD83, UTM Zone 14	Feet [ft]
Z_ft	Topography at 1000ft sampling (NAVD 1988)	Feet [ft]
Distance	Down line distance from start of flight line	Feet [ft]
RHO_I[0] through RHO_I[29]	Inverted resistivity of each later	Ohm-m
DEP_BOT[0] through DEP_BOT[29]	Depth to the bottom of individual layers	Feet [ft]
DEP_TOP[0] through DEP_TOP[29]	Depth to the top of individual layers	Feet [ft]
RESDATA	Residual of individual sounding	NA
RESTOTAL	Total residual for inverted section	NA
DOI_LOWER	Less conservative estimate of DOI from Workbench	Feet [ft]
DOI_UPPER	More conservative estimate of DOI from Workbench	Feet [ft]
DOIPT1FLT	Estimate of DOI as discussed in Appendix 3	Feet [ft]
SPIESDOI2FTFLT	Estimate of DOI as discussed in Appendix 3	Feet [ft]
WT_1995	Elevation of the top of the water table from the Nebraska School of Natural Resources Configuration Report, 1995.	Feet [ft]
Bedrock	Elevation of interpreted bedrock surface	Feet [ft]
PrincipalAquifer_Top	Elevation of top of principal aquifer material (>20 ohm-m)	Feet [ft]
CoarseAquifer_Top	Elevation of top of coarse aquifer material (>50 ohm-m)	Feet [ft]
CoarseAquifer_Bot	Elevation of bottom of coarse aquifer material (>50 ohm-m)	Feet [ft]
PrincipalAquifer_Bot	Elevation of bottom of principal aquifer material (>20 ohm-m)	Feet [ft]
To	Elevation of the top of the Tertiary Ogalla Group.	Feet [ft]
Kp	Elevation of the top of the Cretaceous Pierre shale.	Feet [ft]
Kn	Elevation of the top of the Cretaceous Niobrara Formation.	Feet [ft]
Kc_Kgg	Elevation of the top of the Cretaceous Carlile Shale.	Feet [ft]
Kd	Elevation of the top of the Cretaceous Dakota Formation.	Feet [ft]
&	Elevation of the top of the Pennsylvanian Strata.	Feet [ft]
M	Elevation of the top of the Mississippian Strata	Feet [ft]A
*	No data or unit not detected	

7 References

Abraham, J. D., C. P. Carney, and J. C. Cannia, 2013, "Data Report on Mapping the Hydrogeology of the Clarkson Area within the Lower Elkhorn Natural Resources District Using an Airborne Electromagnetic Survey." Project findings report prepared for the Lower Elkhorn Natural Resources District.

Abraham, J. D., Bedrosian, T.H Asch, L. B. Ball, J. C. Cannia, J. D. Philips, and S. Lackey, 2011, "Evaluation of Geophysical Techniques for the Detection of Paleochannels in the Oakland Area of Eastern Nebraska as Part of the Eastern Nebraska Water Resource Assessment." U.S. Geological Survey Scientific Investigations Report 2011-5228.

Bankey, V., A. Cuevas, D. David, C. A. Finn, I. Hernandez, P. Hill, R Kucks, W. Miles, M. Pilkington, C. Roberts, W. Roest, V. Rystrom, S. Shearer, S. Snyder, R. Sweeney, J. Velez, J. D. Philips, D. Ravat, 2002, Digital data grids for the magnetic anomaly map of North America. U.S. Geological Survey Open-File Report 02-414, Denver, CO: U.S. Geological Survey.

Bentall, R. , 1971, "Water supplies and the land, the ELkhorn River Basin of Nebraska; Lincoln." University of Nebraska-Lincoln Conservation and Survey Division Resource Atlas No. 1.

Burchett, R. R., 1986, "University of Nebraska-Lincoln, School of Natural Resources." Bedrock geology of Nebraska, http://snr.unl.edu/data/geographygis/NebrGISgeology.asp#bedrock (accessed Jan 8, 2015).

Carney, C. P., K. S. Pierce, J. D. Abraham, G. V. Steele, A. G. Genco, and J. C. Cannia, 2014, "Hydrogeologic Assessment and Framework Development of the Aquifers beneath the Brainard-Valparaiso Area of the Lower Platte South Natural Resources District in Eastern Nebraska."

Christensen, N. B., J. E. Reid, and M. Halkjaer, 2009, "Fast, laterally smooth inversion of airborne time-domain elecromagnetic data." Near Surface Geophysics, 599-612.

Christiansen, A. V., and E. Auken, 2012. "A global measure for depth of investigation." Geophysics,Vol. 77, No. 4, WB171-177.

Condra, G. E., and C. E. Reed, 1959, The geolgogical section of Nebraska with current revisions by C.E. Reed. Nebraska Geological Survey Bulletin, Lincoln, Nebraska: University of Nebraska-Lincoln, Consevation and Survey Division.

Diffendal, R. F., 1995, "Geology of the Ogallala/High Plains regional aquifer system in Nebraska, field trip No.6 in Geological Society of America." Annual Meetings of the North-Central and South Central Sections.

Divine, D. P., 2012, Geologic cross section across eastern Nebraska from Pierce County to Dakota County. Correlations and Cross Sections, Conservation and Survey Division, School of Natural Resources, Institute of Agriculture and Natrual Resources, University of Nebraska-Lincoln.

Divine, D. P., and J. T. Korus, 2012, "Eastern Water Resources Assessment." Three-dimensional Hydrostratigraphy of the Sprague Nebraska Area: Results from Helicopter Electromagnetic (HEM) Mapping in the Eastern Nebraska Water Resources Assessment (ENWRA), http://www.enwra.org/media/2012ENWRA_Sprague_final.pdf (accessed Jan 8, 2015).

Divine, D. P., R. M. Joeckel, J. T. Korus, P. R. Hanson, and S. O. Lackey, 2009, Eastern Nebraska Water Resources Assessment, Introduction to Hydrogeological Study. University of Nebraska-Lincoln, School of Natural Resources, Conservation and Survey Division.

Divine, D. P., S. Ross, and J. Korus, 2010, Compilation of Geologic Cross Sections of Eastern Nebraska. Open-File Report 109, Lincoln, Nebraska: School of Natural Resources, University of Nebraska-Lincoln.

Elder, J. A., V. H. Dreesen, and E. C. Weakly, 1951, "University of Nebraska-Lincoln, School of Natural Resources." Topographic Regions of Nebraska. http://snr.unl.edu/data/geographygis/NebrGISgeology.asp#topography (accessed Jan 15, 2015).

Ellis, M. J., 1984, "Overview of the Dakota aquifer system in Nebraska, in Jorgensen, D.G. and Signor, D.C., eds., Geohydrology of the Dakota aquifer." National Water Well Association Proceedings, 48-55.

Flowerday, C. A., R. D. Kuzelka, and D. T. Pederson, 1998, The groundwater atlas of Nebraska. Resorce Atlas No. 4A, Lincoln, Nebraska: Conservation and Survey Division, School of Natural Resoirces, Institute of Agriculture and Natural Resoruces, University of Nebraska-Lincoln.

Foged, Nikolaj, Esben Auken, Anders Vest Christiansen, and Kurt Ingvard Sorensen, 2013, "Test-site calibration and validation of airborne and ground based TEM systems." Geophysics 78, No.2, E95-E106.

Fredrick, B. S., J. I. Linard, and J. L. Carpenter, 2006, Environmental setting of Maple Creek watershed Nebraska. Scientific Investigations Report 2006-5037, U.S. Geological Survey.

Gates, J. B., G. V. Steele, P. Nasta, and J. Szilagyi, 2014, "Lithologic influenes on groundwater recharge through incised glacial till from profile to regional scales: Evidence from glaciated Eastern Nebraska." Water Resources 50, 466-481.

Gosselin, D. C., F. E. Harvey, and C. D. Frost, 2001, "Geochemical evolution of groundwater in the Great Plains (Dakota) aquifer of Nebraska: implications for the management of a regional aquifer system." Ground Water 31, 98-108.

Gosselin, D. C., J. Headrick, X. Chen, S. Summerside, and R. Tremblay, 1996, Northeast glacial drift area hydrogeologic summary from domestic well-water quality in rural Nebraska. Lincoln, Nebraska: University of Nebraska-Lincoln, Conservation and Survey Division GIM.

Gutentag, E. D., F. J. Heimes, N. C. Krothe, R. R. Luckey, and J. B. Weeks, 1984, Geohydrology of the High Plains aquifer in parts of Colorado, Kansas, Nebraska, New Mexico, Oklahoma, South Dakota, Texas, and Wyoming. Professional Paper 1400-B, U.S. Geological Survey .

Hanson, P. R., J. T. Korus, and D. P. Divine, 2012, Three-dimensional hydrostratigraphy of the Platte River Valley near Ashland, Nebraska: Results from Helicopter Electromagnetic mapping in the Eastern Nebraska Water Resources Assessment. Bulletin 2, Conservation and Survey Division, School of Natural Resources, Institute of Agricultutre and National Resources, University of Nebraska-Lincoln.

Helgesen, J. O., R. B. Leonard, and R. J. Wolf, 1993, Hydrology of the Great Plains aquifer system in Nebraska, Colorado, Kansas, and adjacent areas. Regional Aquifer-System Analysis—Central Midwest, Professional Paper 1414-E, U.S. Geological Survey.

HydroGeophysics Group Aarhus University, 2011, Guide for processing and inversion of SkyTEM data in Aarhus Workbench, Version 2.0.

HydroGeophysics Group Aarhus University, 2010, Validation of the SkyTEM system at the extended TEM test site.

Johnson, A. I, 1967, Specific yield -- Compliation of specific yeilds for various materials. Water- Supply Paper 1662-D, U.S. Geological Survey.

Jorgensen, D. G., J. O. Helgesen, D. C. Signor, R. B. Leonard, J. Limes, and S. C. Christenson, 1993, Analysis of regional aquifers in the central Midwest of the United States in Kansas, Nebraska, and parts ofArkansas, Colorado, Missouri, New Mexico, Oklahoma, South Dakota, Texas, and Wyoming Geohydrologic framework. Professional Paper 1414-B, U.S. Geologic Survey.

Korus, J. T., 2012, Geologic cross section across eastern Nebraska from Thurston County to Pawnee County. Conservation and Survey Division, School of Natural Resources Institute of Agriculture and Natural Resources, University of Nebraska-Lincoln.

Korus, J. T., and R. M. Joeckel, 2011, Generalized geologic and hydrostratigraphic framework of Nebraska 2011, version 2. Conservation and Survey Division, University of Nebraska-Lincoln.

Korus, J. T., D. P. Divine, P. R. Hanson, and J. S. Dilion, 2012, Three geologic cross sections across portions of eastern Nebraska showing Quaternary lithologic units and stratigraphy of uppermost bedrock. Correlations and Cross Sections, Conservation and Survey Division School of Natural Resources, University of Nebraska-Lincoln.

Miller, J. A., and C. L. Appel, 1997, Ground water atlas of the United States; Segment 3 Kansas, Missouri, and Nebraska. Hydraulic Atlas 730D, U.S. Geological Survey.

Miller, R. D., R. Van Horn, E. Dobrovolny, and L. P. Buck, 1964. "USGS." Geology of Franklin, Webster, and Nuckolls Counties, Nebraska Bulletin 1165, http://pubs.er.usgs.gov/publication/b1165 (accessed Mar 20, 2015).

Nebraska Oil and Gas Conservation Commision, 2008, Nebraska Oil and Gas Conservation Commission Data and Publications, http://www.nogcc.ne.gov/NOGCCPublications.aspx (accessed Jan 5, 2015).

Nolan, B. T., R. W. Healy, P. E. Taber, K. Perkins, K. J. Hitt, and D. M. Wolock, 2007, Factors influencing ground-water recharge in the eastern United States. Journal of Hydrology 332, 187-205.

Olafsen-Lackey, S, 2005a, Specific yield of principal aquifer Sioux City Quadrangle, Nebraska. Conservation and Survey Division, School of Natural Resources, University of Nebraska-Lincoln.

Olafsen-Lackey, S, 2005b, Transmissivity of principal aquifer Sioux City Quadrangle, Nebraska. Conservation and Survey Division, School of Natural Resources, University of Nebraska-Lincoln.

Olafsen-Lackey, S., and S. Summerside, 2005, Specific yeild of principal aquifer Fremont and Omaha Quadrangles, Nebraska. Conservation and Survey Division, School of Natural Resources, University of Nebraska-Lincoln.

Panday, S., C. D. Langevin, R. G. Niswonger, M. Ibaraki, and J. D. Hughes, 2013, MODFLOW–USG version 1: An unstructured grid version of MODFLOW for simulating groundwater flow and tightly coupled processes using a control volume finite-difference formulation. U.S. Geological Survey Techniques and Methods, book 6, chap. A45, 66 p.

Peterson, J. A, 1984, Stratigraphy and Sedimentary Facies of the Madison Limestone and Associated Rocks in Parts of Montana, Nebraska, North Dakota, South Dakota and Wyoming. Professional Paper 1273-A, U.S. Geological Survey.

Platt, 2014, Platts McGraw Hill Financial, http://www.platts.com (accessed Oct 2014).

Schamper, C., E. Auken, and K. Sorensen, 2014, Coil response inversion for very early time modelling of helicopter-borne time-domain electromagnetic data and mapping of near-surface Geologic Layers. European Association of Geoscientistis & Engineers, Geophysical Prospecting.

School of Natural Resources University of Nebraska-Lincoln, 2005, Delineation of 2005 land use patterns for the Sate of Nebraska Department of Natural Recorces. http://snr.unl.edu/data/geographygis/NebrGISland.asp#landuse05 (accessed Jan 12, 2015).

Signor, D. C., J. O. Helgesen, D. G. Jorgensen, and R. B. Leonard, 1996, Geohydrology and simulation of steady-state flow conditions in regional aquifer systems in Cretaceous and older rocks

underlying Kansas, Nebraska, and parts of Arkansas, Colorado, Missouri, New Mexico, Oklahoma, South Dakota, Texas, and Wyoming. Professional Paper 1414-C, U.S. Geological Survey, http://pubs.usgs.gov/pp/1414c/report.pdf

SkyTEM Airborne Surveys Worldwide, 2012, SkyTEM survey: Mary Creek Canada data report.

SkyTem Airborne Surveys Worldwide, 2015, Appendix A, Specifications of the SkyTEM508 System 60 Hz, http://skytem.com/wp-content/uploads/2015/01/SkyTEM508-60-Hz.pdf (accessed March 18, 2015).

Smith, B. D., J.D. Abraham, J. C. Cannia, B. J. Minsley, L. B. Ball, G. V. Steele, M. Deszcz-Pan, 2009, Helicopter Electromagnetic Geophysical Survey Data, Swedeburg and Sprague Areas, Eastern Nebraska. U.S. Geological Survey Open-File Report 2010-1288.

Souders, V. L, 2000, Geologic maps and cross sections showing configurations of bedrock surfaces, Broken Bow 1° x 2° quadrangle, east-central Nebraska. Geologic Investigations Series I–2725, U.S. Geological Survey.

Stanton, J. S., G. V. Steele, and J. R. Vogel, 2007, Occurrence of agricultural chemicals in shallow ground water and the unstaturated zone, northeast Nebraska glacial till, Scientific Investigations Report 2002-04, U.S. Geological Survey.

Stanton, J. S., S. M. Peterson, and M. N. Fienen, 2010, Simulation of groundwater flow and effects of groundwater irrigation on stream base flow in the Elkhorn and Loup River Basins, Nebraska Phase Two. Scientific Investigations Report, U.S. Geological Survey, 78.

Summerside, S. M. Ponte, V. H. Dreezen, S. L. Harung, M. J. Khisty, and J. Szilagyi, 2001, Update and revision of regional 1x2 degree water-table configuration maps for the State of Nebraska. Lincoln, Nebraska: Conservation and Survey Division, Institute of Agriculture and Natural Resoruces University of Nebraska-Lincoln.

Szilagyi, J., and J. Jozsa, 2013, MODIS-Aided statewide net groundwater-recharge estimation in Nebraska. Ground Water 51, 735-744.

Szilagyi, J., F. E. Harvey, and I. F. Ayers, 2005, "Regional estimation of total recharge to ground water in Nebraska." Ground Water 43, 63-69.

U.S. Census Bureau, 2013, Demographic profile, total population. http://factfinder.census.gov/faces/nav/jsf/pages/index.xhtml (accessed Jan 12, 2015).

U.S. Geological Survey, 2015, USGS surface-water data for Nebraska. http://waterdata.usgs.gov/ne/nwis/sw/ (accessed Jan 8, 2015).

United States Department of Agriculture, 2014. USDA Natural Resources Conservation Service. http://www.nrcs.usda.gov/wps/portal/nrcs/detail/oh/technical/dma/gis/?cid=nrcs144p2_029531 (accessed Oct 2014).

University of Nebraska-Lincoln School of Natural Resources, 2014, Nebraska statewide test-hole database. http://snr.unl.edu/data/geologysoils/NebraskaTestHole/NebraskaTestHoleIntro.asp (accessed October 15, 2014).

Viezzoli, A., A. V. Christiansen, E. Auken, and K. Sorensen, 2008, "Quasi-3D modeling of airborne TEM data by spatially constrainted inversion." Geophysics Vol. 73 No. 3, F105-F113.